The Homestake Gold Mine, An Early Proterozoic Iron-Formation-Hosted Gold Deposit, Lawrence County, South Dakota

U.S. GEOLOGICAL SURVEY BULLETIN 1857-J

AVAILABILITY OF BOOKS AND MAPS OF THE U.S. GEOLOGICAL SURVEY

Instructions on ordering publications of the U.S. Geological Survey, along with the last offerings, are given in the current-year issues of the monthly catalog "New Publications of the U.S. Geological Survey." Prices of available U.S. Geological Survey publications released prior to the current year are listed in the most recent annual "Price and Availability List." Publications that are listed in various U.S. Geological Survey catalogs (**see back inside cover**) but not listed in the most recent annual "Price and Availability List" are no longer available.

Prices of reports released to the open files are given in the listing "U.S. Geological Survey Open-File Reports," updated monthly, which is for sale in microfiche from the U.S. Geological Survey Books and Open-File Reports Sales, Box 25425, Denver, CO 80225.

Order U.S. Geological Survey publications **by mail** or **over the counter** from the offices given below.

BY MAIL

Books

Professional Papers, Bulletins, Water-Supply Papers, Techniques of Water-Resources Investigations, Circulars, publications of general interest (such as leaflets, pamphlets, booklets), single copies of periodicals (Earthquakes & Volcanoes, Preliminary Determination of Epicenters), and some miscellaneous reports, including some of the foregoing series that have gone out of print at the Superintendent of Documents, are obtainable by mail from

U.S. Geological Survey, Books and Open-File Report Sales
Box 25425
Denver, CO 80225

Subscriptions to periodicals (Earthquakes & Volcanoes and Preliminary Determination of Epicenters) can be obtained ONLY from

Superintendent of Documents
U.S. Government Printing Office
Washington, DC 20402

(Check or money order must be payable to Superintendent of Documents.)

Maps

For maps, address mail order to

U.S. Geological Survey, Map Sales
Box 25286
Denver, CO 80225

Residents of Alaska may order maps from

U.S. Geological Survey, Map Sales
101 Twelfth Ave., Box 12
Fairbanks, AK 99701

OVER THE COUNTER

Books

Books of the U.S. Geological Survey are available over the counter at the following U.S. Geological Survey offices, all of which are authorized agents of the Superintendent of Documents.

- **ANCHORAGE, Alaska**–4230 University Dr., Rm. 101
- **ANCHORAGE, Alaska**–605 West 4th Ave., Rm G-84
- **DENVER, Colorado**–Federal Bldg., Rm. 169, 1961 Stout St.
- **LAKEWOOD, Colorado**–Federal Center, Bldg. 810
- **MENLO PARK, California**–Bldg. 3, Rm. 3128, 345 Middlefield Rd.
- **RESTON, Virginia**–National Center, Rm. 1C402, 12201 Sunrise Valley Dr.
- **SALT LAKE CITY, Utah**–Federal Bldg., Rm. 8105, 125 South State St.
- **SAN FRANCISCO, California**–Customhouse, Rm. 504, 555 Battery St.
- **SPOKANE, Washington**–U.S. Courthouse, Rm. 678, West 920 Riverside Ave.
- **WASHINGTON, D.C.**–U.S. Department of the Interior Bldg., Rm. 2650, 1849 C St., NW.

Maps

Maps may be purchased over the counter at the U.S. Geological Survey offices where books are sold (all addresses in above list) and at the following Geological Survey offices:

- **ROLLA, Missouri**–1400 Independence Rd.
- **FAIRBANKS, Alaska**–New Federal Building, 101 Twelfth Ave.

U.S. DEPARTMENT OF THE INTERIOR
MANUEL LUJAN, JR., Secretary

U.S. GEOLOGICAL SURVEY
Dallas L. Peck, Director

UNITED STATES GOVERNMENT PRINTING OFFICE: 1991

For sale by the
Books and Open-File Reports Section
U.S. Geological Survey
Federal Center
Box 25425
Denver, CO 80225

Library of Congress Cataloging-in-Publication Data

The Homestake Gold Mine : an early Proterozoic iron-formation-hosted gold deposit, Lawrence County, South Dakota / by Stanton W. Caddey ... [et al.].
p. cm. — (Geology and resources of gold in the United States ; ch. J)
(U.S. Geological Survey bulletin ; 1857–J)
Includes bibliographical references.
Supt. of Docs. no.: I 19.3:1857–J
1. Gold ores—South Dakota—Lawrence County. 2. Homestake Mine (S.D.) 3. Geology, Stratigraphic—Proterozoic. I. Caddey, Stanton W. II. Series. III. Series: U.S. Geological Survey bulletin ; 1857–J.
QE75.B9 no. 1857–J
[TN423.S8]
557 S—dc20
[553.4'1'0978391]

91–13722
CIP

Chapter J

The Homestake Gold Mine, An Early Proterozoic Iron-Formation-Hosted Gold Deposit, Lawrence County, South Dakota

By STANTON W. CADDEY, RICHARD L. BACHMAN, THOMAS J. CAMPBELL, ROLLAND R. REID, and ROBERT P. OTTO

U.S. GEOLOGICAL SURVEY BULLETIN 1857

GEOLOGY AND RESOURCES OF GOLD IN THE UNITED STATES

DANIEL R. SHAWE and ROGER P. ASHLEY, Scientific Editors
L.M.H. CARTER, Technical Editor

CONTENTS

FIGURES

TABLES

The Homestake Gold Mine, An Early Proterozoic Iron-Formation-Hosted Gold Deposit, Lawrence County, South Dakota

By Stanton W. Caddey,[1] Richard L. Bachman, Thomas J. Campbell, Rolland R. Reid, *and* Robert P. Otto

Abstract

The Homestake mine in the northern Black Hills, South Dakota, is the largest iron-formation-hosted gold deposit known. It has produced 1,101 metric tons (35.4 million troy ounces) of gold from 124.9 million metric tons of ore milled; in 1988 the mine produced 12.1 metric tons of gold. The deposit was discovered in 1876, and the mine has operated continuously to the present day. Ore is currently mined from depths as great as 2,438 meters. Gold is the major commodity produced, along with a minor silver byproduct. The gold:silver ratio averages 5:1; base metal content is negligible.

The Homestake gold deposit is hosted within quartz-veined, sulfide-rich segments of an Early Proterozoic, carbonate-facies iron-formation in a sequence of originally calcareous, pelitic to semipelitic, and quartzose rocks. Strata that contain the Homestake deposit were complexly deformed by a series of tight isoclinal and sheath fold events, and synchronous, extensive ductile and ductile-brittle shearing. Mine area rocks have been subjected to upper greenschist–lower amphibolite facies metamorphism. Early-stage ductile shearing appears to have controlled fluid movement in the system, thereby controlling thermal energy and metamorphic processes. Observed prograde metamorphism in the district is therefore characterized as dynamothermal. Intrusion of granite similar to the 1.72 Ga Harney Peak Granite in an area northeast of the mine postdated regional prograde metamorphism, and appears to have been contemporaneous with later stages of semibrittle deformation.

Gold mineralization took place almost exclusively in the Homestake Formation, an iron-formation consisting of siderite and (or) grunerite schist in productive sections of the Homestake mine. The underlying Poorman Formation is composed of an upper sequence of sericite- to biotite-dominant carbonate-quartz and graphitic phyllites and a lower voluminous sequence of hornblende-plagioclase schist of tholeiitic affinity. The overlying Ellison Formation consists of interbedded quartzitic, pelitic to semipelitic, and tuffaceous strata.

Nine ore ledges, or plunging fold structures, have produced gold. From east to west across the mine area, they are Caledonia, Main, 7, 9, 11, 13, 17, 19, and 21 Ledges. Ore ledges are synclinal fold forms composed of a series of subordinate anticlines and synclines. Interconnecting anticlinal fold forms (even-numbered ledges) are less complex structurally and contain locally anomalous gold, but are generally barren. Each ore ledge contains a varied number of ore bodies that are disconnected, discrete entities. Overall, ore bodies constitute less than 3 percent, by volume, of the Homestake Formation in the mine area.

Ore bodies are relatively undeformed, tabular- to pipe-shaped segregations of quartz, siderite, chlorite, pyrrhotite, arsenopyrite, and minor pyrite. Ore bodies have developed within dilated segments of late-stage ductile-brittle shears, and they display sharp, well-defined shear contacts with adjacent country rock. Gold grades in ore bodies abruptly diminish across ore-body contacts from greater than 6.20 grams per ton to less than 0.02 grams per ton, commonly within 0.5 meter.

At least three stages of mineral alteration took place, two of which were synmetamorphic and predated gold mineralization and a third synchronous with gold mineralization. The pre-gold alteration stages were characterized by carbon remobilization, and extensive potassium, magnesium±iron, and carbonate metasomatism. Ore-stage hydrothermal alteration was retrogressive, producing extensive chlorite, siderite, and sericite replacement in and adjacent to the ore bodies.

Manuscript approved for publication February 5, 1991.

[1]All authors, Homestake Mining Company, U.S.A., Lead, SD 57754.

Gold mineralization at Homestake, even though not dated directly, is regarded to have taken place during Early Proterozoic time. Zircon (U-Th-Pb) dating of tuffaceous sedimentary rocks within the Ellison Formation has indicated an age of 1.97 Ga, providing a relative time for Homestake Formation deposition. A 1.84 Ga age provides a good approximation of regional dynamothermal metamorphism and major regional ductile deformation. We favor a post-peak metamorphic age (<1.84 Ga) and epigenetic origin for the Homestake gold deposit. Emplacement of granite similar to the 1.72 Ga Harney Peak Granite and associated deformation appear to have occurred in large part following gold mineralization, although data suggest a strong genetic association of the gold event with early stages of evolution of the granite.

INTRODUCTION

Location, History, and Production

The Homestake gold mine is the largest gold producer from a single deposit outside South Africa and the largest deposit of its type in the world. Owing to the tremendous size of the gold system, the geologic model of this largely stratabound deposit is known worldwide as Homestake-type. The Homestake mine (fig. J1) is within the Whitewood mining district in the town of Lead, in Lawrence County, western South Dakota, at the north end of the Black Hills uplift, at lat 44°22′ N., long 103°45′ W.

The climate of the Dakota region is temperate, characterized by short, warm summers (June-September) and long, cold, harsh winters. Elevation in the mining district area is about 1,650 m (5,400 ft) above sea level.

In 1874, the Custer expedition discovered placer gold in French Creek, near the present village of Custer, in the southern Black Hills. When word of the presence of gold in the Black Hills reached the outside world, the gold rush was on. In 1875, placer gold was discovered in Deadwood Creek, about 5 km east of what was to become the city of Lead. The Homestake lode, source area of placer gold, was discovered in 1876, at what is now referred to as Main Ledge (Open Cut surface mine) and Caledonia ore zones.

Early mining activities (pre-1936) in the Homestake lode followed the Main Ledge and Caledonia ore zones (ledges) underground (down-plunge), utilizing shrinkage and timber stoping methods (without backfilling), which were replaced by drawhole mining (an uncontrolled block-cave system) until previously mined areas began caving to the surface. Today, mechanized cut-and-fill (MCF) and vertical crater retreat (VCR) mining methods are employed. Nine productive ore ledges are known in the mine. Annual gold production, ore-ledge discovery history, and significant historical events are presented in figure J2.

The Homestake deposit has been mined continuously since discovery in 1876 (with the exception of the 1942–1945 (World War II) closure that resulted from government directive L–208). Current mining has reached a depth of 2,440 m (8,000 ft) below surface. An excellent historical review of the Homestake mine era is given by Fielder (1970).

The Homestake deposit in addition to gold yields silver as a minor byproduct; base metal concentrations are very low. The Homestake mine has produced 1,101 t (metric tons; 35.4 million troy oz) of gold from 124.9 million t of ore milled from 1878 through 1988 (Homestake internal reports). In 1988, 2.2 million t of ore was mined and milled from eight active ore ledges, yielding 12.1 t of gold. Of this production, 1.4 t of gold was mined from the Open Cut surface mine. Underground and surface ore reserves are estimated at 22.8 million t averaging 5.97 g Au/t (Homestake Mining Company, 1988).

In addition to the Homestake deposit, the Lead area contains significant gold-bearing deposits of Tertiary age in Phanerozoic rocks, including in the Cambrian Deadwood Formation and Mississippian Pahasapa Limestone, and locally in Tertiary alkali-calcic sills, dikes, laccoliths, and stocks. Tertiary-age ores came from parts of the Deadwood Formation (Irving and others, 1904; Allsman, 1940). According to Shapiro and Gries (1970), recorded production is 52.9 t (1.7 million oz) gold and 112.0 t (3.6 million oz) silver. However, Norton (1989) indicated a production of about 2.3 million oz gold from the Deadwood in the Bald Mountain mining district.

Mined deposits consisted generally of replacements in dolomitic units that are transected by vertical fractures. The close spatial association of ore bodies to Tertiary intrusions led the earliest workers (Irving and others, 1904) to propose a Tertiary age for these deposits. Tertiary deposits differ from the Early Proterozoic iron-formation-hosted gold deposit of the Homestake mine not only in age and host rock, but also in style of deposit and mineralogy. Tertiary deposits are characteristically silver-rich (gold:silver ratios generally below 1:1; Shapiro and Gries, 1970), and have significant lead-zinc concentrations; and a few contain wolframite-group minerals and tellurides. Pyrite is the dominant sulfide gangue. For additional information on Tertiary ore deposits, the reader is referred to Irving and others (1904), Allsman (1940), Noble (1950), and Shapiro and Gries (1970).

This report is restricted to the Homestake gold deposit, although gold is also known in Precambrian rocks from other parts of the Black Hills uplift. Some of the data presented are based on previous work and are credited appropriately. Additional new information has been generated by the authors over the past 6 years as a continuing study during exploration, development, and mining of the deposit.

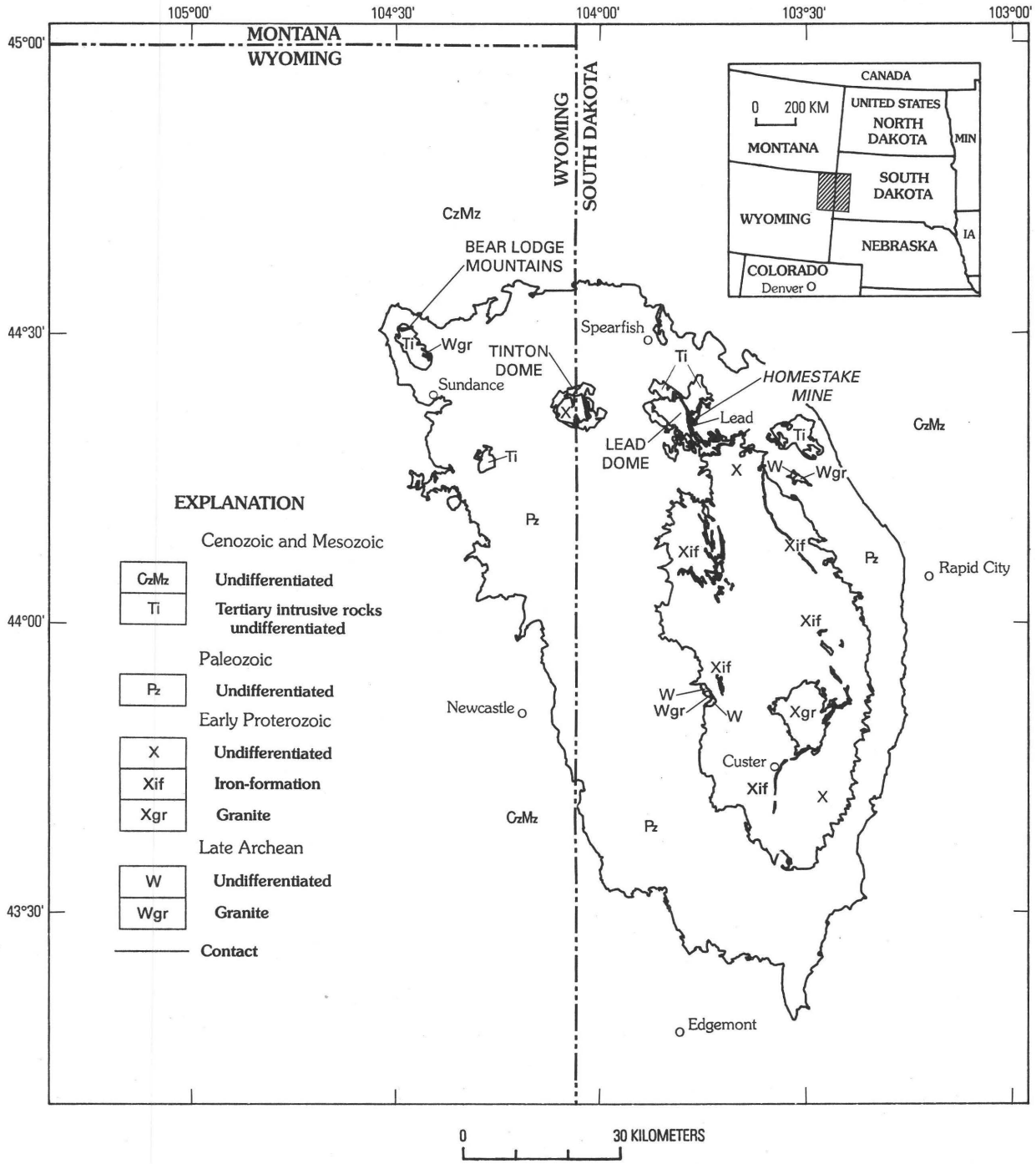

Figure J1. Generalized geology of the Black Hills uplift, South Dakota and Wyoming, modified from DeWitt and others (1986).

Acknowledgments

Inasmuch as it would be virtually impossible to list all of the many geologists who have contributed to the geology of the Homestake mine over the past century, we list some of those who have made major contributions through publications or ore discoveries. Pioneering greats such as Donald McLaughlin, John Gustafson, James Noble, Clarence Kravig, James Harder, and Archie Slaughter, through their discoveries, expanded the Homestake mine, which revealed the truly world-class gold deposit that it is today. Publications by most of these individuals are noted in the references. We are grateful to Homestake Mining Company for permission to publish this report and for continuing support in research.

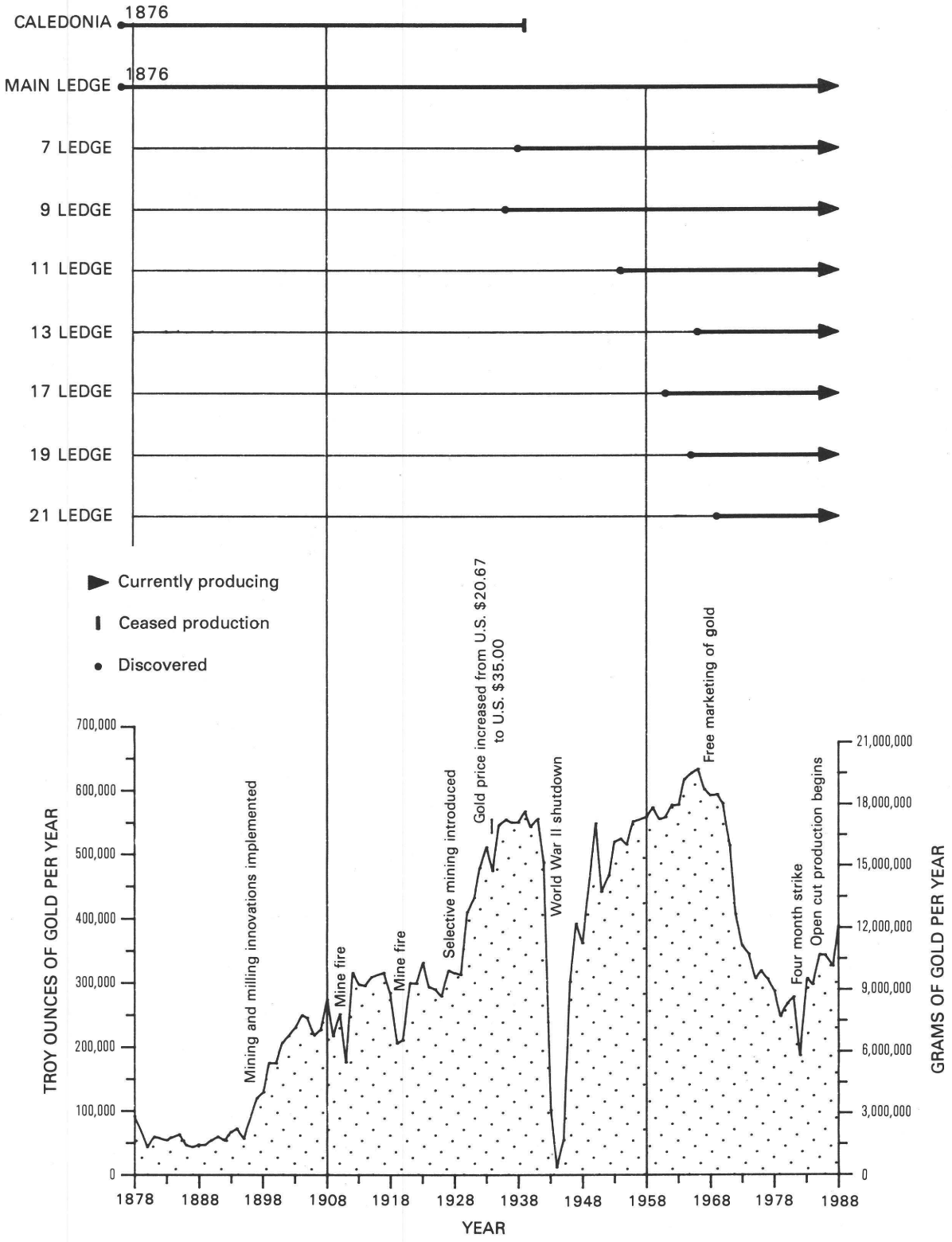

Figure J2. Annual gold production, ore-ledge discovery, and significant historical events, Homestake mine, Lead, S. Dak. Cumulative gold production through 1988 is 35,399,664 troy oz (1,101,053,449 g).

We are particularly grateful to R.E. Green and J.A. Anderson for their support, valuable comments, and guidance that made many results of this paper possible. We appreciate the valuable contributions made by the Homestake mine Geology Department consisting of G.C. Nelson, L.F. Meier, C.J. Hall, J.R. Church, J.H. Rogers, Jr., K.M. Hart, R.L. Brumbaugh, D.M. Vardiman, and G.G. Hamilton. Contributions from the Exploration Division were made by A.G. Hoffman, R.D. Nutsch, D.S. Sneyd, K.L. Triscori, R.M. Bradsky, K.E. Marlowe, T.L. Hruska, E.L. Caddey, and T.M. Rizzi. Appreciation is expressed to Ed DeWitt, D.R. Shawe, C.H. Thorman, J.A. Kerswill, J.A. Redden, and R.M. Honea for their excellent reviews and suggestions. We appreciate the support of C.G. Cunningham and the many valuable discussions with participants who attended the 1986 IUGS/UNESCO Workshop on Mineral Deposit Modeling—Gold in Precambrian Greenstone Belts, Belo Horizonte, Brazil.

GEOLOGIC SETTING

Regional Tectonic and Stratigraphic Setting

The Precambrian core of the Black Hills uplift (Darton and Paige, 1925) in western South Dakota is exposed in an elongate dome approximately 85 km long and 35 km wide (fig. J1). Rocks within the Black Hills uplift range in age from Archean to Holocene and have been described most recently by Redden and Norton (1975), DeWitt and others (1986), and Redden and French (1989). Archean granitic rocks at least 2.5 Ga are known in the Little Elk Creek (Zartman and Stern, 1967; Gosselin and others, 1988) and Bear Mountain areas (Ratté and Zartman, 1970) in South Dakota, where they constitute a minor part of the Precambrian core. Early Proterozoic sedimentary and volcanic rocks are regionally metamorphosed from greenschist to upper amphibolite facies, range in age from 2.20 to 1.87 Ga (Redden and others, 1990), and make up most of the Black Hills core. Protoliths of the Early Proterozoic metasedimentary rocks consisted of clastic sediments, black shale, iron-formation, and volcanic rocks.

The Archean and Early Proterozoic rocks were regionally deformed and metamorphosed prior to emplacement of the 1.72 Ga (Redden and others, 1990) Harney Peak Granite, the youngest Proterozoic rock in the Black Hills uplift. Structural and metamorphic studies at the Homestake mine indicate that regional metamorphism was syndeformational and characterized by a dominant north- to northwest-trending regional foliation in the Lead area (unpublished Homestake reports). The 2.5 Ga Little Elk Granite southeast of Lead is overprinted by this later northwesterly foliation (Zartman and Stern, 1967). Zartman and Stern (1967) tentatively dated this fabric at 1.84 Ga by whole-rock Rb/Sr methods. The 1.84 Ga age likely represents the timing of Lead area regional metamorphism. Contact metamorphic effects associated with the Harney Peak Granite (1.72 Ga) overprint this earlier regional metamorphic fabric in the southern Black Hills.

The Precambrian rocks of the Black Hills were uplifted and eroded by about 530 Ma. The resulting unconformity surface may represent nearly a billion years of time. During a period of relative tectonic quiescence, Paleozoic and Mesozoic sediments were deposited on this surface. The Black Hills area was uplifted again during the Laramide (65–60 Ma) into its present domal configuration. After uplift, a west-northwest-trending belt of early Tertiary (60–50 Ma) alkali-calcic to alkalic stocks, laccoliths, dikes, and sills intruded Precambrian, Paleozoic, and Mesozoic rocks of the northern Black Hills. Renewed erosion exposed the Precambrian core of the uplift. During the Oligocene, a veneer of terrestrial sediments was deposited over much of the Black Hills. Subsequent erosion produced the topography that characterizes the present-day terrain.

District Geology

The Whitewood mining district (known colloquially as the Lead district) is located on the north end of the regional uplift of the Black Hills (fig. J1), within the eroded core of an early Tertiary dome known as the Lead window (67 km^2 in area). The Tertiary Cutting stock, 1.2 km wide by 2.5 km long, is exposed near the center of the window. Emplacement of the Cutting stock, containing numerous dikes and sills, caused a swelling of the Early Proterozoic and Phanerozoic rocks forming the dome. The core of the dome contains Tertiary intrusive rocks of alkali-calcic composition, along with Early Proterozoic metasedimentary and metavolcanic rocks. Although Early Proterozoic rocks have been divided into six formations (Dodge, 1942; Noble and Harder, 1948), as shown in figure J3, only three formations important to the Homestake mine area will be discussed in detail here: (1) the Poorman Formation, comprising a lower unit of voluminous metatholeiite termed herein Yates unit (unpublished Homestake reports), overlain by an upper unit of heterogeneous, calcareous, pelitic to semipelitic phyllite; (2) the Homestake Formation, constituting essentially a carbonate-facies iron-formation; and (3) the Ellison Formation, constituting quartzite and pelitic to semipelitic phyllite. These rocks are intricately folded and metamorphosed (Noble and others, 1949). Geology of the eastern part of the Lead district is shown in figure J4; general geology of the Homestake mine is shown in cross section and plan view (2600 level) in figures J5 and J6, respectively.

Early workers who delineated and described these units appear to have tacitly assumed that the strata are upright (Gustafson, 1933; Noble and Harder, 1948). Sedimentary structures indicative of facing (younging)

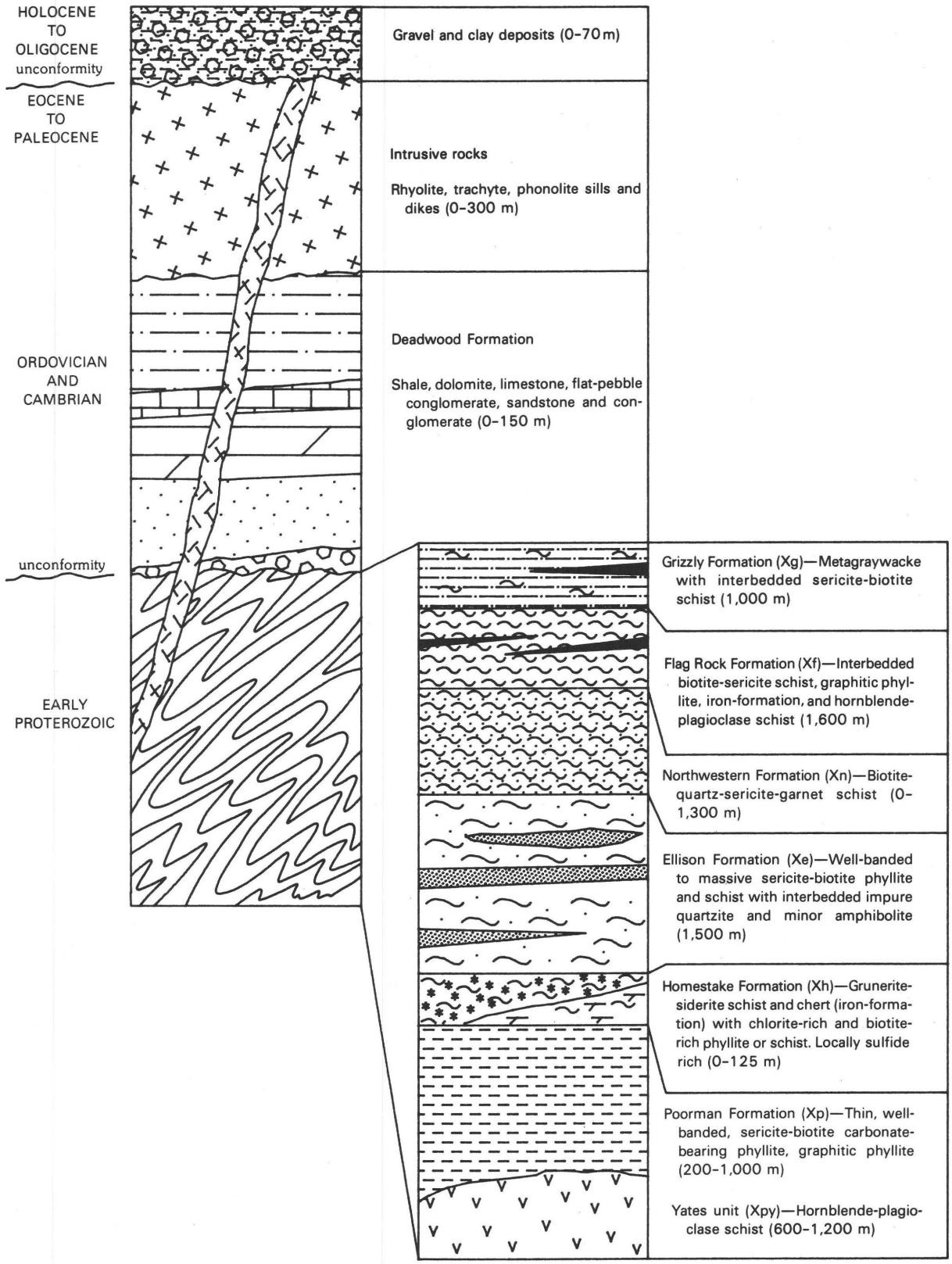

Figure J3. Schematic diagram illustrating stratigraphy (not to scale) of the Homestake area.

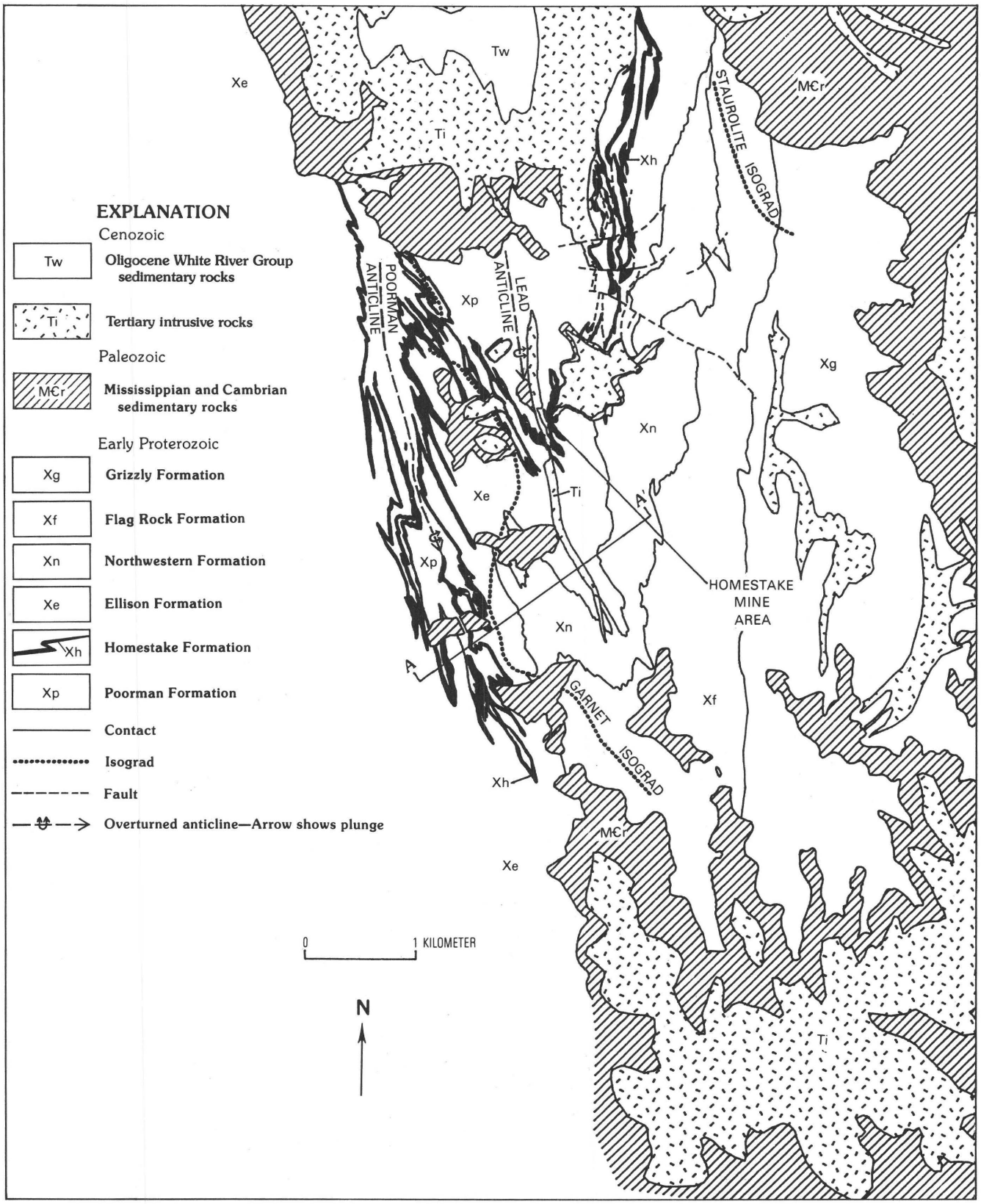

Figure J4. Generalized geologic map of the eastern part of the Lead dome of the Black Hills uplift, South Dakota. Modified from Noble and others (1949). Section *A–A'* shown in figure J5.

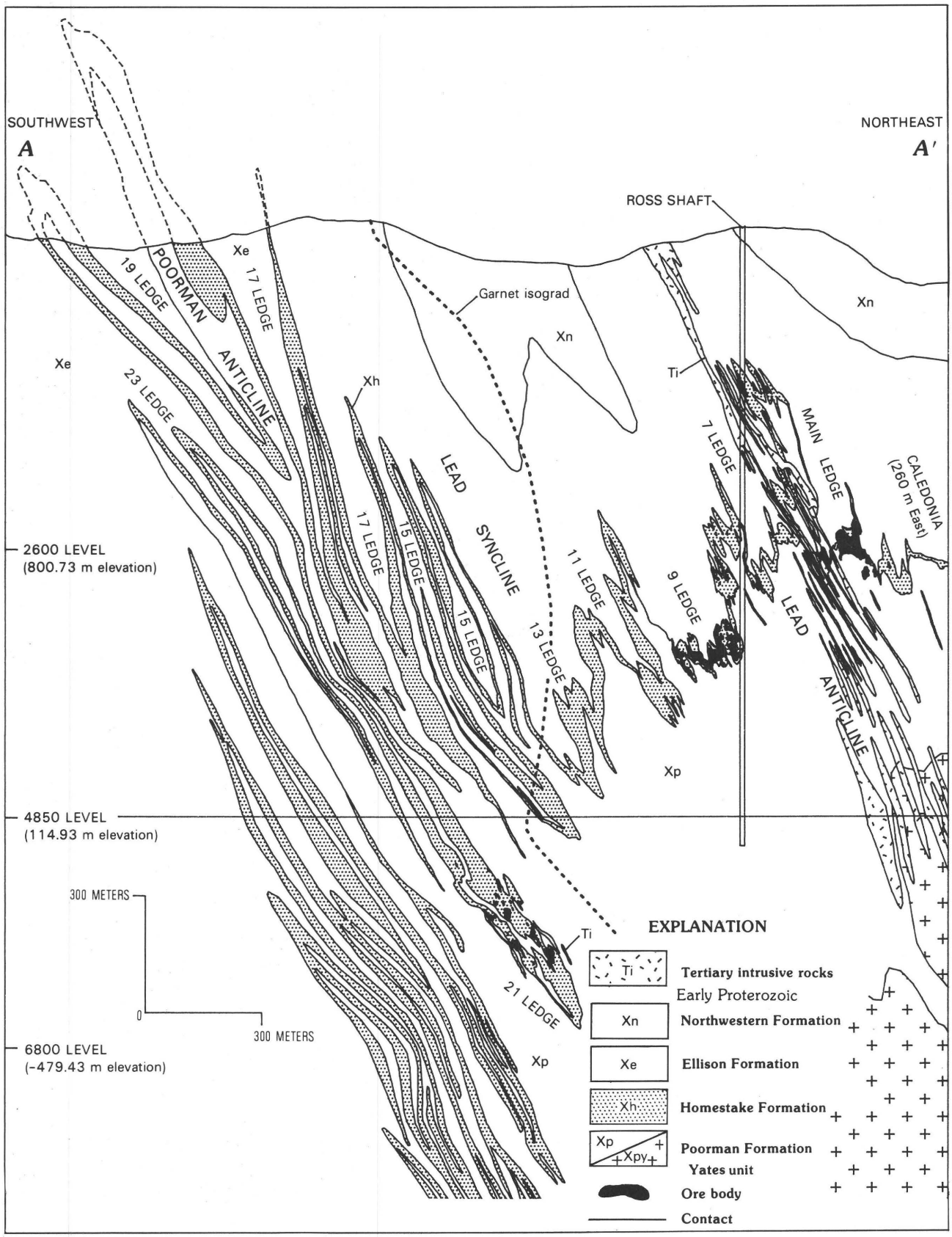

Figure J5. Generalized geologic cross section *A*–*A*′ through 33 Stope, Main Ledge Reference Line, Homestake mine. Position of section is shown in figure J4.

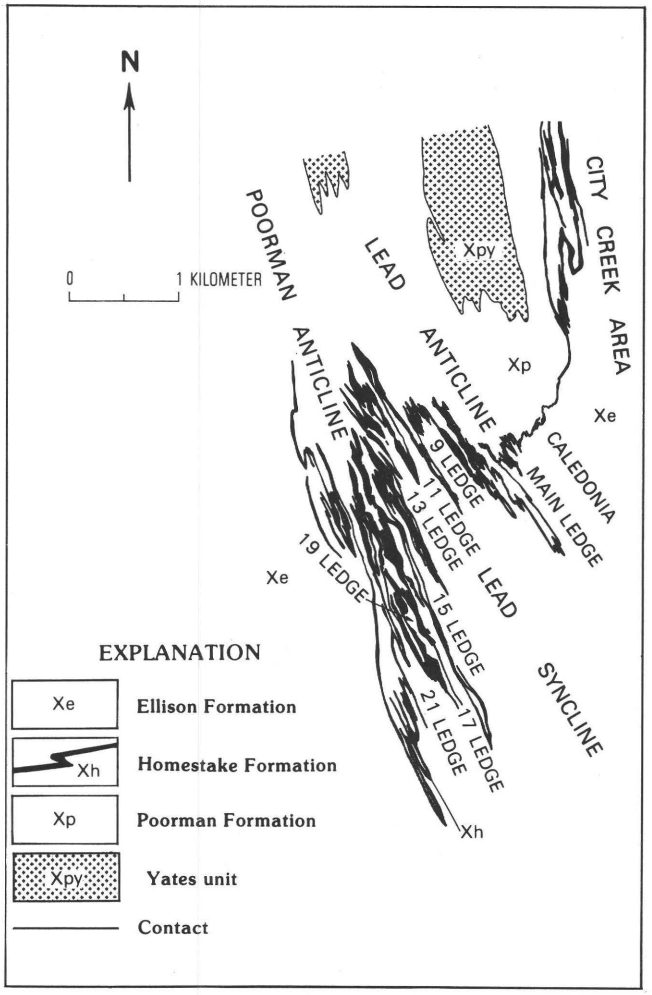

Figure J6. Geology of 2600 level of the Homestake mine, showing significant fold structures and ore ledges.

direction, however, are rarely preserved in these formations. Current workers have noted graded bedding in the Ellison Formation, but the position of this graded bedding in the limbs of isoclinal folds results in ambiguity. In recent years, unpublished facing data from interbedded and deformed basalt pillows in the Flag Rock Formation near the Homestake mine suggest that the stratigraphic sequence is indeed upright, confirming thoughts of earlier workers.

Early Proterozoic rocks of the Lead district have been metamorphosed to middle greenschist facies in the southwest and to middle amphibolite facies in the northeast (fig. J4). Regional metamorphism was centered around a thermal high located northeast of and below the current mine. This thermal high and related metamorphism developed synchronously with early ductile deformation at approximately 1.84 Ga. A sequence of prograde metamorphic isograds (first appearance of metamorphic index minerals, that is, garnet and staurolite) within these metamorphic facies has been established on the surface by mapping (Noble, 1939). The garnet isograd as mapped by Noble (1939) transects the Homestake mine at the surface near the west limb of the Lead anticline (fig. J4). An Early Proterozoic granite at Crook Mountain (Bachman and others, 1990) was penetrated by diamond drilling northeast of the mine. Contact metamorphic effects of the granite emplacement overprinted preexisting regional metamorphic fabric.

This granite, here named the Crook Mountain Granite for the prominent topographic feature 11 km northeast of the Homestake mine designated as the type area, is texturally, geochemically, and mineralogically similar to the 1.72 Ga Harney Peak Granite located in the southern Black Hills. Rb/Sr whole-rock dating is consistent with an Early Proterozoic age, but owing to disturbances indicated by rubidium loss, an absolute age could not be determined. The granite has a pegmatitic texture. The CIPW norm is corundum normative; plagioclase composition indicated by the norm is An_{10}. A peraluminous nature, low CaO content, and presence of minor coarse-grained tourmaline combined with a K:Rb ratio of 160 indicate an intermediate differentiate from a more primitive granite akin to the Harney Peak. Because the Crook Mountain Granite is known only in the subsurface in drill holes, its extent and form are poorly understood.

The Crook Mountain Granite was emplaced into rocks that were previously metamorphosed (at 1.84 Ga) to amphibolite facies. These rocks are characterized by the assemblage muscovite+ biotite+quartz+ garnet+sillimanite+ potassium feldspar. Petrographic evidence suggests that sillimanite and potassium feldspar formed during contact metamorphism near the granite, and the contact metamorphism overprinted the preexisting regional metamorphic fabric.

MINE STRATIGRAPHY AND PETROLOGY

Introduction

Early Proterozoic stratigraphic units encountered within the Homestake mine, from oldest to youngest, are the Poorman, Homestake, and Ellison Formations. Each formation comprises its own unique set of strata and environment of deposition; however, all protoliths and contact relations are not readily inferred, as they are masked by postsedimentary metamorphic, structural, and hydrothermal alteration effects. These three processes have obliterated most sedimentary structures, modified bulk chemistry to varied degrees, complicated contact relations between rock types and formations, and modified unit thicknesses. Owing to the intensity of folding and shearing of the mine rocks, calculated stratigraphic thicknesses for these units represent a tectonic average or range. Poorman and Ellison Formations average 1,500 and 400 m thick,

respectively. The Homestake Formation generally ranges from 0 to 50 m thick and locally attains 125 m in thickened fold hinges (figs. J5 and J6).

Descriptions of the Poorman, Homestake, and Ellison Formations are based largely on intensive structural, rock type, and petrographic studies completed by Homestake geologists in recent years. The Poorman Formation rock type descriptions are taken largely from T.J. Campbell (written commun., 1989).

The term "graphite" is used in the following discussions inasmuch as graphite should be the only stable carbon phase at metamorphic conditions of middle greenschist through middle amphibolite facies (Ed Duke, oral commun., Dec. 12, 1989). Graphite has been confirmed by X-ray diffraction methods on three rock samples. In addition, both grunerite and cummingtonite are found in the Homestake Formation. Their chemical compositions (fig. J7) fall along the line separating the two compositional fields as given in the classification of Leake (1978). Petrographic studies throughout the mine show that the grunerite composition is the more common of the two. Grunerite is used to represent amphiboles of the grunerite-cummingtonite series. In earlier reports on the Homestake deposit (Noble and Harder, 1948; McCarthy, 1976), sideroplesite was described as the diagnostic carbonate mineral of the Homestake Formation. However, sideroplesite is a varietal term for siderite (magnesian siderite; Roberts and others, 1990, p. 786) containing as much as 7 wt. percent magnesium. Therefore, only the term siderite is used in this report. The term sericite is used throughout most of the following rock descriptions in reference to fine-grained muscovite; no other white micas are known to exist in Lead area rocks.

An age of 1.97 Ga has been established from zircons extracted from a metatuff unit in the Ellison Formation (Redden and others, 1990). The metatuff unit lies directly above the upper contact of the Homestake Formation and provides an approximate age for the Homestake.

Poorman Formation

Hosted and Wright (1923) and Gustafson (1933) described the Poorman as dominantly a gray to black, banded to laminated, micaceous phyllite that is ankeritic and locally garnetiferous. We note that the Poorman can be subdivided into lower and upper units based on distinct differences in rock type. The lower unit of the Poorman comprises amphibolite (interpreted as tholeiitic metavolcanic deposits), and the upper unit of the Poorman consists of a carbonate-rich rock, sericite- and biotite-rich carbonate and quartz-bearing phyllite, and graphitic phyllite. Other subordinate rock types are also present.

The Poorman has generally been described as greater than 600 m thick (Hosted and Wright, 1923; Noble and Harder, 1948). However, recent diamond drilling within the mine and to the north indicates that the Poorman is generally 1,500 m thick (measured from northeast to southwest); the observed base is at the center of an isocline.

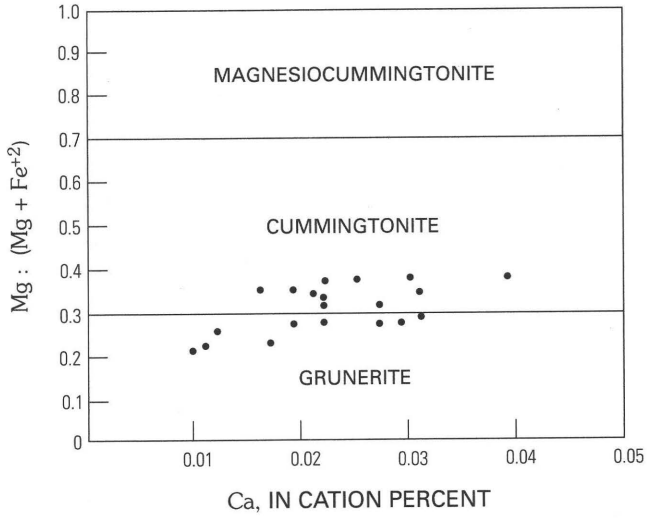

Figure J7. Plot of Mg:(Mg+Fe^{+2}) versus Ca (cation percent) for selected grunerite-cummingtonite–series amphiboles from the Homestake mine. Petrographic studies of amphiboles in iron-formation across the mine show that grunerite composition is most abundant. Diagram modified from Leake (1978); data from T.J. Campbell (unpublished Homestake report).

Lower Unit of the Poorman Formation (Yates Unit, Informal)

The lower unit of the Poorman Formation, and the lowest exposed unit, is amphibolite. Diamond drilling revealed a large volume of this unit north of the Homestake mine and in the core of the Lead anticline. The main body of the unit is hidden under Paleozoic and Tertiary cover north of Lead; it forms an elongate north-south-trending mass, and its southern margin plunges south into the mine workings where it is observed in the Yates Shaft and Number 4 Winze areas. The unit extends along strike from north to south of Lead for at least 10 km. This amphibolite unit is significant enough that we have denoted it in this report as the Yates unit, an informal unit of the Poorman Formation. It is characteristically a dark-green, massive to faintly banded, fine-grained, and moderately well lineated hornblende-plagioclase schist. Ubiquitous, 2-mm- to 2-cm-thick, white calcite bands and veinlets are also characteristic. Minerals composing the Yates unit, in decreasing order of abundance, are ferro-magnesio-hornblende, oligoclase-andesine, calcite, dolomite, ankerite, and trace amounts of ilmenite, magnetite, titanite, "leucoxene," pyrrhotite, and pyrite (table J1). Hornblende exists as 0.1- to 4-mm, subhedral, prismatic, subnematoblastic to randomly

Table J1. Modal mineral percentages in thin sections of representative Poorman Formation, Homestake mine

[Data from unpublished Homestake reports. Chemical data on table J2 are for different samples than shown here. Trace amounts of unusual minerals are not shown. HPS, hornblende-plagioclase schist (Yates unit); HBCS, hornblende-biotite-carbonate schist; CS, carbonate-rich schist; GQSP, graphitic quartz-sericite phyllite; SCQP, sericite-carbonate-quartz phyllite; BQCP, biotite-quartz-carbonate phyllite; X, <1 percent]

Rock type	Matrix quartz	Grunerite	Hornblende	Na-amphibole	Biotite	Sericite (muscovite)	Fe-chlorite	Mg-chlorite	Clinochlore	Garnet	Albite	Intermediate plagioclase	Tourmaline	Titanite or "leucoxene"	Epidote or clinozoisite	Zircon	Ilmenite or rutile	Magnetite	"Graphite"	Siderite	Ankerite	Calcite	Pyrrhotite	Arsenopyrite	Pyrite	Location
HPS	2		84									12					1	1			X					3800 level, Yates Shaft area
HPS	4		77									18		X	X		X	X			1					4100 level, Yates Shaft area
HPS	5		75									20					X				X					4850 level, Yates Shaft area
HBCS			40		40												5					15				7700 level, No. 6 Winze
CS	33				20	3													3		9	30	2			4100 level, Yates Shaft area
GQSP	38				4	18													11		12		13		9	8000 level, 21 Ledge
GQSP	38				9	28													9		15		1			8000 level,19 Ledge
GQSP	28				10	30													20		10		12			4850 level,15 Ledge
SCQP	30					27													2		40		X			4100 level, Ross Shaft area
SCQP	18					45													1		35		X		1	4850 level, 4 Winze area
SCQP	22				5	30										X			3		27		2		1	6800 level, near Main Ledge
BQCP	35				56														3		6					4850 level, 15 Ledge
BQCP	25				55			15													X		5			7700 level, 6 Shaft area

oriented grains. Anhedral, 0.05- to 0.2-mm, untwinned grains of plagioclase are interstitial to hornblende and commonly occur as poikilitic inclusions in the amphibole. In polished section, pyrrhotite is seen to replace ilmenite and magnetite, and all three are replaced by Tertiary-age pyrite. Minor to moderate amounts of biotite and chlorite are found locally.

In greenschist-facies metamorphic rocks, actinolitic hornblende and albite are present instead of ferro-magnesio-hornblende and oligoclase-andesine. Amphiboles are in 0.1- to 3-mm, subhedral to euhedral, prismatic grains. Subhedral, less than 1-mm grains of plagioclase, carbonate minerals, and accessory minerals are interstitial to hornblende. Locally, the Yates is partially to totally replaced by the assemblage chlorite-calcite-biotite.

Strata intercalated with the schist include graphitic quartz-sericite phyllite, crudely banded grunerite-bearing iron-formation without sulfides (eastern mine), coarse-grained amphibole-bearing units, and chert containing minor stilpnomelane, graphite, and pyrrhotite.

Interpretation

Hornblende-plagioclase schist, or amphibolite of the Yates unit, forms the lithologic base of the known Poorman. The protolith, as determined from geochemistry and field relations (conformable contacts, various intercalated sediments, structures interpreted as relict pillows), was a mixture of tholeiitic basalt, tuffaceous and (or) epiclastic debris, and subsequently reworked material. The chemical composition of three hornblende-plagioclase schist samples in table J2 indicates a basalt protolith. Of 18 samples plotted in figure J8, all but three fall within the compositional range of tholeiitic basalt and all but one fall within the iron tholeiite field. Three samples have higher MgO values and are tentatively interpreted as basaltic komatiite. Samples plotted on an AFM diagram (fig. J9) are entirely within the tholeiitic field, as defined by Irvine and Baragar (1971). Geochemical data for amphibolite samples of the Yates from the Lead area are similar to available data on amphibolite throughout other sectors of the Black Hills (Norby,

1984; Tapper, 1984), but differ somewhat in having slightly lower TiO_2 values.

Because tholeiitic basalt is known in both continental and oceanic settings, the hornblende-plagioclase schist samples were plotted in a KTP diagram, as used by Pearce and others (1975), to discriminate between continental and oceanic basalt (fig. J10). All but three (possibly four) samples from the Poorman Formation plot in the oceanic basalt field. Tholeiitic basalts are common features of Archean greenstone belts worldwide. Komatiite sequences, deep in the greenstone belts, are commonly cited as possible source terrains for remobilized gold in Archean gold deposits categorized as epigenetic (Groves and others, 1987). The voluminous nature of the Yates unit at Lead suggests possible greenstone affiliation of earliest Proterozoic rocks, not fully appreciated from limited surface exposures. Iron-tholeiites of the Yates, and possibly other iron-tholeiites of similar Early Proterozoic rocks in the northern Black Hills, may represent basalts related to a rifting event and development of a back-arc or possibly intracontinental basin as suggested by Redden and others (1990). The Poorman, Homestake, and Ellison metasedimentary rocks are interpreted as infillings of the northern part of the basin during Early Proterozoic (1.97 Ga) contemporaneous with a period of rift failure or allochthon development.

Upper Unit of the Poorman Formation

Carbonate-rich Schist

Directly overlying the lower unit of the Poorman (the Yates unit) is a carbonate-rich schist of the upper unit of the Poorman. Locally the carbonate-rich schist is absent or thin

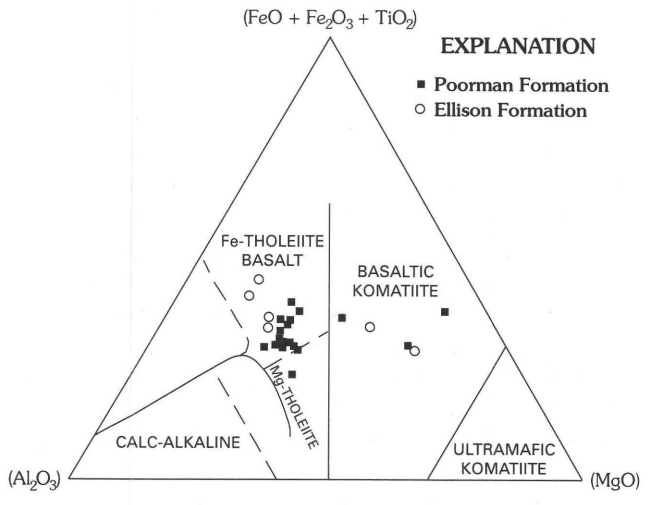

Figure J8. Jensen cation plot for mafic metavolcanic rocks of the Poorman Formation (Yates unit) and Ellison Formation, Homestake mine. Data are calculated in cation percent. Field boundaries from Jensen (1976).

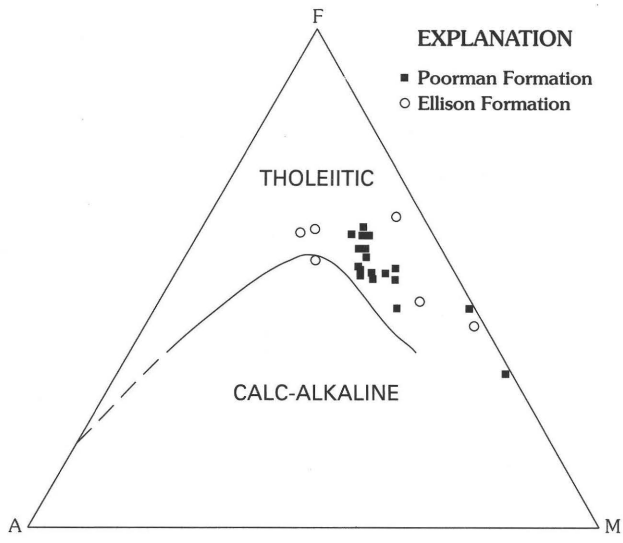

Figure J9. AFM diagram for metabasalt samples from the Poorman Formation (Yates unit) and Ellison Formation, Homestake mine. Field boundaries from Irvine and Baragar (1971).

at the Yates contact; in some areas it is interbedded with the Yates. The carbonate-rich schist is less than 1 m to 30 m thick, and is slightly graphitic, fine grained, light gray to gray, and moderately well foliated although locally massive. In places, nearly white chert layers as much as 2 cm thick are interbedded with the carbonate-rich layers. Quartz, biotite, and sericite are moderately abundant (table J1). Alternating carbonate-, sericite-, and biotite-bearing layers generally define bands that range from 3 mm to 2 cm wide. Proportions of carbonate minerals (calcite; minor dolomite and ankerite), sericite, biotite, and quartz are varied. Quartz commonly shows a high modal abundance (±30 percent).

Sericite-Carbonate-Quartz Phyllite

The dominant carbonate-rich, semipelitic rock of the upper unit of the Poorman is a sericite-carbonate-quartz phyllite (table J1), which is present wherever complete sections are cut by the mine workings. It ranges in thickness from a few tens of meters to 170 m. Its characteristics are somewhat varied, but generally the rock is very fine to fine grained with thin (<1 mm) to medium-wide (<1 cm), moderately well to very well developed alternating light-gray to very dark gray layers; these layers are graphite poor and graphite rich, respectively. Graphite content ranges from 1 to 7 percent, averaging 4 percent overall by volume of the sericite-carbonate-quartz phyllite. Thin (<1 mm), discontinuous streaks and lenses of pyrrhotite oriented parallel to layering compose 1–2 percent (by volume) of the rock; pyrite is present locally. Sericite is the dominant mineral, followed by varied proportions of carbonate minerals, quartz, and biotite. Carbonate minerals are calcite, dolomite, and ankerite; two carbonates may be present in

Table J2. Major and minor element geochemistry of Poorman Formation units, Homestake mine

[Unpublished Homestake data. Chemical data are for samples different from those shown on table J1. All values in weight percent; samples analyzed by atomic absorption and ICP methods, Skyline Labs, Wheatridge, Colo. CO_2 determined by gas evolution. Leaders (--), not determined). HPS, hornblende-plagioclase schist; CS, carbonate-rich schist; HBCS, hornblende-biotite-carbonate schist; GQSP, graphite-quartz-sericite phyllite; SCQP, sericite-carbonate-quartz phyllite; BQCP, biotite-quartz-carbonate phyllite]

Rock type	SiO_2	Al_2O_3	Fe_2O_3	FeO	MgO	CaO	Na_2O	K_2O	MnO	TiO_2	P_2O_5	elemental S(tot)	CO_2
HPS	48.90	13.10	1.30	10.30	6.80	10.30	2.40	0.54	0.210	0.93	0.06	0.37	0.68
HPS	49.30	14.40	3.15	10.20	6.90	10.70	2.70	.22	.210	1.00	.07	<0.05	.60
HPS	51.20	13.00	2.10	11.50	6.10	8.80	2.40	.32	.230	1.30	.09	.58	.45
CS	46.30	9.70	2.96	5.50	6.40	10.20	1.20	1.90	.170	.43	.26	1.70	7.10
HBCS	36.40	10.90	2.04	10.00	3.70	16.30	2.00	1.80	.220	2.50	.55	<0.02	11.40
GQSP	45.00	7.60	12.20	--	3.60	4.50	.15	2.70	.130	.24	.02	7.20	6.39
SCQP	46.80	7.50	.73	2.30	6.60	11.60	.56	3.00	.040	.11	--	2.20	8.80
BQCP	63.30	13.40	1.21	7.30	2.90	.13	.50	5.10	.078	.42	.04	.28	1.37

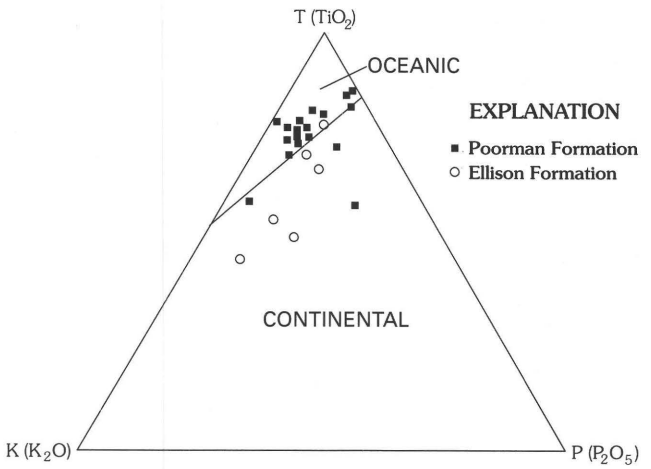

Figure J10. KTP diagram for metabasalt samples from the Poorman Formation (Yates unit) and Ellison Formation, Homestake mine. Field boundary from Pearce and others (1975).

the same sample. Chlorite is present locally in trace amounts; other trace accessories include plagioclase, zircon, titanite, and clinochlore (variety of leuchtenbergite). Garnet is sparsely distributed, and is found mostly in the eastern ledges.

Biotite-Quartz-Carbonate Phyllite

The biotite-quartz-carbonate phyllite (table J1), commonly found close to Homestake Formation, is characterized by a high biotite content, and varied proportions of carbonate minerals, sericite, and quartz. It ranges in thickness from a few meters to 30 m. Like the sericite-carbonate-quartz phyllite, the rock is well foliated and thin (1 mm) bedded to medium (1 cm) bedded, with alternating, well-developed brown-gray and dark-gray layers; the difference in color is due to variations in graphite concentrations. Vein quartz and chert bands less than 1 cm thick are locally present. Trace to minor amounts of chlorite are found in some areas, and the amount of pyrrhotite streaks ranges from a trace to 2 percent (by volume). Chlorite concentration generally increases close to the Homestake Formation. Minor amounts of garnet and tremolite are locally present, the former predominantly in the eastern ledges.

Graphitic Quartz-Sericite Phyllite

The graphitic quartz-sericite phyllite (table J1) generally is found in the upper part of the Poorman beneath the Homestake Formation, but it is found interbedded with other Poorman units as well. This phyllite, colloquially termed "graphitic phyllite," is found as layers from less than 1 m thick to sequences more than 30 m thick, especially in the western ledges. In highly sheared areas of the mine, graphitic phyllite occurs as transgressive zones.

Overall, the graphitic phyllite is dark gray to black, and very fine grained, and it exhibits moderately well developed banding that is locally disrupted. A lepidoblastic texture is observed in thin section; however, foliation is generally obscured in hand specimen by the high graphite content. The rock contains quartz as grains interstitial to the graphite-sericite-biotite-ankerite matrix. In higher concentrations, graphite imparts a greasy feel to the rock.

Sulfide concentration ranges from a trace to more than 60 percent (by volume); pyrrhotite and pyrite are present and pyrrhotite is dominant. Pyrrhotite is in two forms, streaks and blebs. The streaky variety is present as less than 0.1- to 5-mm-thick and 1-mm- to 2-cm-long aggregates that are oriented parallel or subparallel to foliation. Irregular blebs or masses of pyrrhotite are also common and range from 2 mm to several centimeters thick. Pyrrhotite blebs locally contain fragments of quartz veins and enclosing phyllite. Pyrrhotite blebs replace streaks and are associated with quartz veins. The pyrrhotite-rich zones containing irregular blebs are commonly anomalous in gold; values reach as much as 0.5 g/t. Pyrite is partly intergrown with and partly replaces both varieties of pyrrhotite, generally occurring as euhedral, 0.5- to 1-cm cubes.

Interpretation

The upper unit of the Poorman is a carbonate-rich metasedimentary rock dominated by calcite and ankerite, and containing a significant pelitic component along with minor dolomite (tables J1 and J2). Carbonate is abundant in sericite-carbonate-quartz phyllite and graphitic quartz-sericite phyllite as well as in the carbonate-rich schist. Biotite-quartz-carbonate phyllite, and perhaps only local parts of it, may be the only true pelitic rock in the Poorman, containing 13.4 wt. percent Al_2O_3 (table J2). Original detrital components were very fine grained (<0.02 mm) silt consisting of clay, mica, and quartz grains. The detritus was incorporated with varied amounts of chemical precipitates in the form of calcitic to ankeritic carbonate and chert in addition to tuffaceous material locally.

The lack of coarse clastics, the presence of abundant carbonate, and the rhythmic thinly layered to laminated character of the rock indicate a low-energy depositional environment with very limited current agitation for the sediment. Either a deep marine abyssal plain or a restricted shallow to intermediate-depth oceanic basin is a good possibility. We favor the shallow to intermediate-depth basin environment largely because of ubiquitous graphite found in the Poorman and because some of the graphite manifests itself in thin (<1 mm) laminae possibly representing algal mats. Much of the graphite, however, probably represents a combination of bacteria and algal organisms.

Alternating graphite-rich and graphite-poor layers characteristic of most strata composing the upper unit of the Poorman may represent seasonal fluctuations that were pervasive up until deposition of the Homestake Formation. Rare elliptical structures found locally in graphite-rich layers of some phyllites may represent sporelike structures similar to those described by Bondesen (1970) in the 2.0 Ga Early Proterozoic rocks in the Graenseland area of southwest Greenland.

The abundance of microorganisms in the Poorman, evident from the pervasive graphite, is not characteristic of abyssal plain environments. Detrital quartz grains (<0.02 mm) are ubiquitous in the upper unit of the Poorman, comprising anywhere from 5 to 25 modal percent. Detrital quartz grains are not transported for long distances as a suspended load into the deep ocean, especially not in the abundances just given. In addition, the overlying Ellison Formation is currently interpreted as a deltaic deposit (at least in the eastern ledges), an unlikely succession if the Poorman is interpreted as an oceanic abyssal plain sediment.

The pelitic component of the original Poorman is represented in the equivalent metamorphosed rocks by the presence of layer silicates. Probably, clays and extremely fine grained micas, along with detrital quartz grains, were transported basinward by terrestrial drainages emptying into the basin. Upon mixing with saline oceanic waters, the clay fraction flocculated and deposited. This fine detritus was deposited concomitantly with chemical precipitates forming on the basin floor.

Bottom conditions in the basin must have been reducing and euxinic, given the ubiquitous presence of graphite and pyrrhotite streaks. The occurrence of graphite and its coexistence with carbonate indicate that fO_2 was low and that conditions were close to the C-CO_2 buffer. Pyrrhotite streaks are interpreted as sedimentary owing to their mode of occurrence, widespread distribution, crosscutting relations with younger pyrrhotite, and lack of association with quartz veins or gold. Their abundance thus suggests that fS_2 was relatively high throughout most of the basin. The presence of chert also indicates bottom conditions characterized by low Eh, and relatively low pH and temperature. The majority of the sedimentary sulfides (pyrrhotite streaks with minor pyrite) probably formed as a result of bacteriogenic reduction of seawater sulfate, as suggested by sulfur isotope analyses (William Hallager and Peter Holland, unpublished Homestake reports). Organic material obviously was present in metasedimentary rocks of the upper unit of the Poorman throughout sedimentation. The organic material may have had a significant influence on processes governing the formation of chemical precipitates. If the organisms were photosynthetic, they might have contributed significantly to the development of an oxygenic atmosphere (for example, Roscoe, 1969, p. 83) and possibly to the development of iron-formation.

The restricted nature of the Poorman sedimentary basin inferred from preserved structures and from the evidence of the physico-chemical conditions of the metasedimentary rocks may have been due to peripheral carbonate shoals. The concept of such restriction was introduced by Button (1976) for chemical sediments, including iron-formation, comprising the Olifants River Group of the Transvaal Basin, South Africa. As in the Transvaal example, the restrictive barrier in the Poorman basin may have been composed of stromatolites or of clastic carbonate. The barrier might also be attributed to a combination of chemical precipitation of carbonate and

growth of stromatolites. That restrictive barriers affected iron-formation deposition was suggested long ago by Woolnough (1941), James (1954), and Goodwin (1956). James (1954) also introduced the concept of restriction caused by anticlinal warps in a basin floor, the scale of which might vary. Slight compression at deformation in this particular Early Proterozoic rifting environment may have been responsible for production of a warp in the development of a restricted basin. Such compression seems likely because basin closure directions were dominated by east-west compressive forces as noted by Redden and others (1990).

During prograde metamorphism some carbonaceous material and sulfur were remobilized into shear zones and structural traps, which explains the structurally transgressive character of some occurrences of graphitic phyllite. The source of iron in the Poorman sediments may have been (1) a volcanic component already present within the basin, and (2) paleo-hot spring activity on the seafloor providing not only iron, but possibly silica and carbonate as well.

Homestake Formation

Mineralogy of the Homestake Formation reflects more the metamorphic intensity and extent of devolatilization reactions (that is, amount of H_2O and CO_2) that affected the rocks than does mineralogy of the underlying Poorman or overlying Ellison Formations. For example, in the Homestake in upper greenschist facies, siderite phyllite is dominant, whereas in lower amphibolite facies, grunerite schist is dominant. Chloritic schist is important as a "transitional" phase into Ellison or Poorman Formations and locally occurs as discontinuous lenses in the Homestake. Prior to metamorphism, the Homestake may have been 20–30 m thick (Noble and Harder, 1948), although present thicknesses range from zero to 125 m (the latter in thickened fold hinges). Thickness contrast is attributed to intense deformation (differential strain) and metamorphism (devolatilization).

Overall, the Homestake is a sequence of carbonate-dominated and (or) silicate-dominated rocks, depending upon location in the mine. The formation is locally massive to thin bedded, marked by abrupt stratigraphic changes. Mixtures of iron-carbonate and iron-silicate minerals characterize the central mine area. End members of exclusively iron-carbonate and iron-silicate exist in the extreme western and eastern mine areas, respectively. Thin chert beds are commonly interlayered with carbonate- and silicate-dominated rocks. Layering (commonly called "banding") in the Homestake is characteristic in the western ledges but less common in the eastern ledges. In the eastern ledges the Homestake is largely massive; layering is obliterated (local islands preserved) by grunerite growth that accompanied increasing metamorphic intensity. In the western ledges, layering is well developed, consisting of alternating thin laminae of chert, siderite, and biotite, locally with interlayered thin chlorite, sericite, and pyrrhotite.

Siderite-Dominant Phyllite

Homestake Formation in which siderite is relatively more abundant than grunerite contains siderite, quartz, biotite, and locally chlorite as major minerals along with varied but subordinate amounts of ankerite and graphite (table J3). Siderite occurs in two morphologically distinct varieties that are probably related to different events and modes of formation. The first siderite type is very fine grained and is found in a heterogranular polygonal texture with quartz; it characterizes the siderite-dominant phyllite. The second type occurs as coarse-grained, postkinematic porphyroblasts that crosscut earlier formed minerals; its development was related to gold mineralization. Much of the Homestake in the upper eastern and middle to upper western parts of the mine is dominated by siderite-dominant phyllite. Minor amounts of grunerite, stilpnomelane, muscovite, and almandine garnet may occur in the phyllite.

Siderite-dominant rocks are olive green to gray green, with layers moderately well to very well developed, alternating between 1–5-mm-thick, graphite-rich layers and millimeter- to centimeter-thick, graphite-poor or graphite-free layers. Graphite-poor layers are biotite rich and (or) chlorite rich. Alternating carbonate-quartz- and biotite-chlorite-rich layers also constitute layering. Locally, layering is disrupted and exhibits diagonal fractures filled by carbonate minerals (siderite and (or) ankerite) and quartz. Chert beds are ubiquitous and varied in thickness. Locally, chert layering is common at the lower contact with the Poorman and rare at the upper contact with the Ellison.

Grunerite-Dominant Schist

Iron-formation in which grunerite dominates over siderite ranges widely in texture and mode (table J3). The most typical example is a variably layered, olive-green, fine- to coarse-grained, grunerite+biotite+quartz±siderite± chlorite schist. Increasing metamorphic grade brings a concomitant reduction in siderite and quartz content. An end-member rock type typical of lower amphibolite facies metamorphic grade is a grunerite-biotite-quartz schist. This rock type dominates the deep eastern part of the mine and is fine to coarse grained, dark green, massive to thick banded with common minor chert. The grunerite is in 2-mm to 2-cm subradial aggregates that lack preferred orientation and generate a very competent rock. Hornblende has been observed petrographically as a trace component in the deep eastern part of the mine. Overall, hornblende in the Homestake is rare. Almandine garnet and chlorite are important constituents locally.

Table J3. Modal mineral percentages in thin sections of representative Homestake Formation, Homestake mine

[Data from unpublished Homestake reports. Chemical data on table J4 are for different samples than shown here. Trace amounts of unusual minerals are not shown. GDS, grunerite-dominant schist; SDP, siderite-dominant phyllite; CQS, chlorite-quartz schist; X, <1 percent; *, equivalent mine level encountered in drill core. No visible gold present]

Rock type	Matrix quartz	Grunerite	Hornblende	Na-amphibole	Biotite	Sericite (muscovite)	Fe-chlorite	Mg-chlorite	Clinochlore	Garnet	Albite	Intermediate plagioclase	Tourmaline	Titanite or "leucoxene"	Epidote or clinozoisite	Zircon	Ilmenite or rutile	Magnetite	"Graphite"	Siderite	Ankerite	Calcite	Pyrrhotite	Arsenopyrite	Pyrite	Location
GDS	4	51			34					5									4				2			4550 level, Main Ledge
GDS	30	56			5						2								3	3			1			4550 level, 9 Ledge
GDS	2	78			6		3			3	6								2							6800 level, 21 Ledge
GDS	4	38			13		36												1	8						6800 level, 21 Ledge
GDS (ore)		40			5				5	40													5	5		7200 level, 9 Ledge*
GDS	8	75		8	8					1											X		X			8300 level, Pierce Structure (Main Ledge)*
SDP (ore)	6				4		4				6								4	72			4			800 level, 7 Ledge
SDP	24				10		4				X								2	60						1700 level, 7 Ledge
SDP (ore)							24			2									13	50			11			6650 level, 9 Ledge
SDP	18						18												4	60			X			5750 level, 17 Ledge
SDP	28				2		24												2	41			3			5900 level, 17 Ledge
SDP (ore)	26						20												6	42			6			6800 level, 21 Ledge
CQS	38				15		36			16	1								2	11			X			800 level, 7 Ledge
CQS	14						49													12			6			5600 level, 11 Ledge
CQS	26				4		37													33						6950 level, 21 Ledge

Miscellaneous Iron-Formation Rock Types

Other rocks interbedded with and constituting iron-formation include biotite-quartz-siderite phyllite or schist and cherty chlorite-quartz-siderite (CQS, table J3) phyllite. The biotite-quartz-siderite phyllite or schist is found locally as a distinct unit within the Homestake in upper greenschist facies rocks, and the cherty chlorite-quartz-siderite phyllite constitutes a significant part of the Homestake in the west limb of the Poorman anticline. Cherty chlorite-quartz-siderite phyllite also is found within the Poorman Formation in the core of the Lead anticline. It represents either structurally displaced Homestake or a distinct iron-formation horizon in the Poorman that was not subjected to higher grades of metamorphism. These units range from absent to 10 m thick.

Chloritic Biotite-Sericite-Quartz-Carbonate Phyllite (Transitional Homestake Formation)

Chloritic biotite-sericite-quartz-carbonate phyllite, averaging 1 m thick, is present locally at the upper and lower contacts of the Homestake, grading into Ellison or Poorman, respectively. Conventionally, this phyllite has been assigned to the Homestake, owing to the presence of chlorite, although it is transitional with either underlying Poorman or overlying Ellison Formations. The rock is very fine to fine grained, well foliated, and moderately well to well layered, with alternating gray, greenish-gray, and dark-gray layers. Gray layers are sericite and carbonate rich; greenish-gray layers are chloritic and contain biotite with trace amounts of siderite and (or) ankerite. As in other rocks, dark-gray layers are graphitic. Garnet is recognized locally, and chert content is varied.

Table J4. Major, minor, and trace element geochemistry of barren Homestake Formation units, Homestake mine

[Unpublished Homestake data. Chemical data are for samples different from those shown on table J3. Trace element values in parts per million (ppm), gold values in parts per billion (ppb), major and minor element values in weight percent. Samples analyzed by atomic absorption and ICP methods, Skyline Labs, Wheatridge, Colo. CO_2 determined by gas evolution. GDP, grunerite-dominant phyllite; SDP, siderite-dominant phyllite]

	Major and minor elements													Trace elements				
														ppb	ppm			
Rock type	SiO_2	Al_2O_3	Fe_2O_3	FeO	MgO	CaO	Na_2O	K_2O	MnO	TiO_2	P_2O_5	elemental S(tot)	CO_2	Au	Ag	Cu	Pb	Zn
GDP	52.60	2.60	9.35	17.70	4.90	3.60	2.00	1.10	1.180	0.12	0.22	2.30	1.90	10	0.4	55	<5	15
GDP	54.60	4.00	7.19	23.50	4.30	.17	.09	.71	.300	.15	.05	<0.02	.30	8	<0.02	<5	<5	20
GDP	48.50	2.60	8.13	25.10	5.90	1.40	.65	.77	1.550	.15	.16	13.50	1.00	51	.6	50	10	25
GDP	48.80	4.40	3.50	24.60	6.10	1.20	.06	1.30	.720	.38	.37	.08	1.04	100	<0.2	90	5	25
SDP	48.70	3.20	3.96	23.70	4.40	.79	.05	.57	.410	.11	.19	<0.02	.73	14	<0.2	100	<5	20
SDP	37.30	5.10	28.14	23.90	6.20	1.50	.13	.63	.630	.15	.33	.08	1.10	30	<0.2	20	<5	60
SDP	48.50	4.80	1.69	24.20	6.00	1.40	.10	.96	.380	.37	.15	.35	.59	18	<0.2	25	<5	35
SDP	48.70	5.90	1.90	27.00	6.50	.45	.07	1.20	.620	.48	.15	.02	.66	21	<0.2	70	10	40

Interpretation

We interpret the iron-formation in the Homestake to represent a carbonate-facies chemical sediment (table J4) precipitated in a low-energy restricted basin, as discussed previously and hypothesized by Bidgood (1977). The iron source, as with other iron-formations worldwide, is enigmatic. Rye and Rye (1974) suggested a hot spring model or seafloor exhalative origin for the Homestake based on oxygen and sulfur isotope data. We believe that the onset of volcanic exhalations or hot spring activity influenced precipitation of iron and may have supplied a portion thereof. We suggest that iron probably accumulated under reducing conditions in basin waters, having been derived largely from deep weathering of iron-rich rocks in an adjacent, low-lying land mass. Ferrous iron concentration increased to saturation, triggering precipitation. We propose that iron precipitation was induced by volcanic exhalative activity and evaporative processes that caused changes in physico-chemical conditions in the basin.

Siderite, like other carbonates, is more soluble under high CO_2 activity, attributed to low temperatures (Krauskopf, 1967) and the presence of organic matter. It follows that siderite solubility is reduced with decreased activity of CO_2 by warming, by increase in pH, or by photosynthetic activity of microorganisms, causing precipitation. All three mechanisms could have operated during deposition of the iron-formation. Discharging vents on the seafloor influence heat and pH variation in basin waters or brines. Photosynthetic microorganisms, probably neritopelagic, may have been present in the basin water and could have influenced siderite precipitation. Microorganisms use iron to obtain energy, and they serve as catalysts to initiate chemical reactions. Warming and evaporation would heat basinal waters, causing iron precipitation. A portion of the iron-formation components in the Homestake may have originated by a replacement process (sideritization) analogous to dolomitization, whereby siderite replaced calcite- or dolomite-bearing chemical sediments, as postulated by Button (1976) for parts of the Malmani Dolomite in the Transvaal. Transitional Homestake Formation (the chloritic biotite-sericite-quartz-carbonate phyllite) may represent a metamorphic reequilibration product of iron-formation and semipelitic rocks; metamorphic fluids channeled through rock strata of differing competencies promoted chemical reactions between two chemically diverse rock types.

Ellison Formation

The Ellison Formation consists of phyllite, quartz-mica schist, and quartzite. Noble and Harder (1948) subdivided the Ellison into upper, middle, and lower "members" on the basis of surface mapping; however, rocks of the formation are intermixed, and such distinctions within the Homestake mine are not practical. Ellison thickness was given as 1,500 m (Noble and Harder, 1948), although indicated thicknesses in the mine area generally do not exceed 400 m. Apparent Ellison thickness in the western part of the district approaches 1,500 m, but owing to stratigraphic and structural ambiguities the 1,500-m value is not considered an original stratigraphic thickness.

Quartzite

Quartzite (table J5) is fine grained, gray to dark gray, massive to faintly bedded, and moderately well sorted, containing well-rounded grains. Graded bedding and contained rock fragments are rare. Foliation is poorly

discernible owing to the paucity of layered silicates. Most quartzite units are impure and contain subordinate sericite, biotite, and plagioclase. Based on the classification of McBride (1963) and Folk (1968), Ellison quartzite is best termed a subarkose, or rarely a quartz arenite. Minor accessories include microcline, ankerite, titanite, tourmaline, ilmenite, rutile, xenotime and (or) monazite, pyrite, and pyrrhotite streaks. In cross section, quartzite units are lenticular bodies. Individual strata are 0.3 to 4 m thick, and composite beds are several tens of meters thick. Long-axis dimensions are not precisely known, although a quartzite bed west of the mine extends for at least 1,000 m along strike. Lenticular quartzites are interbedded with other Ellison rocks.

Quartz-Mica Schist

Quartz-mica schist is mineralogically similar to quartzite but contains more mica and garnet, particularly in rocks of the garnet grade of metamorphism. The quartz-mica schist is moderately well foliated; layering is poorly developed and locally absent. Layers where present range in thickness from 1–2 cm to several centimeters. Color varies from light gray to tan to pale brown, depending on relative abundance of sericite and biotite. Quartz-mica schist is generally dominated by sericite; locally, biotite is abundant. Individual schist units are characteristically more extensive (laterally and vertically) than quartzite. They are locally interbedded with quartzite and mica-dominated phyllites.

Sericite-Quartz Phyllite

Sericite-quartz phyllite is very fine to fine grained, light gray to gray, and well foliated, and has 1-cm- to greater than 5-cm-thick layers that are poorly developed (table J5). Sericite-quartz phyllite is discontinuous, is commonly interbedded with quartzite, and is as much as 30 m thick. Sericite content ranges from 35 to 70 percent (by volume); quartz, ankerite, and biotite are subordinate. Trace to minor amounts of garnet, graphite, tourmaline, and chlorite exist locally.

Biotite-Quartz Phyllite

The biotite-quartz phyllite is very fine to fine grained, light brown, thick bedded to massive, and contains 1–3-mm-thick, local graphite-bearing layers (table J5). This unit is discontinuous and is as much as 100 m thick. Interstitial ankerite is minor but ubiquitous. Sericite and tourmaline are locally present. Content of 1–4-mm, anhedral to euhedral, pink to red, almandine or spessartitic almandine garnet ranges from a trace to more than 15 percent (by volume). Carbonate minerals are generally a minor component but locally may constitute a significant part of the rock. Sulfide minerals (pyrrhotite streaks, pyrite) are generally absent, or present in trace amounts.

Amphibolite

Amphibolite (table J5) occurs as discordant to concordant, fine- to coarse-grained, dikelike bodies and as concordant, fine-grained bodies interbedded with other rocks. These units are lenticular and locally are 65 m thick. The coarse-grained discordant bodies are interpreted as metagabbro (Dodge, 1942). Concordant, fine-grained, interbedded amphibolite strongly resembles the Yates unit of the Poorman. Chemical analysis of one representative sample is given in table J6. Contact relations and textures of the concordant units suggest probable altered mafic volcanic rocks (figs. J8, J9, and J10).

Interpretation

Protoliths of the phyllite, schist, and quartzite of the Ellison Formation have been interpreted as shale, impure siltstone, and sandstone, respectively (DeWitt and others, 1986). Redden and others (1990) interpreted the Ellison as a shallow-water shelf quartzite correlated to deeper water turbidite and quartzite deposits in the Rochford area. Based on recent detailed underground mapping, key surface outcrops, and petrography, we interpret the majority of Ellison in the mine area as a deltaic sequence. Specifically, the rock types and their distribution probably represent a lobate or constructive-type delta (Fisher and others, 1969) in which fluvial processes dominated. Selected chemical analyses for major rock types appear in table J6.

Pelitic to semipelitic and psammitic Ellison strata are characterized by their medium to thick, poorly developed to moderately well developed bedding, and some massive quartzite and quartz-mica schist units. Relict sedimentary structures preserved in lenticular quartzite units include moderately well rounded to well-rounded grains exhibiting moderate to good sorting, graded bedding, and rare cross-bedding; local scour surfaces are developed in underlying phyllite. Most original sedimentary structures, however, have been destroyed by metamorphism and structural deformation. Conglomerate beds in the Ellison are rare.

Ellison rock types and their geometric distribution can be correlated to specific deltaic environments, as discussed in Broussard (1975). Graphite-rich phyllites may be ascribed to marsh, backswamp, and meander-loop channel environments of delta-plain facies. Associated sericite- and biotite-rich quartz-phyllites may represent levee and tidal-flat deposits in the same facies. Carbonate-bearing phyllites in proximity to these rock types may have been evaporite deposits within tidal flats. Quartz-mica schist units of large areal extent are interpreted as delta-front facies. Extensive sericite- and biotite-rich quartz phyllites may represent prodelta and offshore marine facies.

Table J5. Modal mineral percentages in thin sections of representative Ellison Formation, Homestake mine

[Data from unpublished Homestake reports. Chemical data on table J6 are for samples different from those shown here. Trace amounts of unusual minerals are not shown. SQP, sericite-quartz phyllite; BQP, biotite-quartz phyllite; QMS, quartz-mica schist; X, <1 percent]

Rock type	Matrix quartz	Grunerite	Hornblende	Na-amphibole	Biotite	Sericite (muscovite)	Fe-chlorite	Mg-chlorite	Clinochlore	Garnet	Albite	Intermediate plagioclase	Tourmaline	Titanite or "leucoxene"	Epidote or clinozoisite	Zircon	Ilmenite or rutile	Magnetite	"Graphite"	Siderite	Ankerite	Calcite	Pyrrhotite	Arsenopyrite	Pyrite	Location
Quartzite	83				3	5										X			3			3				4550 level, 11 Ledge
Quartzite	95					X						X				X			X		X	X			X	6500 level, Main Ledge
Quartzite	91				X	5				X							X		X				X			6800 level, 9 Ledge
QMS	60				20	15				4		1	X						X		X		X			5900 level, 13 Ledge
SQP	30				X	65				5			X	X									X			2600 level, east of Yates Shaft
SQP	30				20	50																				6800 level, Main Ledge
SQP	12				15	70																	3			6800 level, 13 Ledge
SQP	35					35															30		X			8000 level, 15 Ledge
BQP	45				45	10		X		X										X	X		X			2600 level, east of Yates Shaft
BQP	23				30														3		35		10			6500 level, Main Ledge
BQP	40				45					15											X					6800 level, 9 Ledge
Amphibolite			72		4							20		X	3		X									Drill hole north of Lead, S. Dak.

Table J6. Major and minor element geochemistry of Ellison Formation units, Homestake mine

[Unpublished Homestake data. Chemical data are for samples different from those shown on table J5. All values in weight percent. Samples analyzed by atomic absorption and ICP methods, Skyline Labs, Wheatridge, Colo. CO_2 determined by gas evolution. SQP, sericite-quartz phyllite; BQP, biotite-quartz phyllite]

Rock type	SiO_2	Al_2O_3	Fe_2O_3	FeO	MgO	CaO	Na_2O	K_2O	MnO	TiO_2	P_2O_5	elemental S (tot)	CO_2
Quartzite	86.30	5.30	1.13	1.30	0.69	0.59	0.06	1.90	0.065	0.13	0.02	0.39	0.75
SQP	58.90	16.20	1.84	6.70	2.20	.19	.59	4.70	.340	.58	.04	1.10	.60
BQP	60.90	12.30	1.13	5.80	3.40	3.10	.68	4.10	.940	.47	.05	.03	1.50
Amphibolite	40.20	12.70	1.07	11.10	4.70	9.40	2.80	1.90	.180	2.00	.42	.32	6.00

Thin-banded to laminated phyllites of the Ellison may in part be offshore marine facies developed on and above the Homestake upper contact and are difficult to distinguish from similar phyllites in the Poorman at its upper contact with the Homestake. Lenticular quartzite units distributed throughout the Ellison, especially within quartz-mica schist units, are believed to represent bar finger complexes of delta-plain and delta-front facies.

Deposition of the Ellison deltaic sequence was probably initiated by major orogenic activity well inside the adjacent landmass, the probable source of the clastic debris. Progradation of the delta complex consisted of slow inundation of at least part of the restricted basin with clastic material. Influx of clastics may have served to extinguish exhalative activity on the basin floor and terminate production of iron-formation. Thus the youngest uppermost

Poorman may be the time equivalent of different parts of the Homestake, or of the oldest lowermost Ellison.

METAMORPHISM OF THE MINE ROCKS

Upper greenschist and lower amphibolite facies rocks of a typical Barrovian sequence (Tilley, 1925) are encountered in the Homestake mine area and related to an Early Proterozoic (1.84 Ga) regional dynamothermal metamorphic event that preceded the emplacement of the (probably) 1.72 Ga Crook Mountain Granite (Bachman and others, 1990). Typical metamorphic assemblages of the principal minerals in the stratigraphic units are listed in tables J1, J3, and J5, and depicted in A′KF, ACF, and AFM diagrams (figs. J12, J13, and J14). Thompson projections (Thompson, 1957) were not used for the Poorman and Ellison because requisite analytical data are insufficient. Assemblages are dominated by carbonate rocks (tables J1–J6) that contain a strong pelitic component. Rocks other than iron-formation, amphibolite, and garnet-biotite-bearing semipelitic rocks do not contain definitive assemblages for facies assignment; they are classified on the basis of neighboring rocks.

Little is known about metamorphic parameters in the complex metamorphic terrain of the Lead area, especially concerning the iron-formation in the Homestake. However, research is currently underway by Homestake's Exploration staff in conjunction with the South Dakota School of Mines and Technology to define parameters such as temperature, pressure, fluid composition, fluid paths, and mineral reactions. Preliminary temperature determinations from garnet-biotite and ankerite-siderite geothermometry across the Lead area by Kath (1989) show values ranging from about 370 °C in the west (upper greenschist facies) to approximately 630 °C in the northeast (middle amphibolite facies). Initial pressure estimates by R. Kath (written commun., 1990), using the plagioclase-biotite-garnet-muscovite geobarometer of Ghent and Stout (1981), range from 3.5 to 4.9 kb in semipelitic rock samples.

A sequence of prograde metamorphic isograds (first appearance of index minerals garnet and staurolite) has been established by surface mapping in the Homestake mine area (Noble, 1939; this report, figs. J4, J5, and J11). The garnet isograd has been extrapolated into the subsurface in the mine area. Although an isograd has been established in the mine itself for garnet (figs. J4, J5, and J11), some very fine grained (<2 mm) pink garnet in the western ledges is manganese-bearing (spessartitic almandine) and not used as an indicator of lower amphibolite facies or the garnet isograd. For mapping purposes, coarse (>3 mm) red garnet, generally of almandine composition, in iron-formation and in metapelites has been used to establish the garnet isograd.

From west to east in the mine area, upper greenschist facies rocks grading into lower amphibolite facies rocks

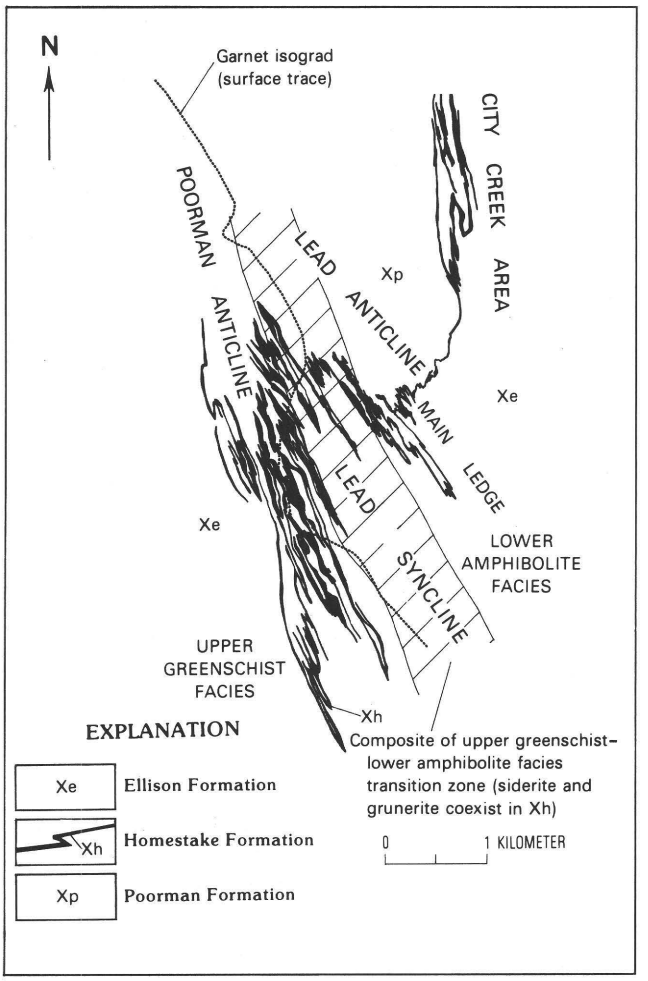

Figure J11. Geology of 2600 level, Homestake mine, showing upper greenschist–lower amphibolite facies and ground surface trace of garnet isograd.

form a metamorphic transition zone that averages 800 m wide (fig. J11). The transition zone strikes, on average, N. 20° W. and dips nearly vertical. The transition zone is defined mineralogically by the coexistence of siderite (fine grained) and grunerite in iron-formation. Within the Yates unit (metatholeiite) of the Poorman, the transition zone is thought to be defined by the coexistence of hornblende and actinolitic hornblende in addition to oligoclase-andesine and albite. The upper greenschist–lower amphibolite facies transition zone is structurally bounded east and west by early ductile shear zones, and it is contained within a structural domain dominated by late upright folds. (See section, "Structural geology.") Ductile shears appear to have exerted strong control on position of the transition zone. The surface trace of the garnet isograd as mapped by Noble (1939) lies near the west margin of the transition zone. A retrograde metamorphic event is also recorded in

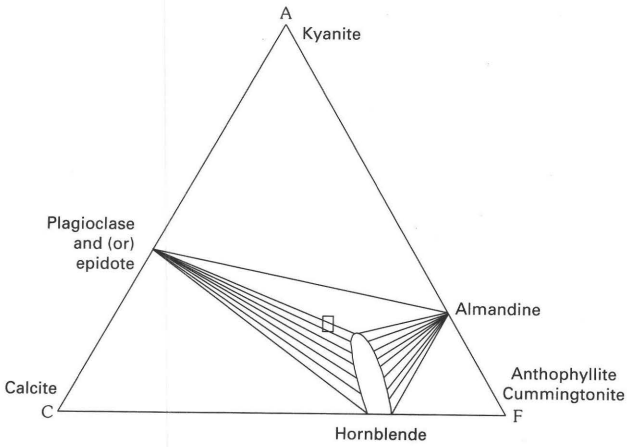

Figure J12. ACF diagram for lower amphibolite facies metamorphism of mafic igneous rocks of the Poorman and Ellison Formations, Homestake mine. Rectangle indicates location of average tholeiitic basalt according to Winkler (1979). Tielines define possible stable mineral-assemblage fields.

Homestake mine rocks and is largely manifested as a biotite halo developed within and peripheral to the iron-formation in the Homestake. This retrograde event occurred soon after the prograde thermal peak.

Prograde Metamorphism

Mafic Rocks

Mafic rocks in the mine are dominated by Yates unit metatholeiite (hornblende-plagioclase schist) of the Poorman Formation. Mineral assemblages within the Yates unit can be used as an indicator of metamorphic grade because of widespread distribution of the unit across the core of the Lead anticline where the unit is encompassed by the garnet isograd. The Yates unit lies largely within the lower amphibolite facies, which is characterized by ferromagnesian hornblende and plagioclase, the latter in the compositional range of oligoclase and andesine (T.J. Campbell, written commun., 1990). Subordinate accessory minerals include epidote-group minerals, carbonates, quartz, ilmenite, and magnetite. Minor parts of the Yates unit that occur in upper greenschist facies terrain consist of actinolitic hornblende, albite-oligoclase, carbonates, and epidote group minerals (T.J. Campbell, written commun., 1990). A possible metamorphic reaction (unbalanced) to account for the assemblages observed in the Yates unit at upper greenschist–lower amphibolite facies transition is: actinolite+albite+ankerite±chlorite = hornblende+andesine+ H_2O+CO_2.

The mineral fabric of the Yates unit is judged to be a particularly important indicator of the degree to which lower amphibolite facies metamorphic grade was attained.

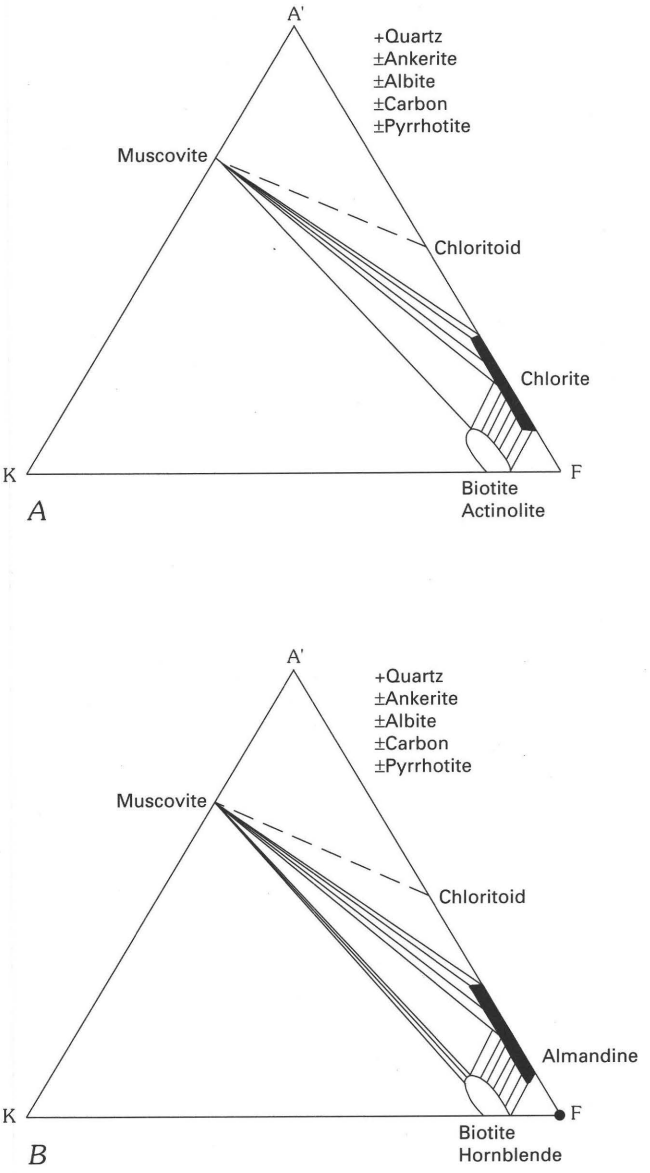

Figure J13. A'KF diagrams for mineral assemblages from the Poorman and Ellison Formations, Homestake mine. *A*, upper greenschist facies; *B*, lower amphibolite facies. Data are not available for Thompson projections (Thompson, 1957). Tielines define possible stable mineral-assemblage fields.

Hornblende and plagioclase are intergrown in a somewhat granoblastic fabric in which all the plagioclase is clearly metamorphic (equant, unzoned, untwinned, 0.1-mm grains). No relict igneous plagioclase persists. Locally, biotite is abundant, replacing hornblende along certain layers. An ACF diagram indicating the mineral assemblage for the Yates unit and Ellison Formation amphibolites is given in figure J12. The formation of hornblende from orthopyroxene, clinopyroxene, and (or) olivine is one of the major transformations of basaltic rock during prograde metamorphism in the presence of water (Winkler, 1979). Reactions forming hornblende must have been essentially

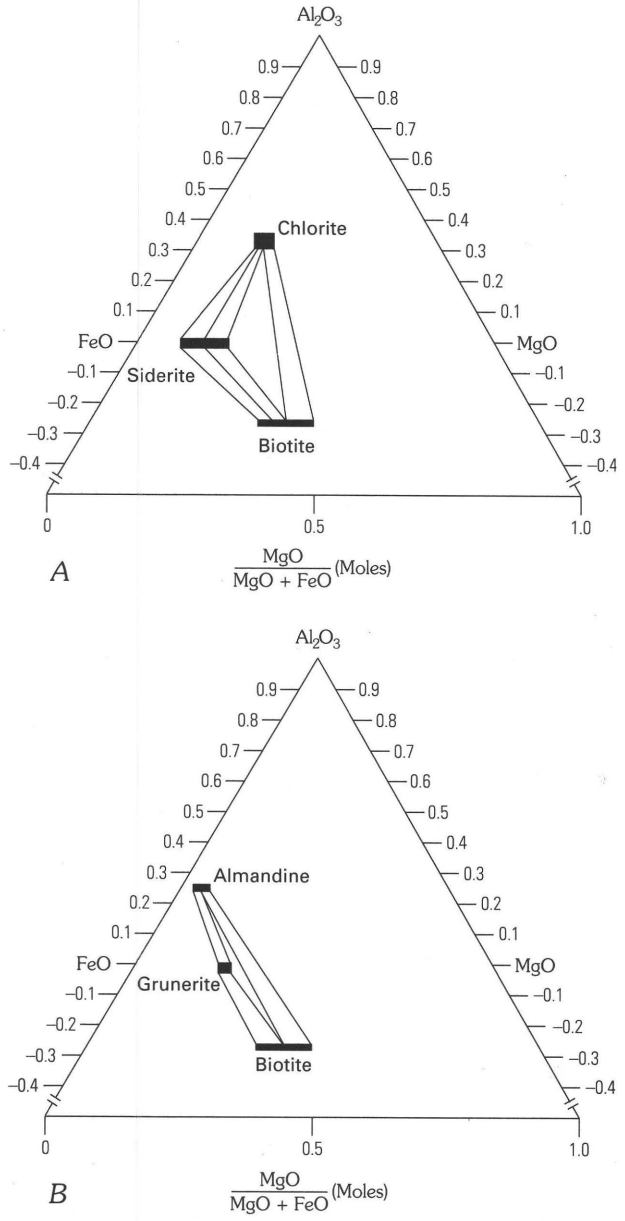

Figure J14. Projected AFM diagrams for *A*, upper greenschist facies, and *B*, lower amphibolite facies mineral assemblages for Homestake Formation, Homestake mine. Tielines define possible stable mineral-assemblage fields.

complete, based on ubiquitous hornblende in the Yates unit throughout the Lead area. The overwhelming abundance of hornblende, indicative of chemical equilibrium, suggests that prograde metamorphism may have taken place over a relatively long time. Grain size of the Yates unit, smaller than that of the tholeiitic basalt protolith, indicates a greater crystal-surface area available for fluid-rock interaction favoring recrystallization and equilibration. Additionally, much of the Yates unit chemistry was either directly or indirectly affected by extensive ductile shearing that facilitated recrystallization and equilibration. Relatively uniform hornblende compositions, implying large-scale redistribution of elements, also suggest isochemical conditions within and adjacent to ductile shears transecting the Yates unit. Such redistribution is supported by the observations of Beach (1980) in rocks of the Lewisian complex in Scotland.

The coexistence of hornblende and oligoclase-andesine in the Yates unit of the eastern mine area corresponds to grunerite-almandine-garnet assemblages in iron-formation. Therefore, the hornblende-plagioclase assemblage provides an estimate for the eastern boundary of the metamorphic transition zone.

Pelitic to Semipelitic Rocks

Metamorphic grade in phyllitic rocks of the upper unit of the Poorman, and to a lesser extent in the Ellison, is difficult to ascertain. This uncertainty exists largely because fine-grained graphite disseminated throughout most of the phyllites inhibited reactions that form minerals indicative of metamorphic grade. Another factor that deterred metamorphic reactions is the presence of abundant carbonate (which deforms plastically, reducing porosity) and fine-grained white mica (muscovite). Most Poorman phyllites cannot be termed pelites based on bulk composition; the rocks contain less than 18 weight percent Al_2O_3 (table J2) and are referred to herein as semipelites. The deficiency of alumina in most Poorman rocks combined with factors deterring mineral reactions precludes the formation of garnet, an indicator of metamorphic grade. Other minerals indicative of metamorphic grade in more aluminous pelitic rocks (>18 wt. percent Al_2O_3), such as chloritoid, stilpnomelane, and spessartitic almandine, are rare in the Poorman. The typical Poorman assemblage of muscovite+biotite+carbonate+quartz is stable (or metastable) in both upper greenschist and lower amphibolite facies.

Locally, where they contain almandine garnet, phyllites of the Ellison Formation (quartz-mica schist, sericite-quartz phyllite, and biotite-quartz phyllite) are indicative of metamorphic grade. Otherwise, mineral assemblages are similar to those of the Poorman: sericite+biotite+quartz±carbonate. (Figure J13 is A′KF diagrams for mineral assemblages in phyllites of the Poorman and Ellison Formations.) Bulk compositions of Ellison phyllites are largely pelitic (not reflected in chemical analyses in table J6) to semipelitic (table J6), and indicator minerals of metamorphic grade are present (table J5), but their distribution is not well known. A possible metamorphic reaction responsible for almandine garnet formation in the Ellison and Poorman is: chlorite+muscovite+quartz =almandine+biotite+H_2O. This is a typical garnet-forming reaction in most pelitic rocks, as noted by Thompson and Norton (1968), and reflects minerals and textures observed in pelitic to semipelitic rocks of the Lead area.

Remobilized graphite is a common feature recognized largely in the western ledges. Based on crosscutting relations, remobilization took place late during prograde metamorphism and continued well into the retrograde event. Its effects are most pronounced in phyllitic rocks controlled exclusively by ductile shearing. Within the mine environment are some shear zones that contain abundant graphite (about 7–25 modal percent) and that are indicative of carbon remobilization by metasomatic fluids. Carbon mobility can be explained by the following reaction (E.F. Duke, oral commun., Dec. 12, 1989):

$$C+2H_2O=CH_4+O_2$$

The inferred reaction also is suggested by methane-rich and methane-bearing fluid inclusions observed in quartz veins and near graphite-bearing phyllites (Homestake internal reports). These dark-gray to black graphite-rich zones exhibit poorly developed or disrupted layering and locally obvious shear fabric. Quartz vein stringers and pyrrhotite blebs are abundant locally in graphite-rich zones; pyrite is a minor constituent but is common in some areas. These zones transect earlier developed metamorphic rocks or mineral assemblages. A more comprehensive discussion is given by Campbell and others (1990).

Iron-Formation

Typical mineral assemblages in upper greenschist facies of iron-formation of the Homestake Formation consist of the equilibrium assemblage siderite+quartz+biotite+ankerite+ferroan clinochlore. The presence everywhere of two carbonates in upper greenschist facies of the Homestake has been verified in numerous samples by X-ray diffraction and electron microprobe techniques. The mineral assemblage may also contain varied amounts of almandine, stilpnomelane, albite, and chlorite group minerals. Figure J14's AFM diagrams represent this assemblage.

Two chlorite varieties are distinguished and interpreted by us to represent prograde metamorphic products. (See description of a third variety in the section, "Retrogressive hydrothermal alteration.") The two varieties treated here are recognized by their optical properties, X-ray diffraction patterns, mineral chemistry, mineral textures, and distribution; they are best developed in iron-formation, but also exist in pelitic to semipelitic rocks. They are as follows:

1. A faintly pleochroic, anomalously birefringent, lepidoblastic chlorite, found in small amounts in iron-formation and selected semipelitic rocks west of the garnet isograd in upper greenschist facies rocks. This chlorite, termed Type I, is considered early metamorphic, possibly a relict of precursor lower to middle greenschist facies regional metamorphism predating the earliest deformation recognized in the mine.

2. A ubiquitous but volumetrically small chlorite component of iron-formation, found as subhedral, randomly oriented, platy grains that are pleochroic from green (X) to yellow (Z) and exhibit anomalously high birefringence. Through X-ray diffraction methods, we have determined this chlorite-group mineral, termed Type II, to be ferroan clinochlore (variety of ripidolite). Ferroan clinochlore is pervasively widespread, and formed during the thermal maximum of prograde metamorphism largely in iron-formation.

It is generally accepted both by past workers (Noble and Harder, 1948; Gustafson, 1930, 1933; and Wayland, 1936) and by present workers that siderite and quartz are products of, and probably the major constituents of, the prograde metamorphic reactions that produced grunerite. Petrographic studies (unpublished Homestake data; Kath, 1990) indicate that several grunerite-forming reactions may have taken place in the iron-formation during prograde metamorphism. These reactions are based on mineral textures and in part on combined mineral and whole-rock chemistry.

The simplest and possibly most important reaction proposed is the following:

$$7\ \text{siderite}+8\ \text{quartz}+H_2O=\text{grunerite}+7\ CO_2 \qquad (1)$$

This was one of several grunerite-producing reactions proposed by Floran and Papike (1978) for the banded Gunflint Iron-formation of the Early Proterozoic Animikie Group in northern Minnesota–southern Ontario. The following two unbalanced grunerite-forming reactions, one involving the production of garnet and the other using stilpnomelane as a reactant, have been suggested by Kath (1989):

$$\text{siderite}+\text{quartz}+\text{chlorite}=\text{grunerite}+\text{almandine}+CO_2 \qquad (2)$$

$$\text{siderite}+\text{stilpnomelane}+H_2O=\text{grunerite}+\text{biotite}+\text{chlorite}+\text{quartz}+CO_2 \qquad (3)$$

Stilpnomelane is known at Homestake locally in lower grade metamorphic rocks (Bidgood, 1977; present authors); however, its distribution is not well documented. Another possible unbalanced reaction, proposed by Bidgood (1977) and by us, which accounts for a commonly observed assemblage, is the following:

$$\text{siderite}+\text{quartz}+\text{chlorite(I)}+H_2O+K=\text{grunerite}+\text{biotite}+\text{almandine}+CO_2\pm\ \text{chlorite(II)} \qquad (4)$$

The proposed reactions 1 through 4 are only a few of many that could be responsible for producing the prograde metamorphic assemblages observed. The end-member prograde assemblage found in the deep eastern ledges comprises grunerite+quartz+biotite+almandine garnet (fig. J14). These four reactions assume an isochemical system, but such a system probably is not entirely likely given the complex assemblages and textures observed in many

Homestake Formation rocks. Potassium (K^+), CO_2, and water have undoubtedly been introduced at some time during the metamorphic/deformational history of the iron-formation; and these components, other than CO_2, have not been taken into account in most of the reactions just listed.

Textural evidence for these reactions consists of crosscutting relations between earlier formed and later formed minerals. Such relations include grunerite sprays transecting locally embayed quartz and siderite grains (reaction 1). Similar textural relations support reaction 2, but in addition euhedral garnet growth is synchronous with grunerite. In reaction 3 siderite and stilpnomelane are overprinted by radial aggregates of grunerite along with metacrysts of biotite and chlorite, but the chlorite may be retrograde in some cases. Although reaction 4 is complex and tenuous, crosscutting textural relations lend support to the proposed reaction. However, quartz abundance in the higher grade mineral assemblage suggests an initial excess of quartz over that required for the reaction.

Prograde reactions in the Homestake Formation were dominantly devolatilization reactions involving the liberation of CO_2 during the breakdown of the carbonates. Liberation of water from pore fluids and dehydration reactions also were significant. Elsewhere, prograde metamorphic reactions in the Gunflint Iron-formation, Minnesota, that have been interpreted as promoted by thermal effects of the Duluth Gabbro emplaced within the Gunflint, coincide with a significant stratigraphic thinning toward the intrusive contact. This thinning is not believed to have resulted from depositional processes, but instead from volume loss from devolatilization reactions (Floran, 1975; Floran and Papike, 1978). Vaniman and others (1980), Labotka and others (1982), and Labotka (1985) made similar observations of volume loss during metamorphism of iron-formation adjacent to the Archean Stillwater Complex, Montana. In both cases, volatile loss was responsible for at least a 20 percent volume reduction of the iron-formation. In the Homestake Formation, volume reduction is apparent as indicated by thicknesses of iron-formation on either side of the garnet isograd on the surface (fig. J4) or on either side of the metamorphic transition zone underground (fig. J11). The Homestake Formation is thicker in upper greenschist facies rocks in the upper western part of the mine than it is in lower amphibolite facies rocks in the deeper eastern part of the mine (not illustrated). As in the Gunflint Iron-formation and Stillwater Complex examples, thickness differences are not believed to have been a result of the original depositional nature of the Homestake. Volume reduction is interpreted to have resulted directly from devolatilization reactions and differential strain along plunge during prograde dynamothermal metamorphic processes operating in early stages of ductile deformation. (See section, "Structural geology.") Additional support is given by the drastic reduction of hydrous and volatile mineral phases from west to east across the mine.

Retrograde Metamorphism

Retrograde metamorphic effects, first recognized by Noble (1939), overprinted prograde mineral assemblages and were superimposed on the upper greenschist–lower amphibolite facies transition zone in the mine area. Retrograde metamorphic assemblages recognized by Noble (1939) are similar to those recognized by us; however, some of Noble's retrograde assemblages are actually temporally related to a later hydrothermal alteration event synchronous with gold mineralization. Based on crosscutting relations, retrograde metamorphism was earlier and distinct from the gold event associated with retrogressive hydrothermal alteration. As noted by Noble and Harder (1948), the effects of retrograde metamorphism make the garnet isograd difficult to trace along its western margin because of incomplete alteration of garnet to chlorite, sericite, quartz, carbonate, and iron oxide. The "prochlorite" zone ("white chlorite") described by Noble and Harder (1948, p. 958–959), extends for some distance into rocks of lower amphibolite facies east of the mine. This zone, however, has not been recognized in the subsurface.

Retrograde minerals associated with the Homestake Formation are primarily biotite, siderite, chlorite, and ankerite. Biotite is the most obvious and best documented retrograde product; siderite, chlorite, and ankerite are less conspicuous. Away from ore zones, chlorite, siderite, and ankerite that are products of the retrograde event are difficult to distinguish from these same minerals that formed during hydrothermal alteration. Altered parts of the Yates unit metatholeiite may be related to the retrograde event.

A biotite halo is prevalent around the iron-formation in the Homestake Formation throughout most of the mine; based on observations made thus far, the biotite halo represents an early stage of alteration not related to subsequent gold mineralization. We suggest here that the biotite halo is a retrograde alteration product formed subsequent to the prograde metamorphic event. However, some metamorphic fluids generated during the prograde event may have reentered the system to produce a biotite halo. Retrograde fluid flow was focused primarily along rheologically contrasting rocks such as iron-formation and enclosing pelitic to semipelitic rocks where ductile shears had preferentially developed. However, the western ledges with their tight, attenuated fold structures were affected differently by ductile shearing owing to rheologic contrasts. Whether biotite formation marking the alteration halo was the result of potassium metasomatism, magnesium±iron metasomatism, or both, is currently unclear.

Potassium metasomatism alone would be difficult to substantiate, except in chlorite-bearing rocks, because the majority of the rocks enclosing the Homestake are pelitic to

semipelitic in composition. The addition of K^+ would have had little effect unless chlorite was a constituent; moreover, biotite replacement of chlorite was rare.

Given the pervasiveness of biotite, the large difference in bulk chemical composition between iron-formation and bounding rock types (tables J1–J6), and competency contrast between respective formations, magnesium±iron metasomatism was very likely. Attainment of equilibrium conditions between highly contrasting bulk chemical compositions was promoted by ductile shearing, competency contrasts, and fluids channeled through potential conduits. Equilibrium would then have been facilitated through the fluid medium by metasomatic exchange between magnesium and iron in the iron-formation, and aluminum and possibly potassium in the enclosing phyllites and schists. The equilibrium reaction involved liberation of magnesium and iron from octahedral sites in grunerite (lower amphibolite facies) and of octahedrally coordinated metal atoms in siderite or ankerite (upper greenschist facies). Aluminum was released from octahedral sites in muscovite: chemical gradients were established across stratigraphic/formational boundaries exchanging magnesium and iron for aluminum with a concomitant release of CO_2 and water from carbonates and amphiboles, respectively. Potassium in pelites and semipelites and silica both in pelites and semipelites and in iron-formation also were available during dissociation and redistribution. A chemical gradient developed with respect to K^+, causing its migration into the iron-formation, and the production of biotite. A silica gradient was negligible. Mobilized iron and silica in iron-formation were combined with introduced aluminum that had been released from pelites and semipelites to form garnet in the iron-formation. A reverse process is also possible, whereby aluminum liberated in semipelites, along with silica, may have combined with introduced iron to form garnet in pelitic to semipelitic rocks.

Fluid migration along units of contrasting competence (that is, ductile shears) and bulk chemical composition may have induced metasomatism and promoted equilibrium conditions through development of chemical gradients with respect to aluminum and potassium in phyllites, and magnesium and iron in iron-formation. Such a process may explain mineral assemblages and rock-type distributions found along lower and upper contacts of the Homestake, within both the iron-formation and the enclosing Poorman and Ellison Formations. Biotite is found in all rock types at formational boundaries in the upper western ledges and is accompanied by garnet in the lower eastern ledges. Based on limited data, the suggested fluid migration along ductile shears at contacts may explain the apparent increase in modal abundance of dolomite (or ferroan dolomite), ankerite, and locally siderite, at the expense of calcite and ankerite in the Poorman toward its contact with iron-formation.

Additional biotite alteration took place locally along the western sheared margins of metatholeiite of the Yates unit. The altered metatholeiite is characterized by biotite, calcite, and minor chlorite that replaced hornblende-andesine or locally actinolitic-hornblende-albite. The alteration was largely a hydration-carbonation reaction incorporating the addition of K_2O and CaO with a concomitant depletion in MgO and possibly Al_2O_3 and SiO_2 (table J2; unpublished Homestake data). Whether this alteration was related to retrograde metamorphism and synchronous with biotite alteration associated with iron-formation, or was the manifestation of a later temporally and spatially distinct hydrothermal alteration event is not clear.

Interpretation

Prograde metamorphic reactions in the Lead area were initiated synchronously with transposition of the mine rocks from an originally flat lying position to their present steeply dipping orientation. The transposition was accompanied by a more focused phase of ductile shearing creating large-scale shear systems. Prior to ductile shear development, metamorphic processes were largely preceded by intergranular fluid migration, along microcracks and larger scale widely spaced fractures, as described by Yardley (1986) for metamorphic rocks in general. Fractures propagated as a wave front away from a heat source. The large ductile shear zones served as conduits for fluid flow during prograde and retrograde events. Fluid flow regimes in the mine area can be compared to several examples discussed by Kerrich (1986). He indicated that, in general, flow regimes in shears follow an order from locally derived fluids at low water:rock ratios and at high temperature-pressure conditions during inception of the structures, to large volumes of fluid flow along conduits as the structures propagate. In the Lead district large shear zones were initiated during early tectonism synchronously with prograde metamorphism. High temperature-pressure conditions accompanied by low water:rock ratios probably characterized the early stages of deformation, and the thermal maximum occurred late in ductile deformation. Prograde fluid-volatile generation culminated late in ductile deformation and was characterized by high fluid fluxes in the shear zones; the high fluid fluxes promoted chemical disequilibrium that in turn initiated and then accelerated the mineral reactions. Metamorphic conditions progressed from a largely internally buffered, essentially closed, and possibly isochemical system during early tectonism, to an externally buffered and open system during later stages of the ductile event as ductile shears propagated. Prograde metamorphic reactions, reaction progress, and associated pressure-temperature-time (P-T-t) paths were highly modified as a result of fluid flow in these shear zones during the prograde and subsequent retrograde metamorphic

events. Ductile shear zones also delimited the development of the garnet isograd by focusing fluids and heat, buffering rocks west of the mine area from higher temperature metamorphic effects. Thus, lower to middle greenschist facies rocks west of the mine may represent a primitive regional burial metamorphic event; the regional dynamothermal event at 1.84 Ga had minimal effect on the rocks.

STRUCTURAL GEOLOGY

Deformational Events

Early Proterozoic structural geology in the vicinity of the Homestake mine was characterized by two major deformational events termed the older event, D1a, and the younger event, D1b. Deformation phases for these events include early D1a (regional "plate-scale" shearing and folding), middle D1a (flattening event, no lineation), late D1a (sheath[2] folding with axial fabric and stretching lineation), latest D1a (ductile shearing with planar mylonitic fabric), early D1b (upright folding with vertical axial plane foliation), middle D1b (ductile-brittle shearing accompanied by ore-stage mineralization), and late D1b (post-ore brittle shearing, and crenulation/kink fabric). Following conventional terminology, the folding and subsequent shear events are defined by planar, folded, and linear elements (table J7). Deformation D1 occurred during the Early Proterozoic. Deformation phases in D1a are believed to have taken place during a single thermal event, as deduced from metamorphic assemblages and mineral textures. Available data suggest that this thermal event was a regional prograde metamorphism that probably was initiated during early D1a, reached its maximum in late D1a, and possibly continued into latest D1a. Regional prograde metamorphism is generally dated at 1.84 Ga (Zartman and Stern, 1967). Retrograde metamorphism was apparently short lived and was synchronous with latest D1a. A subsequent retrogressive hydrothermal event and associated gold mineralization were synchronous with middle D1b, possibly initiated in early D1b. Deformation associated with the emplacement of the Crook Mountain Granite (this report; Bachman and others, 1990) is represented by late D1b even though early initial phases may have coincided with middle D1b. Folds correlated with the successive deformational events are termed F1a, F1b, ...*n*, and related shears and lineations are termed S1a, S1b, ...*n*, and L1a, L1b, ...*n*, respectively. Some much younger faulting of Laramide and early Tertiary age occurred, but it has no bearing on the Early Proterozoic deformation and metamorphism and thus has not been studied.

Noble (1939) generated a structural model at the mine involving early folds cut by crossfolds. Our work has several points of similarity to Noble's model. Noble (1939, p. 214) stated that, "***the directions*** [of crossfolding] ***range from N. 17° W. to N. 35° W., and the dips of the shear planes, all eastward, range from 50 degrees to nearly vertical." His data on crossfolds pertain to our early F1b fold sets recognized in the current study. Chinn (1969) analyzed Homestake structure and suggested three important fold events. His F1 appears to correlate with our late F1a; his F2 to our early F1b. Our crenulation cleavage and kink folds (late F1b) may be structures that he described as F3. Apparently, neither Noble nor Chinn recognized early F1a folds or D1a and D1b ductile shears.

Structural geology in the mine area is characterized by the overprinting of successive individual deformation phases. The complex fold structures and shear zones that were produced present a composite of the deformation history. The Lead anticline, Lead syncline, and Poorman anticline (fig. J11) are "structural composites" of the total deformation. Figure J15 shows the distribution of dominant D1a structural domains relative to the Homestake Formation on the 2600 mine level. Domain boundaries are transitional and, in detail, commonly overlap. These structural domains represent areas where a particular deformation phase dominates and various combinations of other phases are subordinate. As an example in figure J15, the dominant latest D1a ductile shearing domain contains subordinate components of middle S1a fabric, late F1a sheath folds and fabric, and minor D1b folds and shears.

Early D1a

We believe that the early D1a deformation in the Lead area (table J7) developed during major transcurrent movement, related to the Trans-Hudson orogen, along the eastern margin of the Wyoming Archean craton (Bachman and Campbell, 1990). The resulting "plate-scale" shear zone is expressed in the Early Proterozoic core of the northern and central Black Hills as a series of anastomosing ductile shear zones that truncate and postdate nappe-style folding described by Redden and others (1990), and R.R. Reid (internal Homestake report, 1983). We suspect the presence of transposed minor nappe fold elements in the Lead area, although no definitive stratigraphic evidence for larger scale nappe fold closures has yet been found in the district. Possibly early F1a folds discussed here may have had their origin related to nappe-style folding. If so, these early nappe folds are likely to have developed while the rock units were flat lying, prior to early D1a deformation.

Transcurrent ductile shearing during early D1a, coincident with initial stages of prograde metamorphism,

[2]"Sheath fold" is used in this report to denote a fold of conical form generated within a strain regime where the strain release path is directed along a single direction and contains a single stretching lineation (late L1a) parallel to its fold axis (figs. J16 and J17).

Table J7. Structural deformation history in the Homestake mine and vicinity

TIME	Deformational event	Surface(s) folded/sheared	Surface formed	Folds	Stretching lineation	Thermal event	Description of deformation (folding and shearing)
→ EARLY PROTEROZOIC →	Late D1b	all earlier S1b, S1a	Late S1b	Late F1b	Late L1b	Lower T	Post-ore semibrittle kink-shear and kink-fold phase, minor fault displacement of ore bodies, steep to shallow fold plunges, NE.-NW. trend kink-shear surfaces (Stage III quartz veins).
	Middle D1b	all S1a Early S1b	Middle S1b	Middle F1b	Middle F1b	Retrogressive hydrothermal alteration ≈ 1.72 Ga ?	Post-upright folding ductile-brittle shear phase, shears develop on bedding planes and earlier foliation surfaces, shears trend NS.-N. 60° W., predominant dip-slip shearing, drag folds develop, horizontal plunge (Stage II quartz veins with ore mineralization).
	Early D1b	Late, latest S1a	Early S1b	Early F1b	Early L1b		Upright open to isoclinal folding phase, vertical axial-plane foliation developed, NS.-N. 60° W. fold trends, SE. plunge.
	Change of strain and thermal conditions in continuing deformation						
	Latest D1a	Late S1a	Latest S1a	Latest F1a		Prograde metamorphism (thermal maximum ≈1.84 Ga)	Post-sheath ductile shear phase, ductile shears develop on bedding planes and earlier foliation surfaces, shears trend N. 20° W., predominant strike-slip, minor dip-slip shearing, reclined and semi-reclined drag folds (Stage I quartz veins). Developed late, with retrograde metamorphism.
	Late D1a	Middle S1a	Late S1a	Late F1a	Late L1a		Sheath folding phase, apparent constriction flow in axial-planar early S1a, axial symmetric fabric, average fold trends N. 35° W., plunges SE., axial planes dip NE.
	Middle D1a		Middle S1a			Initial prograde metamorphism	Flattening phase, minor flow along the axial plane.
	Early D1a	S0	Early S1a	Early F1a			Early regional "plate-scale" ductile shear phase, predominant strike-slip shearing, mega-reclined drag folds develop, north-south trends (Lead-Poorman anticlinorium). During early D1a deformation Black Hills Proterozoic rocks were transposed to their current steeply dipping position.

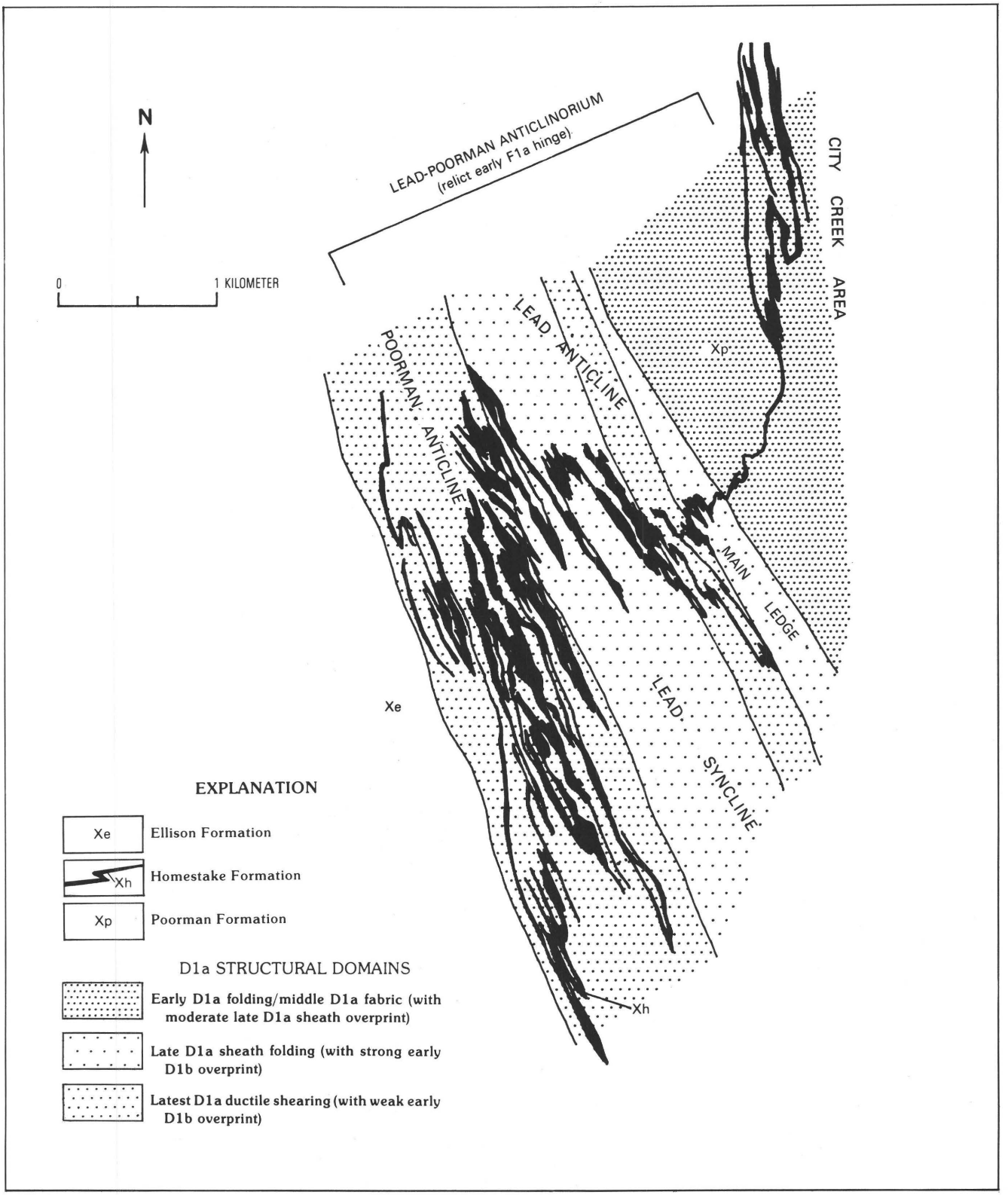

Figure J15. Geology of 2600 level, Homestake mine, showing D1a structural domains.

transposed the originally flat lying Early Proterozoic strata into the steeply dipping rocks that characterize the Black Hills today. A major component of this model is the importance of district-scale variations in rock competence. Relatively competent masses such as the Yates unit metatholeiite acted as strain buttresses during shearing, focusing

shearing and folding along margins and in frontal positions of the "metatholeiite" (fig. J16, shears not shown). The folded iron-formation in the Homestake Formation which defines the Lead-Poorman anticlinorium (fig. J15) is believed to have developed in a strain shadow created by the Yates unit metatholeiite. Folds generated as a result of this deformation (early D1a) are effectively shear-induced drag folds, isoclinal in form; and they trend north-south in the Lead area. Nontransposed early F1a folds plunge east-northeast down the dip line (reclined folds) in the shear foliation plane, indicating a dominant component of strike-slip shearing during fold generation. Drag fold asymmetry suggests sinistral slip.

Small-scale, early F1a drag folds are best preserved in the east limb of the Lead anticline and in the adjacent City Creek area (fig. J15) where deformational shear strain was weakest. Distribution of the early D1a structural domain is shown in figure J15. Generally, the east limb of the Lead anticline (fig. J17) and the City Creek area are characterized by moderately east dipping foliation (late S1a, fig. J18) that roughly parallels but locally crosscuts compositional layering and an early foliation (S0/early S1a) in limb positions. Within the mine environment, where late and latest D1a deformational phases were most intense, linear and planar elements related to early D1a are entirely transposed. In most cases, early F1a folds are indistinguishable from younger folds except where local differences in fold orientation and style are noted, or where refolded fold profiles are observed.

Figure J18 shows medium-sized early F1a folds and inferred early S1a foliation overprinted by late S1a foliation in profile section (perpendicular to late F1a axial orientation), developed in Homestake Formation. Figure J18 is enlarged from the fold labeled "transposed early F1a" on the east limb of the Lead anticline in figure J17. The fold shows large and small elements both symmetrical about late

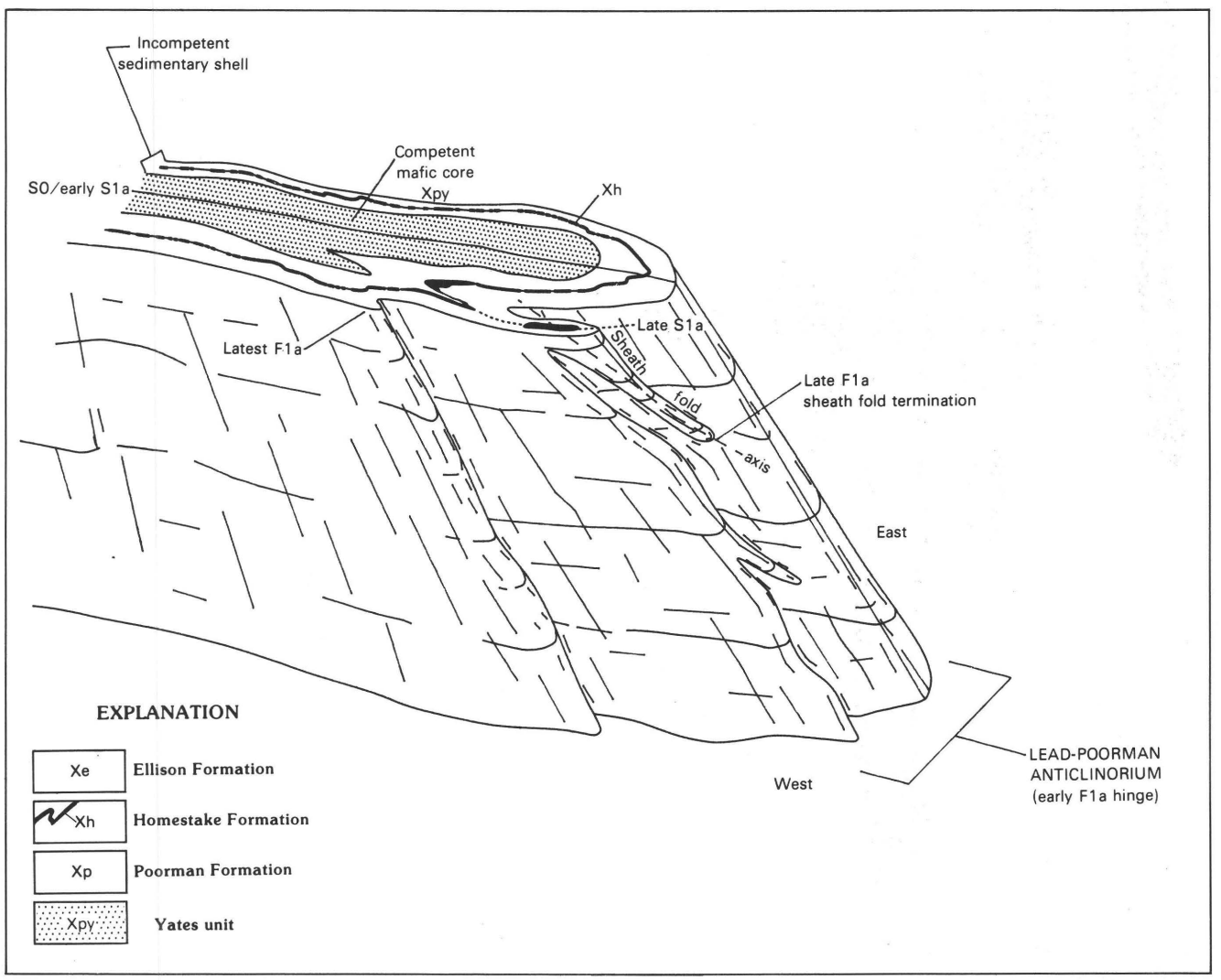

Figure J16. Schematic perspective diagram showing D1a fold events at Homestake mine.

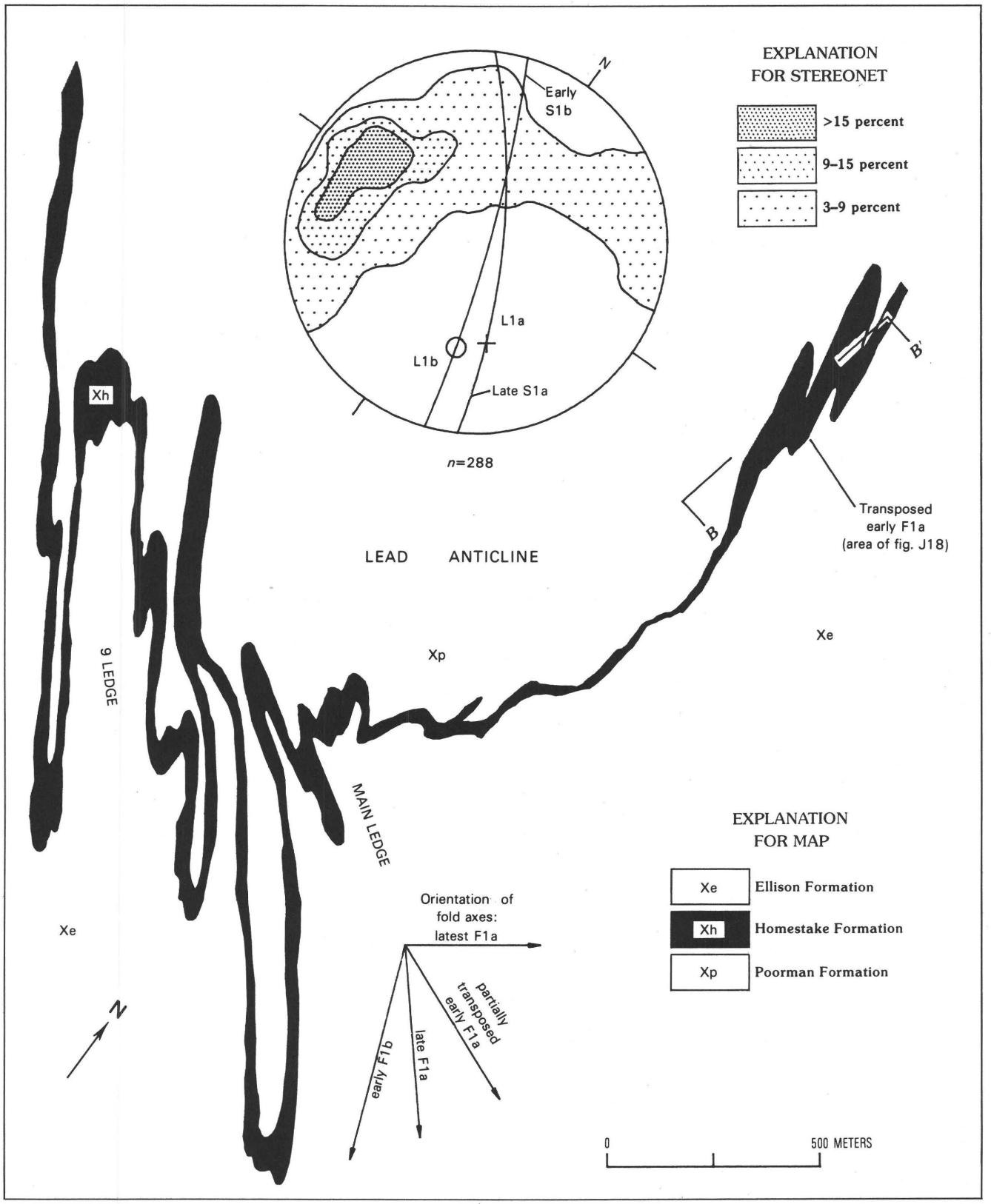

Figure J17. Generalized geologic map of 2600 level, Homestake mine, showing lower hemisphere, equal-area stereonet with 288 poles to folded foliations of late S1a from the Lead anticline (eastern ledge area). Poles contoured at 3, 9, and 15 percent per 1 percent area. L1a (+) and L1b (o) are average stretching lineations and fold axes in late F1a (sheath fold phase) and early F1b, respectively. Details of structural domains are not shown.

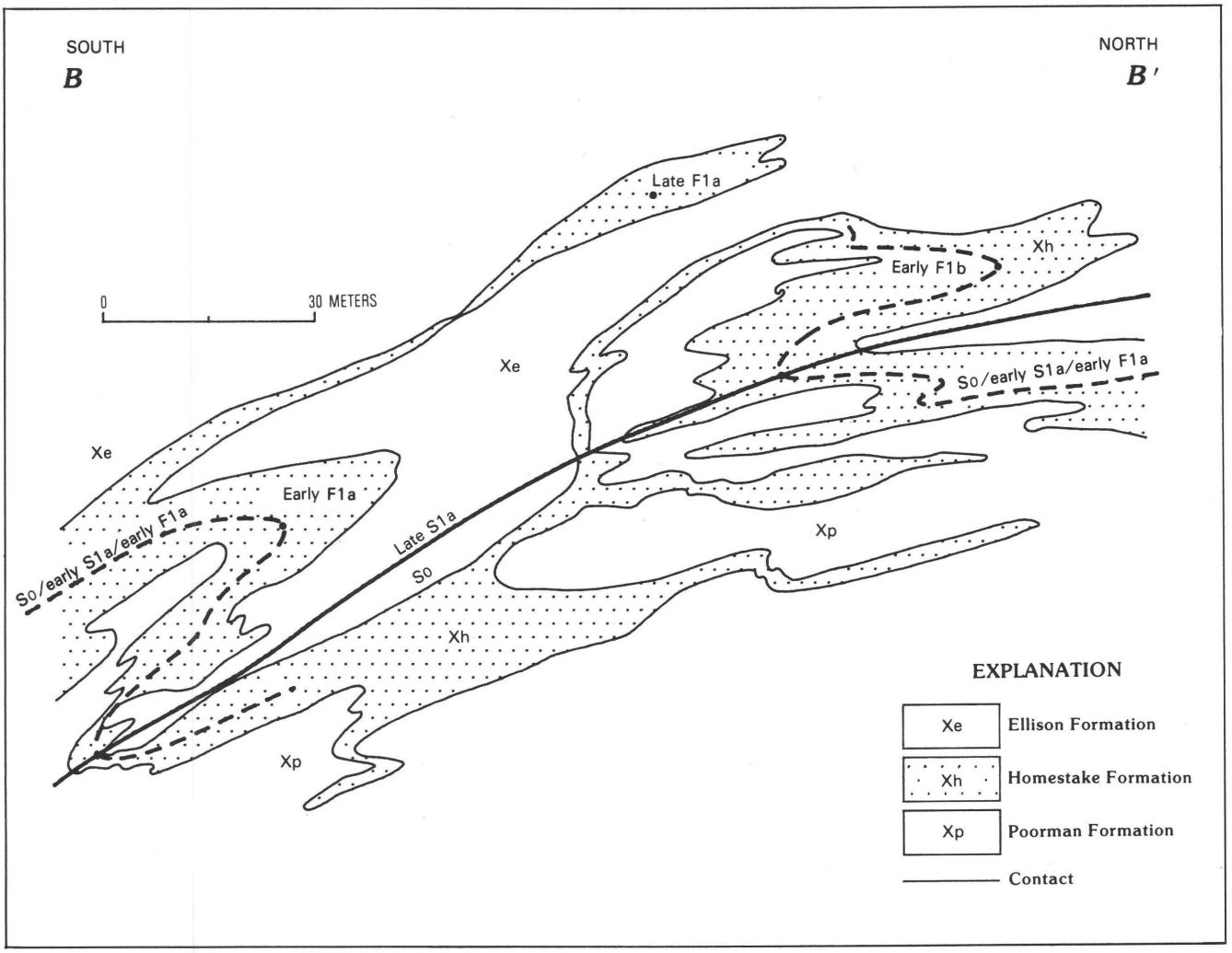

Figure J18. Iron-formation fold profile of the Gentle Annie structure (east limb of the Lead anticline), 2600 level, Homestake mine, observed down plunge to east-southeast and along sheath fold axis in figure J17. Late F1a sheath folding refolded transposed early F1a folds.

S1a. The symmetry and style of folding, in folded early S1a foliation and early F1a folds in figure J18, indicate the effect of superimposed deformation fabrics. Early F1a fold structures are not well understood owing to the intensity and pervasiveness of subsequent shearing and transposition.

Middle D1a

Middle D1a deformation (table J7) is characterized by a flattening fabric (middle S1a) that developed in a field of coaxial strain. No folds or lineation were produced during middle D1a.

We identified flattening fabric petrographically by evaluating three orthogonal thin sections taken from oriented specimens, one perpendicular to each fabric axis. Flattening fabric of middle S1a apparently overprints and is thought to lie parallel to preexisting early S1a foliation; early S1a fabric commonly is transposed. Mineral grains are deformed into oblate spheroids. Where minimal overprinting has occurred, these "pancake-shaped" grains are not rotated, and they lie parallel to the early S1a foliation plane, indicating a post-early D1a development. Middle D1a flattening fabric is preserved in relatively few domains, generally in the eastern mine area and in the adjacent City Creek area (fig. J15). Flattening fabric is overprinted in various degrees by axially symmetric fabric (late S1a foliation). In cases of extreme strain, no evidence of the flattening phase survived late D1a deformation.

Flattening fabric is present in the Yates unit metatholeiite and in phyllite and schist of the Poorman and Ellison Formations. Iron-formation in the Homestake Formation is generally recrystallized and massive in lower amphibolite facies and shows little directed fabric at microscopic scale. In amphibolitic rocks, flattening fabric is expressed by random orientation of hornblende prisms lying in the foliation plane. In phyllite and schist, it is expressed

by garnet that forms partly equant and partly oblate spheroids parallel to foliation. These garnet crystals contain small inclusions of platy quartz grains that are also aligned parallel to foliation. Garnet probably grew synkinematically during early stages of prograde metamorphism in a field of coaxial strain. Additionally, quartz, plagioclase, and pyrrhotite streaks in phyllite and schist, as well as plagioclase in Yates unit metatholeiite, have the form of tiny oblate spheroids whose principal axes parallel foliation; these observations support the interpretation of flattening fabric.

Late D1a

Folds generated in late D1a (table J7) are sheathlike (conical) in form (fig. J19), trending on average N. 35° W., with inclined axial planes dipping northeast. Sheath fold plunge is varied, averaging 45° SE. A penetrative axial symmetric fabric (late S1a foliation) was developed in conjunction with sheath folding, as was a distinctive stretching lineation (late L1a). Sheath folding (see Park, 1988) characteristically resulted in marked changes in structural profile along fold-axis plunge in iron-formation and nearby schist or phyllite (fig. J16). Sheath folds develop within a field of apparent constriction flow (Ramsay and Huber, 1983, p. 172), where stretching lineation (late L1a) indicates the direction of tectonic transport. During the initial stages of sheath development, minor folds, isoclinal in form (fig. J19*A-C*), are generated in response to flow along the plunge line. As strain weakens and flow subsides, sheath fold terminations are created. Sheath fold terminations are closed and elongate structures (figs. J16 and J19*D*) with shallow taper. Fold-axis plunge is varied near sheath fold terminations.

Axially symmetric fabric (late S1a foliation) is most common in schist and phyllite near iron-formation. It overprints and generally destroys early flattening fabric (middle S1a) and transposes early F1a folds. In metatholeiite, the fabric is expressed as hornblende prisms with parallel *c*-axes; the resulting lineation is subparallel to hinges of late F1a sheath folds. Locally, individual prisms are boudinaged, and resulting openings are filled with quartz, feldspar, or minor epidote-group minerals. In mica-rich schist, the axially symmetric fabric (late S1a) is expressed by rodded mineral grains, commonly quartz and pyrrhotite streaks. Small grains attain the general form of prolate spheroids having long axes subparallel to hinges of late F1a sheath folds. Some grains are locally boudinaged, and resulting openings are filled with chlorite and quartz.

Late S1a fabric is also expressed by mica orientations in phyllite and schist. In petrographic thin sections normal to the lineation, edges of mica flakes exhibit random orientations. In orthogonal sections parallel to the lineation, mica flakes are seen randomly oriented, from edgewise flakes to basal sections, reflecting the axial symmetry. Micas are not curved or bent, as might be the case if the fabric were produced by folding perpendicular to the axis of symmetry.

In domains of axially symmetric fabric (late S1a), garnet porphyroblasts are commonly rotated so their planar inclusion fabric occurs at all angles to foliation in the enclosing matrix of schist or phyllite. From this, we interpret garnet as a relic from the flattening phase (middle D1a) and suggest that it was rotated during the later F1a sheath fold phase. This rotation attests to non-coaxial strain character in the late D1a strain history.

Late F1a sheath folds overprint early F1a folds and middle S1a flattening fabric throughout the central mine. How much early F1a fold forms are retained within sheath-dominated fold domains is not known. Probably a significant portion of the isoclinal component in the mine rocks is relict early F1a that has been transposed and overprinted by late F1a sheath folds (fig. J18). Within the mine area sheath folds are best preserved, and they represent the dominant fold domain in the Lead syncline (fig. J15). Sheath folds are overprinted by the latest D1a ductile shear phase in the Poorman anticline and a part of the Lead anticline. We interpret that peak prograde metamorphism was attained late during this deformation phase, probably extending somewhat into latest D1a.

Latest D1a

Deformation associated with latest D1a (table J7) was dominated by ductile shearing that formed extensive shear zones as much as 1,000 m wide within the mine area (fig. J15). Latest D1a shearing, where most intense, generated a planar mylonitic fabric (latest S1a) with an average foliation of N. 18° W., 52° NE.

Latest D1a shears formed on bedding planes and earlier foliation surfaces, to create a complex series of smaller anastomosing meso-shears that exist in sets several meters wide. These meso-shears are composed of even smaller micro-shears that form anastomosing strands around competent rock masses. Variations in rock competence controlled shear-set geometry. Strain intensity was highly varied and was dependent on rheologic contrasts. Ductile shear zones are characterized by disrupted macro- and micro-sheath fold hinges, well-developed flow fabric, drag folds, and high-temperature mylonites (fig. J20).

We believe that movement within D1a shear zones was predominantly strike slip with a minor dip-slip component producing reclined and semireclined folds that plunge to the northeast and southeast, respectively. Reclined and semireclined folds (latest F1a) represent various degrees of transposition of early F1a folds and late F1a sheath folds. These transposed folds are effectively drag folds (latest F1a) formed by ductile shear movement. Figure

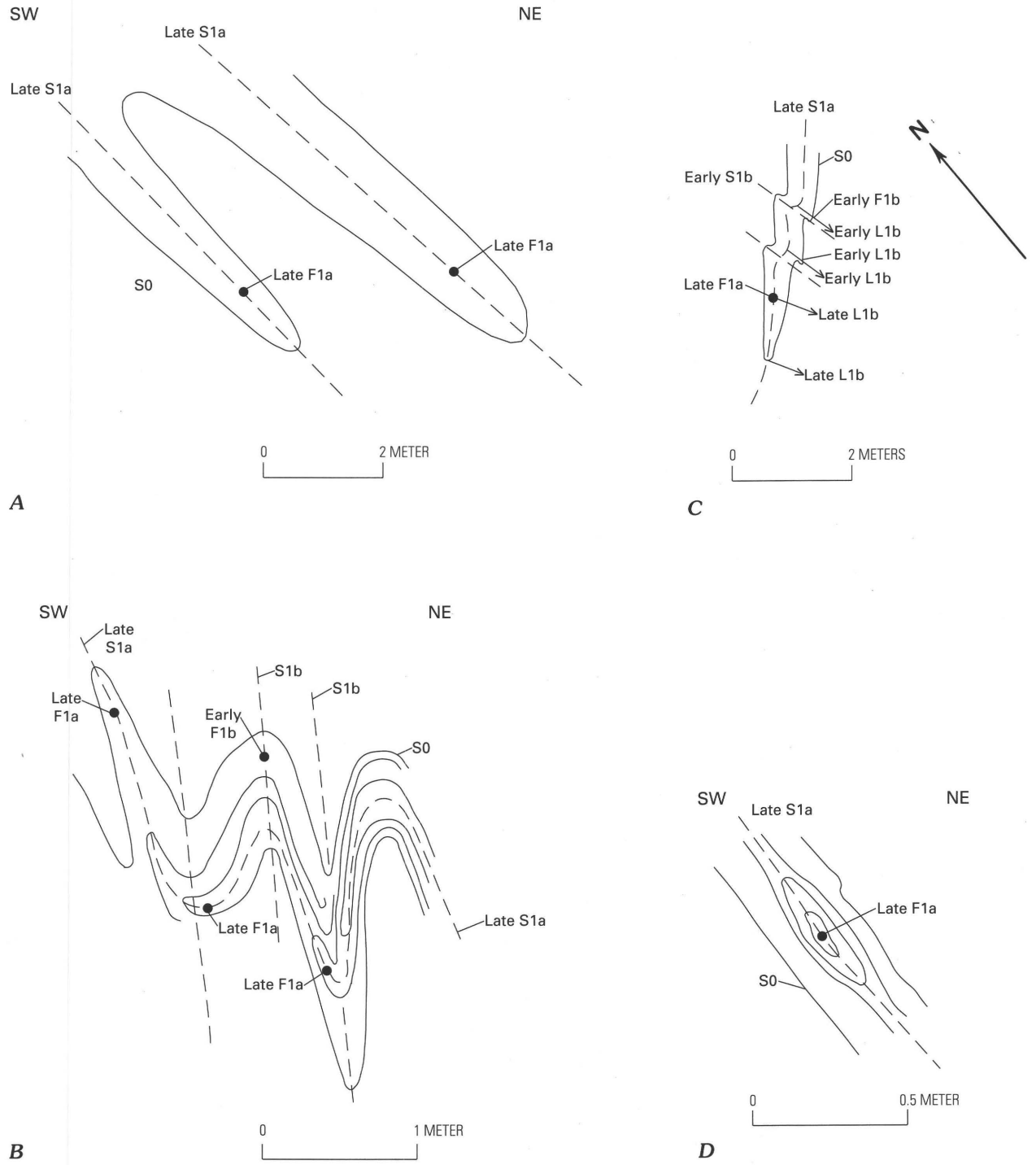

Figure J19. Sketches of late F1a (sheath) and early F1b minor folds in Poorman and Ellison Formations in the eastern ledge area of the Lead anticline, Homestake mine. *A*, typical late F1a fold in profile section; *B*, meso-scale late F1a–early F1b refolded combination in profile section; *C*, late F1a–early F1b refolded combination in plan view—this style of fold interference is seen at all scales; *D*, meso-scale late F1a sheath fold termination in profile section. Profile sections viewed up plunge along the fold-axis direction.

J21 shows effects of ductile shearing on late F1a fold plunge in the Poorman anticline area (6800 level). This event coincided with the transition from prograde to retrograde metamorphism (table J7) and emplacement of the oldest recognized set of quartz veins, that is, veins of Stage I. (See section, "Quartz veins.")

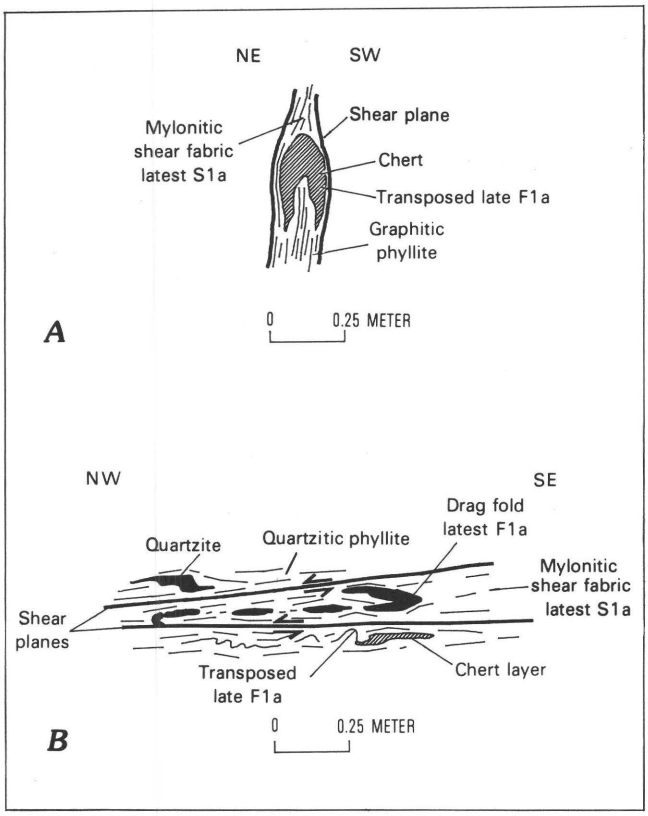

Figure J20. Structural sketches in profile sections of minor folds in latest D1a shear zones, western ledge area on the Poorman anticline, Homestake mine. *A*, Poorman Formation; floating, detached fold hinge. *B*, Ellison Formation; dishar-monic reclined drag folds. Single-barb arrows show direction of shear.

Early D1b

Folds generated in early D1b (table J7) are upright, are open to isoclinal in form, and have nearly vertical axial planes trending on average N. 20° W. (fig. J19*B*, *C*). In detail, F1b fold trends range from N.S. to N. 60° W. Fold plunge is generally moderate, averaging 35° SE. An axial-plane foliation (early S1b) and intersection lineation (early L1b) developed in conjunction with folding (fig. J17). The foliation and lineation are best developed in phyllite.

In general, the D1b deformation was substantially weaker than all previous phases. Early F1b fold domains are restricted to selected locales in the mine, chiefly the Lead syncline area (fig. J15); but they do exist in the other domains as well. In places, early F1b folds locally refold late F1a minor folds, late S1a foliation, and the planar mylonitic fabric of latest D1a. They do not substantially modify the form of large-scale late F1a sheath folds or latest D1a ductile shears (not shown). The early F1b overprint on late F1a resulted in development of conical folds that locally modify structural profile along plunge. These conical folds are characterized by the presence of two lineations: a crossing lineation defined as late L1a and a lineation parallel to early F1b defined as early L1b (fig. J17). The early F1b-parallel lineation is due to the intersection of early S1b with S0/S1a fabric (if preserved), or the F1b hinge.

Middle D1b

Deformation in middle D1b (table J7) was a late-stage ductile-brittle shear phase that is considered a continuation of the D1b deformation with strain conditions changing from upright folding to reverse shearing. Gold mineralization was synchronous with middle D1b shearing.

Middle D1b shears formed on bedding planes and earlier foliation surfaces. They also consist in part of reactivated older shear zones. Middle D1b ductile-brittle shears dip 45° NE. to vertical. Asymmetric drag folds (middle F1b) with nearly horizontal axes are developed within or adjacent to the shears, indicating reverse shearing with northeast sides up. Middle D1b ductile-brittle shear trends are varied, generally ranging from N.S. to N. 60° W. Strike and dip of middle D1b ductile shears were controlled by the attitude of existing foliation surfaces, which was in turn influenced by the attitude of more competent grunerite-dominant Homestake Formation and Ellison Formation quartzite. Similar to latest D1a shears, middle D1b shears anastomose through the mine. Certain selected segments were dilated; many of these dilated shears developed synchronously with ore bodies and many coincide spatially with ore bodies. As shearing continued, parts of some ore bodies were drag folded, sheared, and boudinaged. The middle D1b shearing event was synchronous with retrogressive hydrothermal alteration and emplacement of a second set of quartz veins, that is, Stage II veins. (See section, "Quartz veins.")

Late D1b

Deformation textures characterized by late D1b (table J7) are distinctly postmetamorphic and obviously postdate gold mineralization; they developed in an environment of semibrittle strain and lower temperature. Kink folds (late F1b) and associated kink shear surfaces (late S1b) with north-south as well as northeast to northwest trends were generated in late D1b.

Structures associated with late D1b are interpreted to have developed in response to injected phases of the Crook Mountain Granite (this report; Bachman and others, 1990) northeast of the mine. The northeast- to northwest-trending kink shear surfaces are steeply dipping and apparently formed earlier than the north-south kink set characterized by shallow dips (R.R. Reid, 1982, Homestake internal report). Kink shears produced minor displacement (a few meters),

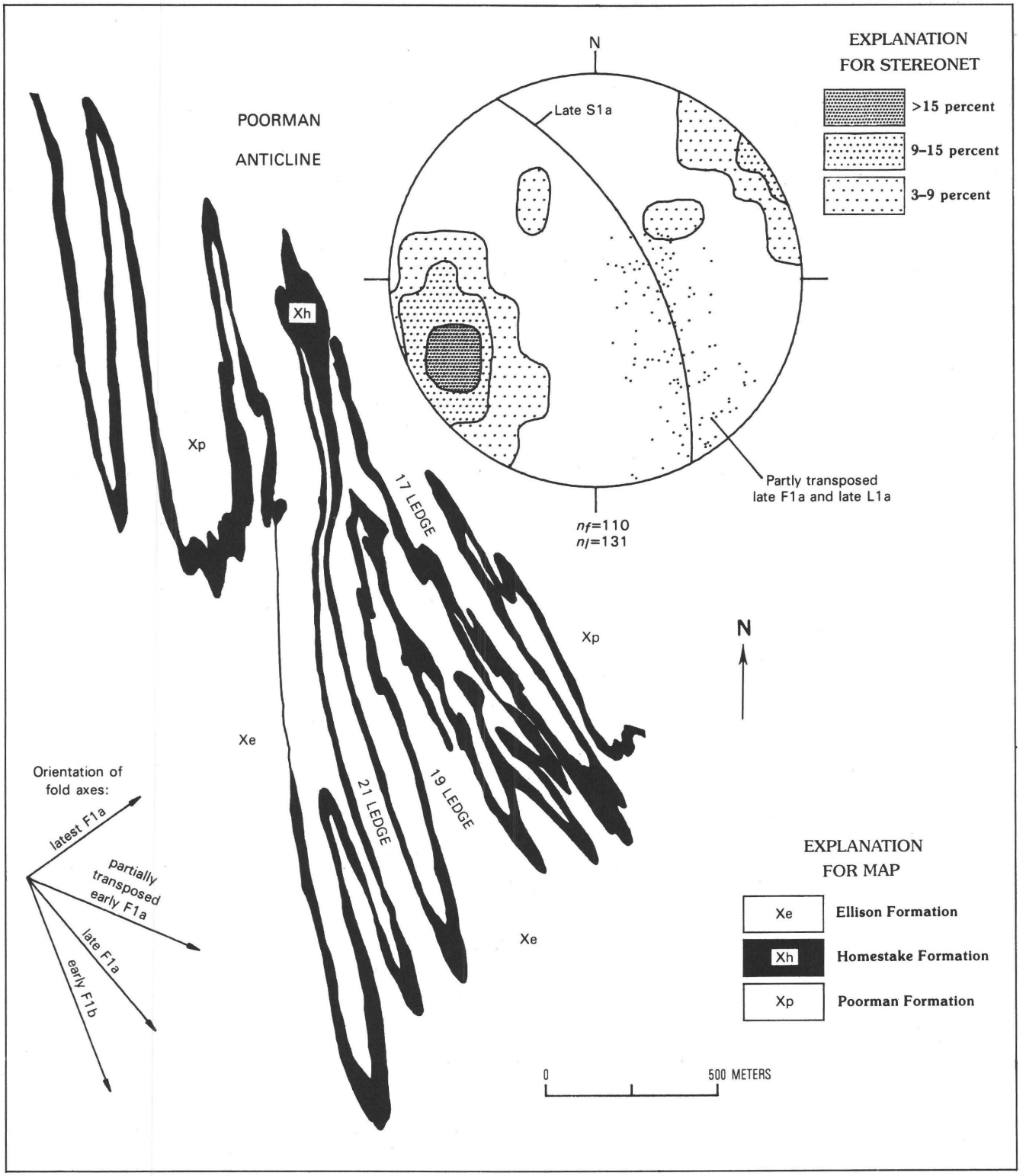

Figure J21. Generalized geologic map of part of 6800 level, western ledge area, Homestake mine, showing lower hemisphere, equal-area stereonet with 110 poles to transposed late S1a foliation (*nf*) from the 6800 to 8000 levels, contoured to 5, 10, and 15 percent per 1 percent area. Tight isoclinal folding (late F1a) is indicated by the strong point concentration of fold axes with varied plunge. Great circle defines average axial plane of partly transposed late F1a isoclinal folds with parallel limbs. Linear features (*nl*) in western ledges are represented by 131 points: 69 minor fold axes and 62 stretching lineations that are parallel in part to neighboring minor fold axes. Lineation attitudes range from strike line to dip line. Linear elements lie in plane of foliation. Structures related to D1b not developed in this domain. Details of structural domains not shown.

commonly on flat shear surfaces, in the ore bodies. Late D1b kink fabrics exist in narrow restricted domains that are more prevalent in the eastern mine area and adjacent City Creek area. A third set of quartz veins (Stage III) was emplaced during this phase of deformation. (See section, "Quartz veins.")

Interpretation

The tectonic evolution of Early Proterozoic rocks in the mine area was complex; the major observed deformation was related to dynamics of the Trans-Hudson orogen and its subsequent reactivation (Bachman and Campbell, 1990). Tectonic events occurring prior to deformation D1a (that is, nappe folding) are not considered here because, at least in the mine area, they were not substantiated by stratigraphic relations. A logical tectonic break existed between the generation of recumbent nappe fold structures in flat-lying sedimentary rocks and transposition of those sedimentary rocks to nearly vertical in a transpressional environment during the D1a phase of deformation at 1.84 Ga.

Movement of the Superior craton northwestward relative to the Wyoming craton is a probable mechanism for development of transpressional forces that initiated the Trans-Hudson orogenic event and early D1a sinistral transcurrent shearing in the Black Hills (Bachman and Campbell, 1990). This plate movement coincided with plate collision along the Great Lakes tectonic zone and the Penokean orogen at 1.85 Ga (Sims and others, 1987). Within this transpressional environment (southeast-northwest) during early D1a, Early Proterozoic rocks were transposed to nearly vertical attitudes, and structures such as the Lead-Poorman anticlinorium began to develop. In continuing deformation during middle and late D1a, the stress field progressively rotated to an inclined east-west to northeast-southwest compressional configuration. Ductile shearing of latest D1a was initiated in response to changing stress conditions that occurred late in D1a sheath fold development. Following latest D1a shearing, we interpret that significant active deformation ceased, and was followed by a period of quiescence.

In our view, renewed tectonism related to D1b was initiated in response to reactivation of the Trans-Hudson zone as a result of continent-arc collision during the Central Plains orogen, active between 1.80 and 1.63 Ga (Bickford and others, 1986; Sims and others, 1987). Early F1b folds appear to have developed during a simple northeast-southwest compression; middle S1b shears with dominant reverse movement indicate a similar stress configuration. Generation of late D1b kink shears and folds is attributed to late-stage granite emplacement (Bachman and others, 1990).

ORE DEPOSIT GEOLOGY

The Homestake gold deposit is largely stratabound within the Homestake Formation and is mined for gold; silver is extracted as a byproduct. Overall, ore bodies make up less than 3 percent of iron-formation in the Homestake Formation in the mine area. Through 1988, cumulative production plus ore reserves was 147.7 million t (metric tons) at an average grade of 8.36 g Au/t.

Main and Caledonia ore ledges were mined initially in 1876 where they were exposed at the surface. Main Ledge is the largest, and it continues to produce ore from the Open Cut and from underground intermittently to the 6800 level, 3,380 m down plunge from the surface. Levels in the mine are referenced in feet below the collar of the Incline shaft, at an elevation of 5,227 ft or 1,594 m above sea level. Twenty-one Ledge, on the 7400 level, is the deepest ore-producing area in the mine. The 8000 level, at which active drifting and exploration drilling are taking place, is the deepest work area.

Ore Ledges

The word "ledge" as used in this report refers to a plunging fold structure containing Homestake Formation. Where economically mineralized with gold, a ledge is referred to as an ore ledge. Nine ore ledges have produced gold from the Homestake mine and eight remain producers (fig. J2). From east to west across the mine area the nine ore ledges are: Caledonia, Main Ledge, 7, 9, 11, 13, 17, 19, and 21 Ledges (fig. J6). Odd-numbered ledges are synformal folds composed of a series of subordinate anticlines and synclines. Where ore mineralization was most intense, as in Main Ledge on the surface and 9 Ledge on the 3200 level, these subordinate fold structures are all ore bearing. Even-numbered ledges are anticlinal fold forms that are less complex structurally; they are generally barren but may be weakly mineralized. The Independence anticline (6 Ledge, located between Main and 7 Ledges and not illustrated) was a minor gold producer.

The mine is divided into two general areas: eastern ore ledges and western ore ledges. Eastern ore ledges include Caledonia, Main, 7, 9, 11, and 13. Western ore ledges include 17, 19, and 21. The orientation of an ore ledge reflects the attitude of folded and sheared iron-formation in the Homestake, and this attitude varies throughout the mine depending on the deformation domain in which the ore ledge lies. Eastern ore ledges trend on average N. 35° W. parallel to late F1a sheath folds, and they lie predominantly within the late D1a sheath fold domain (figs. J6 and J15). Two noted exceptions to the trend are Caledonia between the surface and 1400 level (fig. J22) and Main Ledge below the 6200 level (fig. J23). In these areas ore ledge trends are deflected eastward owing to the

influence of early D1a deformation on the Homestake Formation. Eastern ore ledges plunge on average 40° SE.

Western ore ledges trend on average N. 80° E. parallel to latest F1a reclined folds and lie predominantly within the latest D1a shear domain (figs. J6, J15). An exception to this is 21 Ledge below the 6800 level, where the southernmost ore bodies project into the late D1a sheath fold domain. These ore bodies accordingly deflect southward and trend N. 50° W. (not illustrated). The plunge of western ore ledges is varied, ranging between 60° NE.

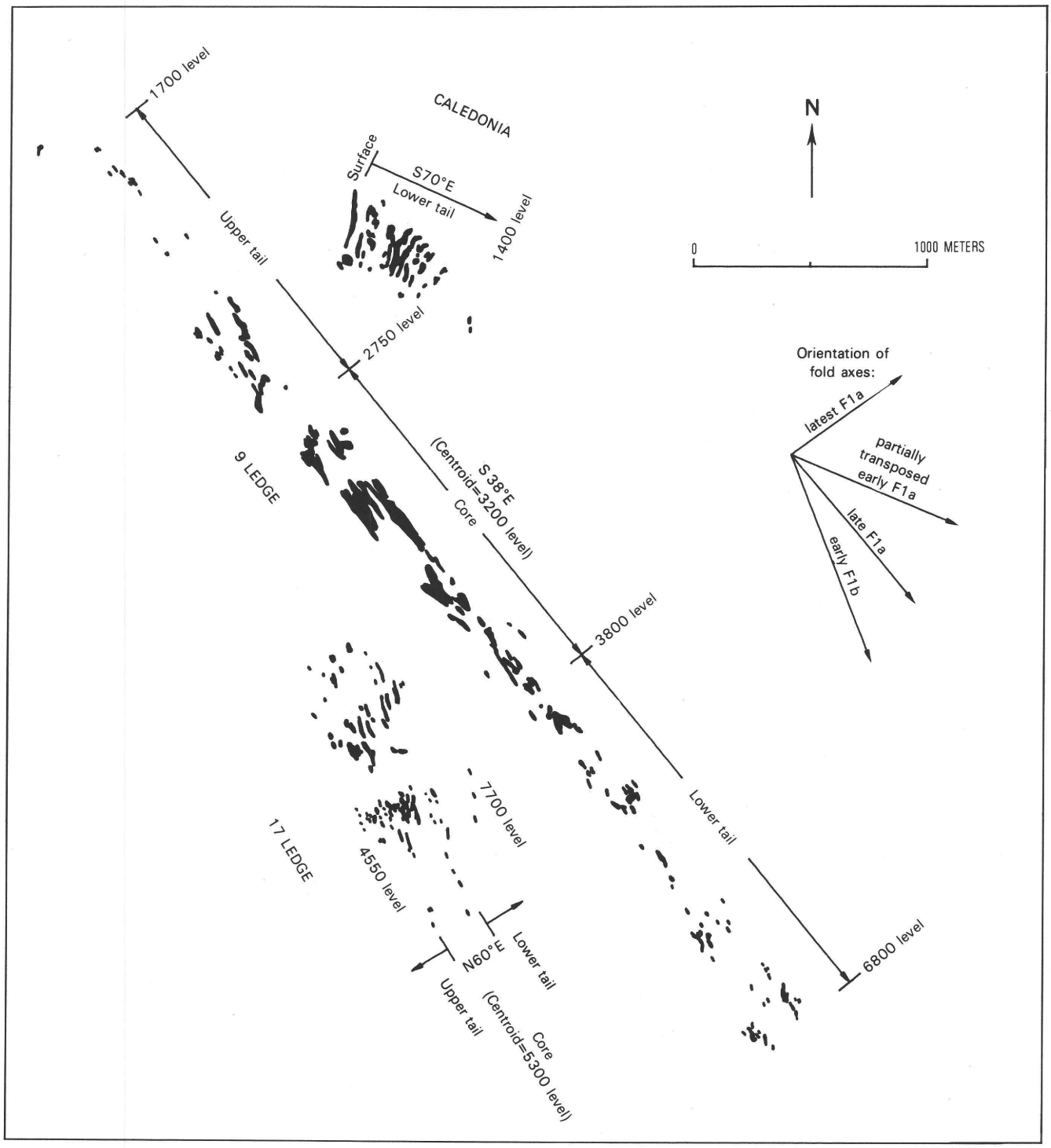

Figure J22. Vertical projection of selected horizontal slices of the Caledonia, 9 Ledge, and 17 Ledge ore bodies to a horizontal plane, showing the geometric elements of an ore ledge.

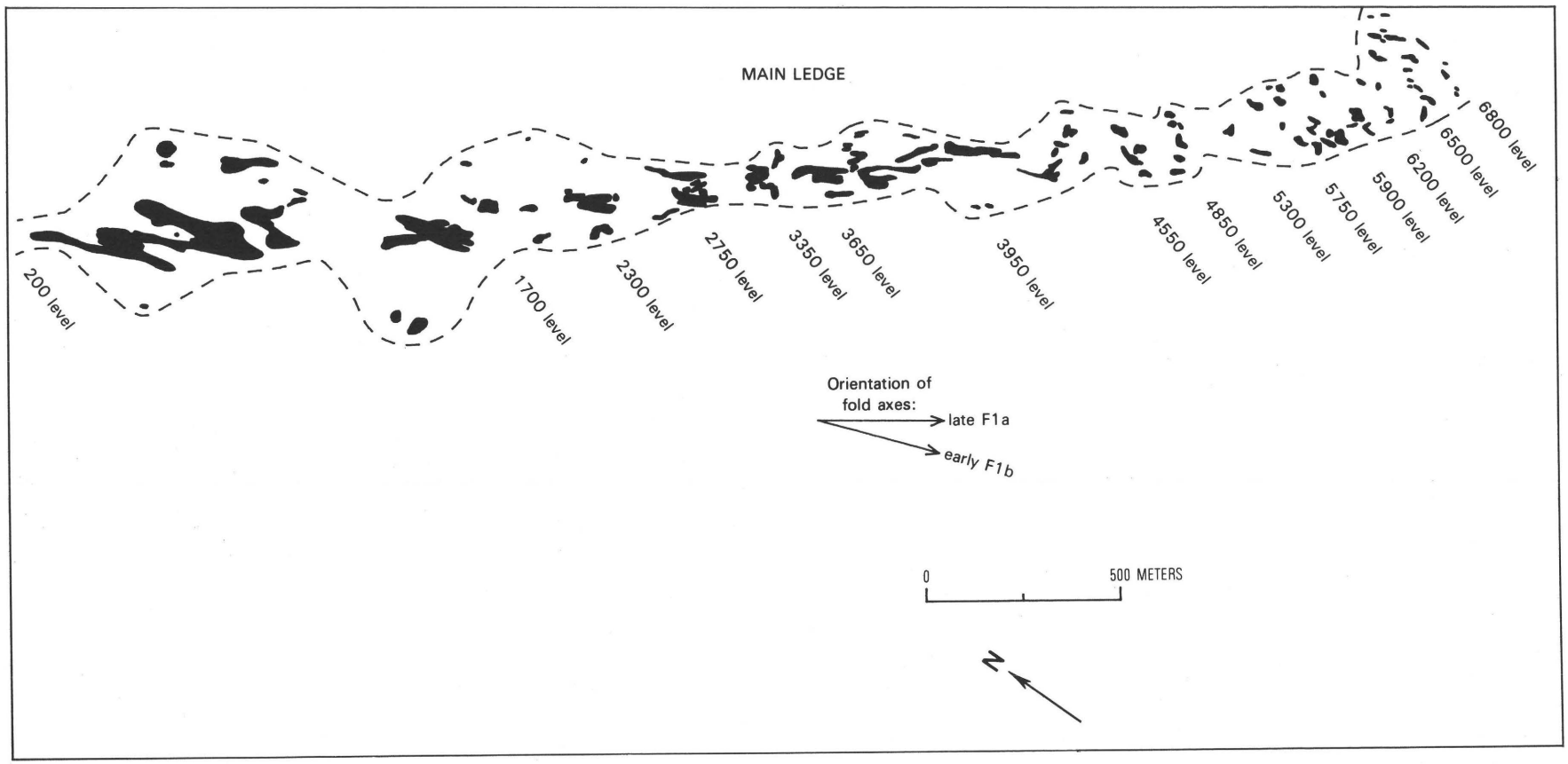

Figure J23. Vertical projection of selected horizontal slices of Main Ledge ore bodies to a horizontal plane. Dashed line, boundary of Main Ledge late F1a sheath folds.

and 40° SE. Average ore ledge plunge in both eastern and western ledges is a function of the fold and shear domain in which the ore ledge occurs.

Composite plan view projections (figs. J22, J23) illustrate the distribution of ore bodies within an ore ledge. To avoid superposition, the figures show ore bodies on selected mine levels; horizontal ore-body slices in the figures represent numerous individual ore bodies that are discontinuous between mine levels.

Ore ledges are defined by three geometric elements: core, upper tail, and lower tail areas (fig. J22); the core area contains the largest and most continuous ore bodies. The volume of ore in the core area generally exceeds 50 percent of the total ore in the ore ledge. The vertical height (mine level to level) occupied by a core area ranges from 200 m (13 Ledge) to more than 800 m (Main Ledge). The mine level within a core area containing the largest cross-sectional ore area is termed the ore ledge centroid. Each ore ledge has a defined ore centroid. The number and size of ore bodies decrease away from the centroid level, both up and down plunge. Distal ends of each ore ledge are longitudinally asymmetric, divided into upper (up plunge) and lower (down plunge) tail areas (fig. J22, 9 Ledge). Lower tail plunge lengths are generally two times greater than upper tail lengths. Overall, average ore ledge grade remains relatively constant, decreasing slightly as the transition is made into upper and lower tail areas. As an example, in Main Ledge, geologic grade varies 1.5 g Au/t between the core and lower tail areas (2,100 vertical meters). Beyond tail areas, economically mineralized Homestake grades into barren Homestake Formation (<20 ppb Au), which continues undisrupted along plunge. Observed physical changes beyond economic limits include a marked decrease in sulfides, chlorite, and quartz veins, all intimately associated with ore bodies. Beyond a few hundred meters from upper and lower tail limits (not clearly defined), trace geochemical signatures for gold, silver, and arsenic are near detection limits (not illustrated).

The metamorphic and physical character of the Homestake Formation within an ore ledge varies along plunge (fig. J24). The Homestake in upper tail areas is siderite dominant, reflecting the effects of upper greenschist facies metamorphism. In the core areas, siderite and grunerite generally coexist, indicating a transition zone that progresses down plunge into lower amphibolite facies. Lower tail areas are grunerite dominant. A volume reduction of the Homestake Formation corresponding to the transition from upper greenschist to lower amphibolite facies is observed along plunge from upper to lower tail areas. This volume reduction is due in part to devolatilization of iron-formation during metamorphism and the varied nature of deformational strain along plunge. In 9 Ledge, a 69 percent relative volume decrease of the Homestake is observed between upper (1700 level) and lower tail (6800 level) areas.

An ore ledge centroid represents the mine level containing the largest ore bodies. The ore centroid theoretically corresponds to a zone of optimal gold deposition. In plan projection, ore ledge centroids generally lie on a line that has an average bearing of S. 20° E. and varied plunge averaging 26° SE. (fig. J25). This centroid trend parallels the latest D1a shear zones, lies within the metamorphic transition zone, and superimposes early D1b folds and shears.

Known ore ledges are elongate and varied in plunge length. Larger ore ledges, such as Main or 9 Ledge, display general continuity of ore bodies along tremendous plunge length. As an example, 9 Ledge has been mined along plunge for more than 5 km (fig. J24). Ore ledges are of varied sizes (fig. J26) ranging from 75 million t (Main Ledge) down to less than 2 million t (19 Ledge).

With the exception of Main Ledge and Caledonia, all other ore ledges at Homestake are blind to the surface even though the Homestake Formation fold structures in which they occur are well exposed. The eastern ore ledges, except 13 Ledge, were discovered prior to 1958 (fig. J2). The western ore ledges were discovered during the 1960's, the last of which was 21 Ledge in 1969. The method of discovery during the past 52 years consisted of systematic underground drifting and drilling. Exploratory drilling in 1987 on the 6200 level (Caddey and others, 1990) intersected 7 m of mineralized rock averaging 24.4 g Au/t in 15 Ledge, making this ledge a probable new producer for the future (fig. J6).

Ore Bodies and Ore Mineralization

Economic gold within an ore ledge is contained within tabular to pipelike, relatively undeformed ore bodies. Ore bodies occur as segregations of pyrrhotite, arsenopyrite, minor pyrite (pyrite content diminishes below the 800 level), and native gold within a gangue matrix of quartz+chlorite+siderite+biotite±garnet. Sulfide content varies generally from 5 to 30 percent of the total ore volume, averaging 8 percent overall. Ore bodies generally occur at or near the Homestake-Ellison or Homestake-Poorman contact. Where an ore body is contained entirely within the Homestake Formation, the Homestake is generally a siderite- or grunerite-dominant biotite-chlorite-quartz schist.

Figures J27 and J28 illustrate the varied form of folded Homestake Formation and contained ore bodies along plunge. Ore bodies do not conform strictly to the Homestake host stratigraphy. They rake across bedding and the pre-middle D1b folds and foliations. In both figures J27 and J28, ore bodies lie near either the Homestake-Poorman or the Homestake-Ellison contacts, except where the entire

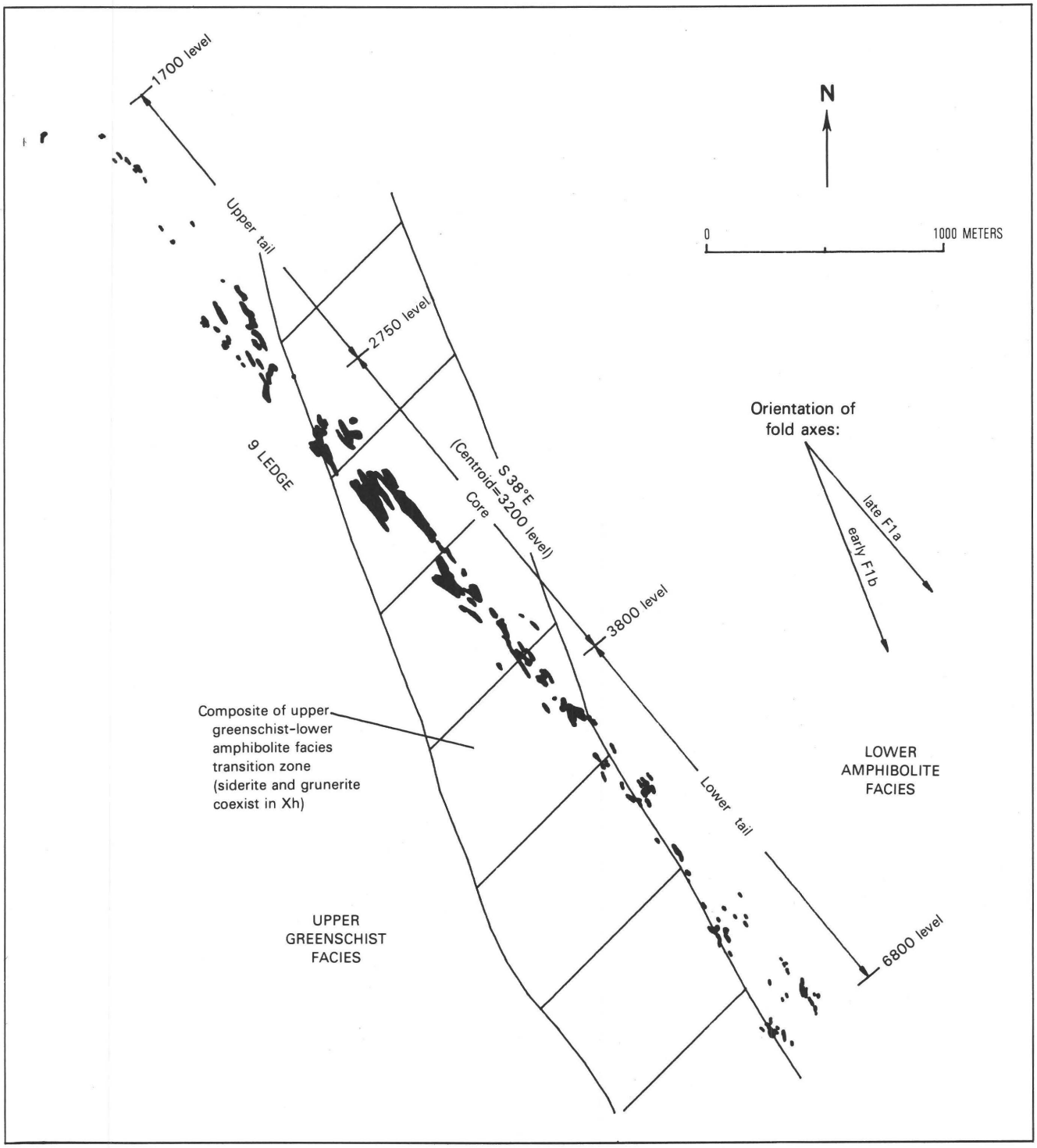

Figure J24. Vertical projection of selected horizontal slices of 9 Ledge ore bodies to a horizontal plane, showing geometric elements of an ore ledge and the upper greenschist–lower amphibolite facies transition zone.

volume of Homestake has been mineralized. Commonly (fig. J28, 6050 level), individual ore bodies lie transverse to compositional layering within the Homestake. Localization of ore bodies near formational contacts is observed throughout the mine and is related to ore-stage ductile-brittle shears (middle D1b) along rheologic boundaries.

The number, size, and relative internal continuity of individual ore bodies are highly varied depending on the position of ore bodies within an ore ledge and on the intensity of middle D1b shearing. Ore bodies in figure J27 represent a transition from the large continuous "core-type" ore bodies on the 1850 level to smaller "lower tail-type" ore

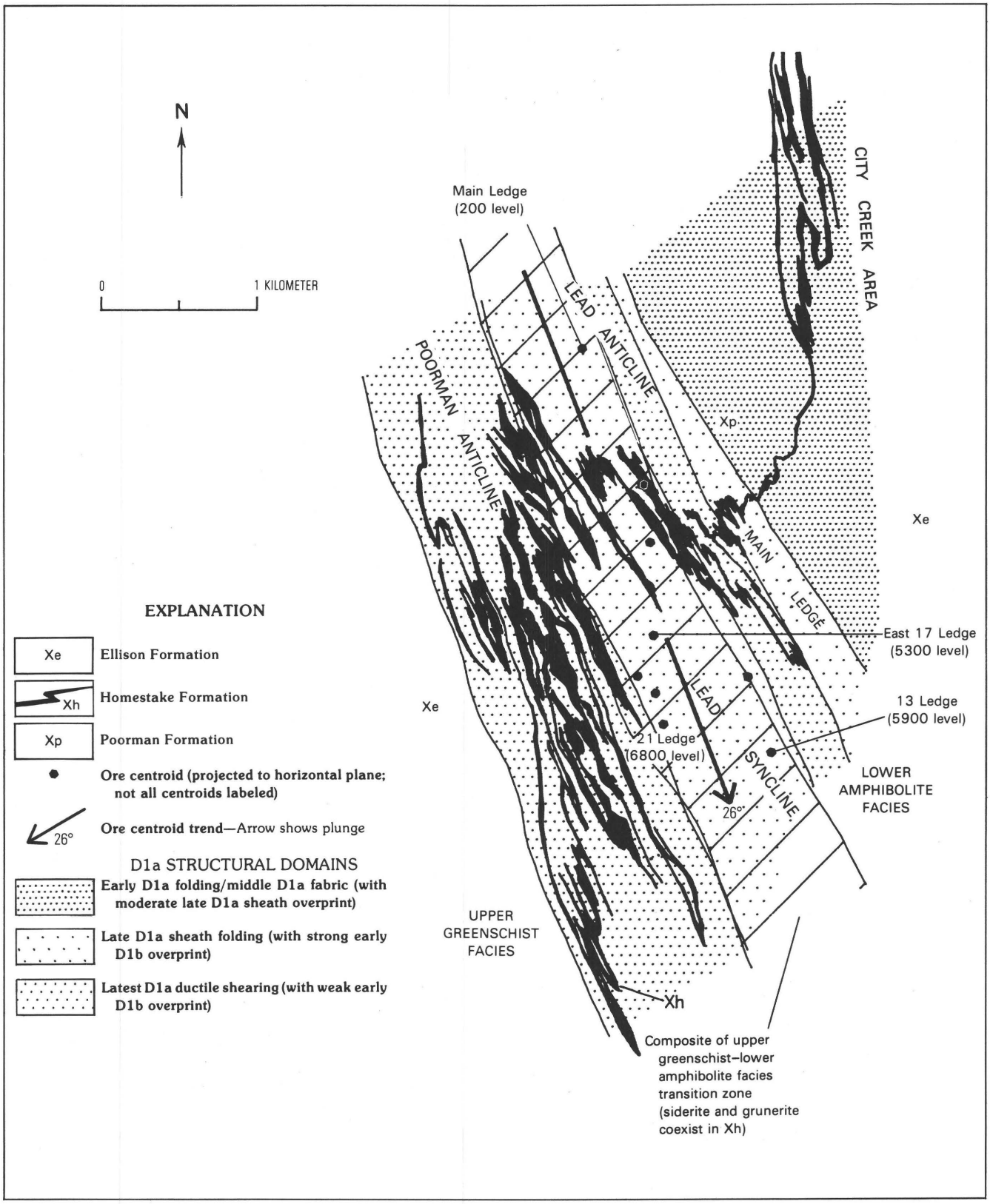

Figure J25. Geology of 2600 level, showing upper greenschist–lower amphibolite facies metamorphic transition zone, D1a structural domains, and ore centroid trend.

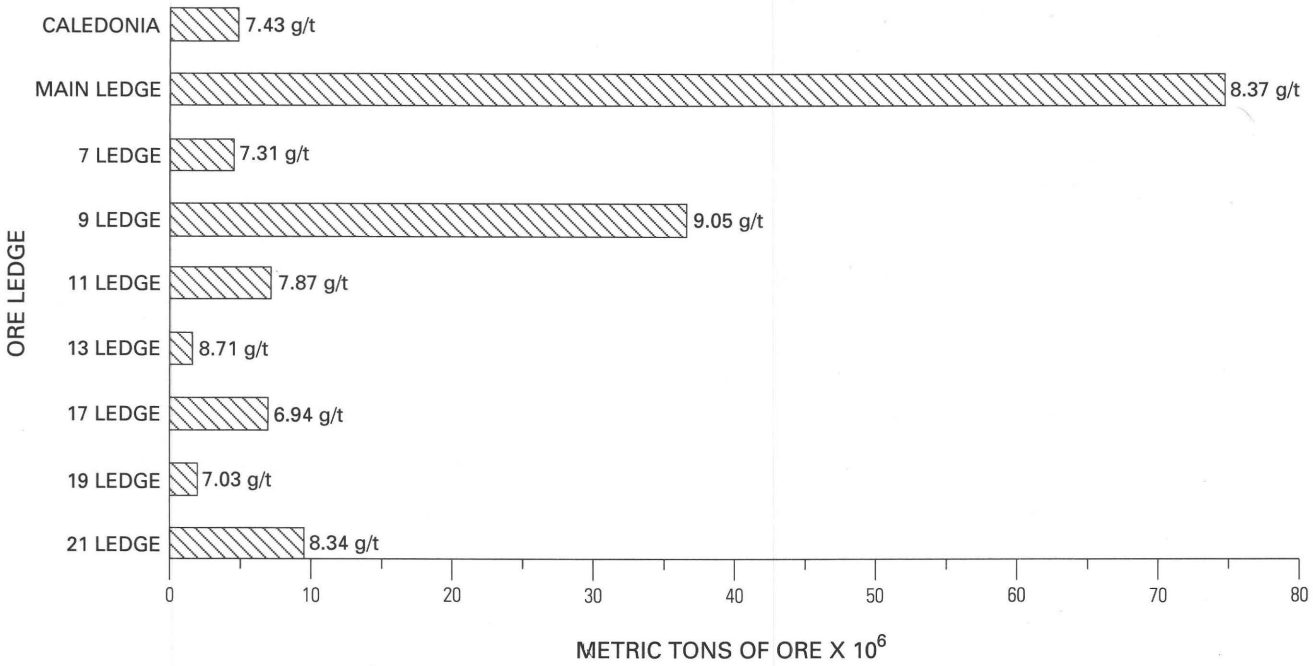

Figure J26. Histogram of ledge production in the Homestake mine, showing average (prerecovery) grade in grams per short ton. Cumulative gold production plus ore reserves (surface and underground) are 147.7 million metric tons averaging 8.36 g Au/t through 1988, shown by ore ledge.

bodies on the 3050 level. Ore bodies in figure J28 occur in the lower tail of 9 Ledge; their forms are generally characteristic of upper and lower tail ore-body geometry in other ore ledges. The detail of figure J28 reveals that individual ore bodies are discontinuous along plunge. The "D" limb structure of 9 Ledge between the 5600 and 6050 levels (fig. J28) contains 12 ore bodies; the largest is 65 m in plunge length. The 9 Ledge ore system as a whole contains 196 individual ore bodies, which range in volume from less than 2,000 to greater than 1 million t.

Ore mineralization took place within and adjacent to dilated segments of middle D1b shears, which tended to dilate preferentially in Homestake Formation. Ore mineralization where confined within the shear segments formed sharp shear contacts between ore and adjacent country rocks (figs. J29, J30). Middle D1b shears throughout the mine show reverse movement with northeast blocks consistently up, and with vertical to moderate northeast dips.

The type of mineralization that occurred within middle D1b shear zones resulted in a mineral assemblage comparable in the classical sense to a mesothermal vein assemblage and referred to herein as "shear ore." "Shear ore" commonly shows little if any original fabric and generally comprises stage II quartz veins with associated chlorite, siderite, arsenopyrite, and minor pyrrhotite (figs. J29, J30). Chlorite replacement of the host rock (largely of biotite) in middle D1b shears has been extensive. "Shear ore" in figure J30 is contained within a middle D1b shear zone, which lies on reactivated late F1a foliation (late S1a) entirely in the Homestake Formation. This ore occurrence is locally devoid of quartz veins and retains some relict original fabric in the form of chert. Gold grades of "shear ore" are generally excellent, as illustrated in figure J30. Elevated gold values (26.74 and 2.74 g Au/t) in the layered pyrrhotite zone left of the middle D1b shear zone represent a second type of ore, referred to herein as "replacement ore." The "replacement ore" (figs. J29, J30) reflects leakage off master middle D1b shears via early S1b axial-plane foliation and earlier foliations. Disseminated pyrrhotite replaced certain siderite-rich beds within the Homestake and is deposited in discontinuous layers along foliation surfaces. Pyrrhotite within the replacement ore zone also occurs in minor dilatant zones along quartz, siderite, ankerite, and chlorite mineral grain boundaries. The replacement process, or sulfidation, was dependent on an increase in permeability developed on existing bedding or foliation surfaces during middle D1b shearing. In addition to sulfidation of siderite-bearing parts of iron-formation units, moderate chlorite and siderite (scattered coarse grains and grain aggregates) alteration occurred within the replacement ore zone. The siderite component within the replacement and shear portion of the ore body is distinctly coarser grained and paragenetically younger than very fine grained matrix siderite observed within layers in barren carbonate-facies iron-formation. "Replacement ore" as currently defined is everywhere spatially associated with gold-bearing and chloritically altered middle D1b shears.

Figure J27. Isometric view of Main Ledge on 1850, 2450, and 3050 levels. See figure J6 for location of Main Ledge relative to Lead anticline.

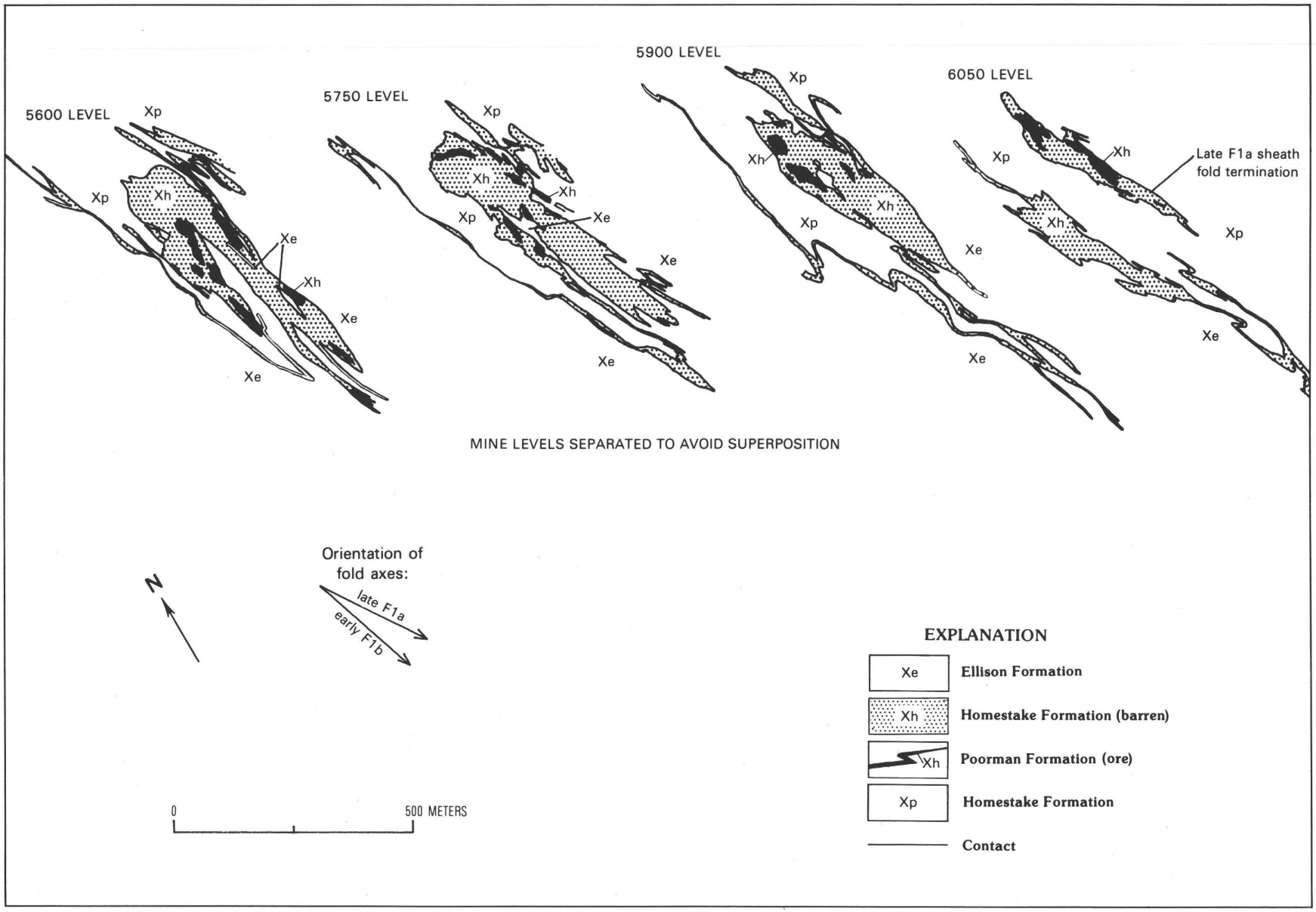

Figure J28. Geologic map of "D" limb of 9 Ledge on the 5600, 5750, 5900, and 6050 levels. Configuration of ore bodies is shown enclosed within late F1a sheath fold structures collectively located in hinge of Lead anticline. Tertiary intrusive rocks not shown.

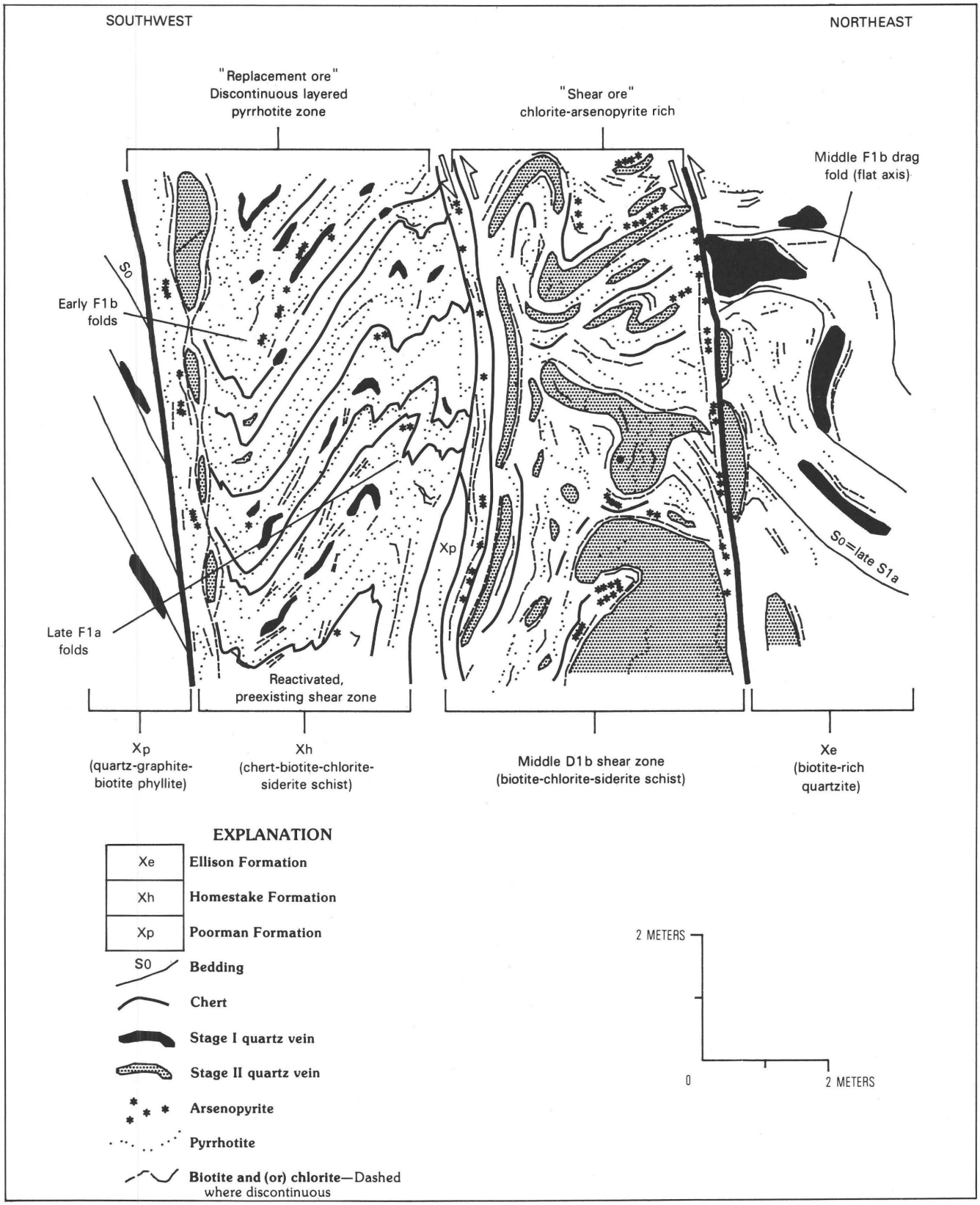

Figure J29. Face sketch, 7 Ledge, 1550 level, 58–61 stope, Homestake mine. Near-vertical line, shear; heavy line, major shear; barbs show relative movement.

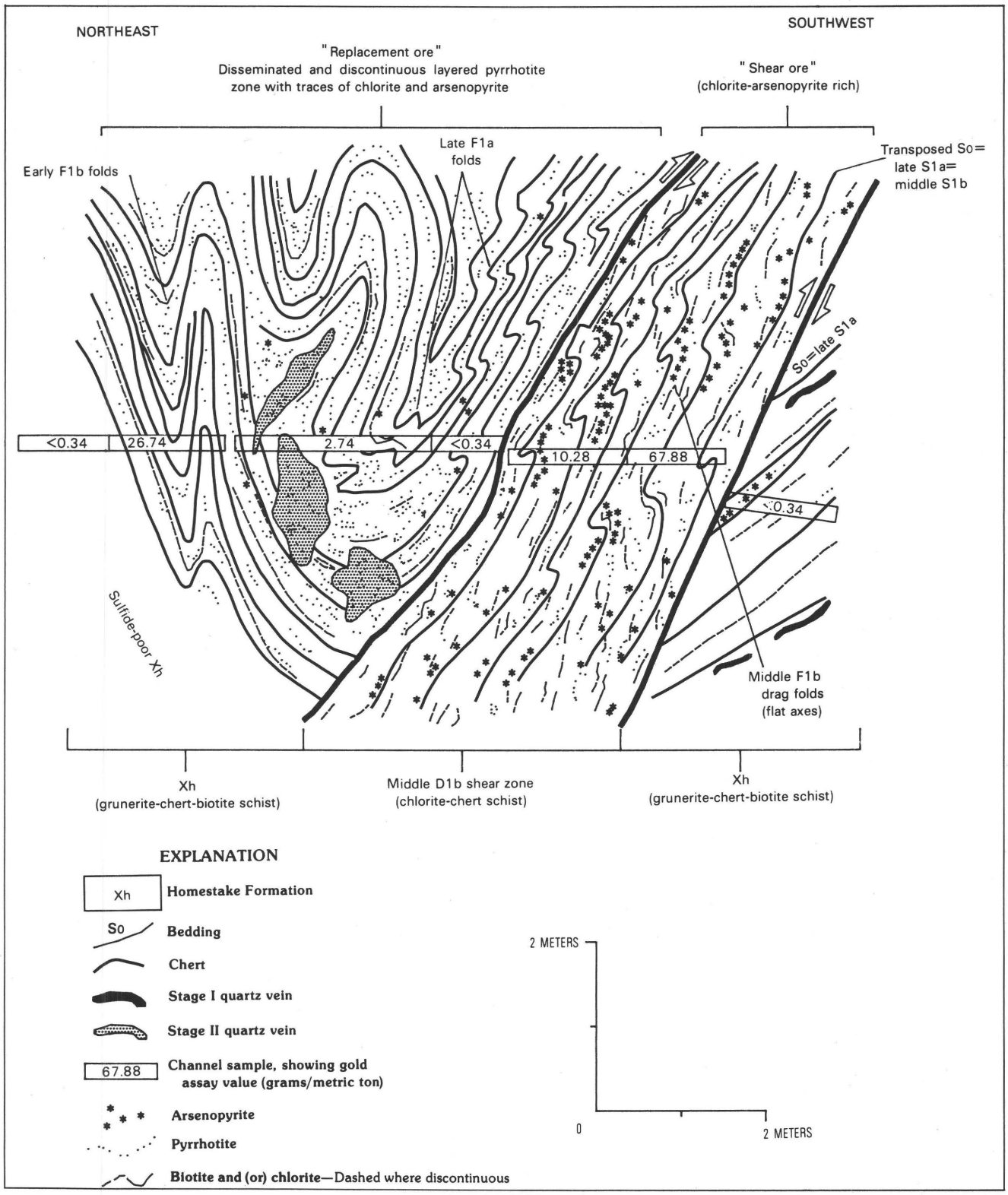

Figure J30. Face sketch, 13 Ledge, 6350 level, 55 stope, west "B" limb, Homestake mine. Heavy line, major shear; barbs show relative movement.

In figure J29, the entire shear zone is ore bearing; it lies disconformably between a steep northeast-dipping and drag-folded Ellison hanging wall and a steep northeast-dipping Poorman footwall. The chaotic middle D1b deformation fabric, Stage II quartz veins (see section, "Quartz veins"), and gold mineralization overprinted all other observed fabrics. Stage II quartz veins within the middle D1b shear zone are unfractured, and most were emplaced in their present tabular to irregular form; all are lined with undisrupted and continuous vein selvages consisting of chlorite, arsenopyrite, and minor pyrrhotite. The right side of the shear zone (toward northeast) is dominated by "shear ore" consisting of arsenopyrite and abundant chlorite. The left side (toward southwest) is dominated by "replacement ore" consisting of pyrrhotite in discontinuous layers with only minor chlorite, a common fabric observed in many ore bodies.

The shear zone in figure J30 is 3 m wide, contains "shear ore" consisting of abundant arsenopyrite and chlorite with minor pyrrhotite, and dips steeply northeast. It is discordant to stratigraphy, contains a transposed and shear-induced foliation, and shows the physical result of middle D1b reverse shearing contemporaneous with gold mineralization. Local disseminated and discontinuous layered pyrrhotite, minor arsenopyrite, and ore-grade gold overprint late F1a and early F1b folds of the hanging wall; both fold sets are truncated by the shear zone. This "replacement ore" was also related to the shear zone; it terminated beyond 6 m into the hanging wall. Mineralization consisted of two styles of coeval development (deposition of "shear ore" within the dilating middle D1b shear zone and "replacement ore" developed outward from the shear zone), and these deposits have been undeformed since.

The gold distribution within an ore ledge centers around high-grade (>15.5 g Au/t) zones that form the nucleus of individual ore bodies (figs. J31, J32). Lower grade material (<4.7 g Au/t) lies lateral to and on strike extensions of these high-grade zones. The size of high-grade parts of an ore body was determined by the intensity of middle D1b shearing, which in turn was controlled by position within the Homestake Formation. The largest high-grade ore zones are found in core areas, as illustrated by gold-grade distribution in Main Ledge on the 2450 level (fig. J31). Also indicated in figure J31 is the extension of ore into Poorman and Ellison Formations, a relatively common feature throughout the mine. Poorman- and Ellison-hosted gold occurs in middle D1b shears near the Homestake Formation and represents only a small percentage of the total gold produced from the mine.

Gold-grade distribution in lower tail areas is sporadic and discontinuous, as illustrated in figure J32. Small zones of subeconomic gold-bearing rock exist in upper and lower tail areas throughout the mine, similar to the grade distribution in figure J32. These zones may contain high-grade (>15.5 g Au/t) gold-bearing rock that is less than a meter wide, or low-grade (1.5–4.7 g Au/t) material that is several meters wide. The frequency of occurrence of subeconomic segments decreases with increasing distance from the core area. The current mining cutoff is a 5 m width assaying 4.7 g Au/t.

Ore Mineralogy

Ore bodies in the Homestake mine are sulfide rich, dominated by pyrrhotite. Ore bodies contain varied amounts of carbonate and silicate gangue minerals including chlorite, siderite, grunerite, quartz, biotite, ±garnet, with minor ankerite, muscovite, and albite, in addition to graphite, listed in decreasing order of abundance (Noble, 1950; present authors). Sulfides include pyrrhotite and arsenopyrite, with subordinate pyrite and chalcopyrite. Pyrrhotite:arsenopyrite ratios in ore bodies are generally estimated in the range of 1:2 to 10:1. In general, ratios increase from eastern to western ore ledges and from upper to lower tails. Magnetite, hematite, ilmenite, galena, sphalerite (microscopic), and visible gold are locally present (Noble, 1950; McLaughlin, 1933). Ore-body mineralogy at Homestake has been described by Gustafson (1930, 1933); McLaughlin (1933); Noble (1950); Slaughter (1968); and Chinn (1969). The most detailed discussion, that of Noble (1950), is valid today even though western ore ledges (17, 19, 21) were not yet discovered in 1950. Hand specimens and polished sections of typical ore specimens are shown in figures J33, J34, and J35.

Pyrrhotite

Pyrrhotite is present in three textural forms: streaks, blebs, and layers. Pyrrhotite is brownish bronze and is either magnetic (2M polytype) or nonmagnetic (6H polytype), the magnetic polytype being more common. Pyrrhotite streaks are commonly found in iron-formation and phyllite of adjacent formations; they are not associated there with anomalous gold. In iron-formation, pyrrhotite streaks are generally oriented parallel to transposed bedding, are crosscut or replaced by pyrrhotite blebs and layers, and are locally replaced by arsenopyrite. They are less than 1 mm to 3 mm thick, 1 mm to 1 cm in length (parallel to foliation), and flattened in the plane of foliation. This pyrrhotite variety is the only sulfide of possible sedimentary derivation.

Pyrrhotite blebs occur in irregular and elliptical morphological varieties. Blebs measure less than 1 mm to several centimeters in maximum dimension. Irregular blebs locally contain fragments of quartz veins and country rock. Blebs are common in disseminated lenses and masses within and adjacent to Stage I (elliptical blebs) and Stage II

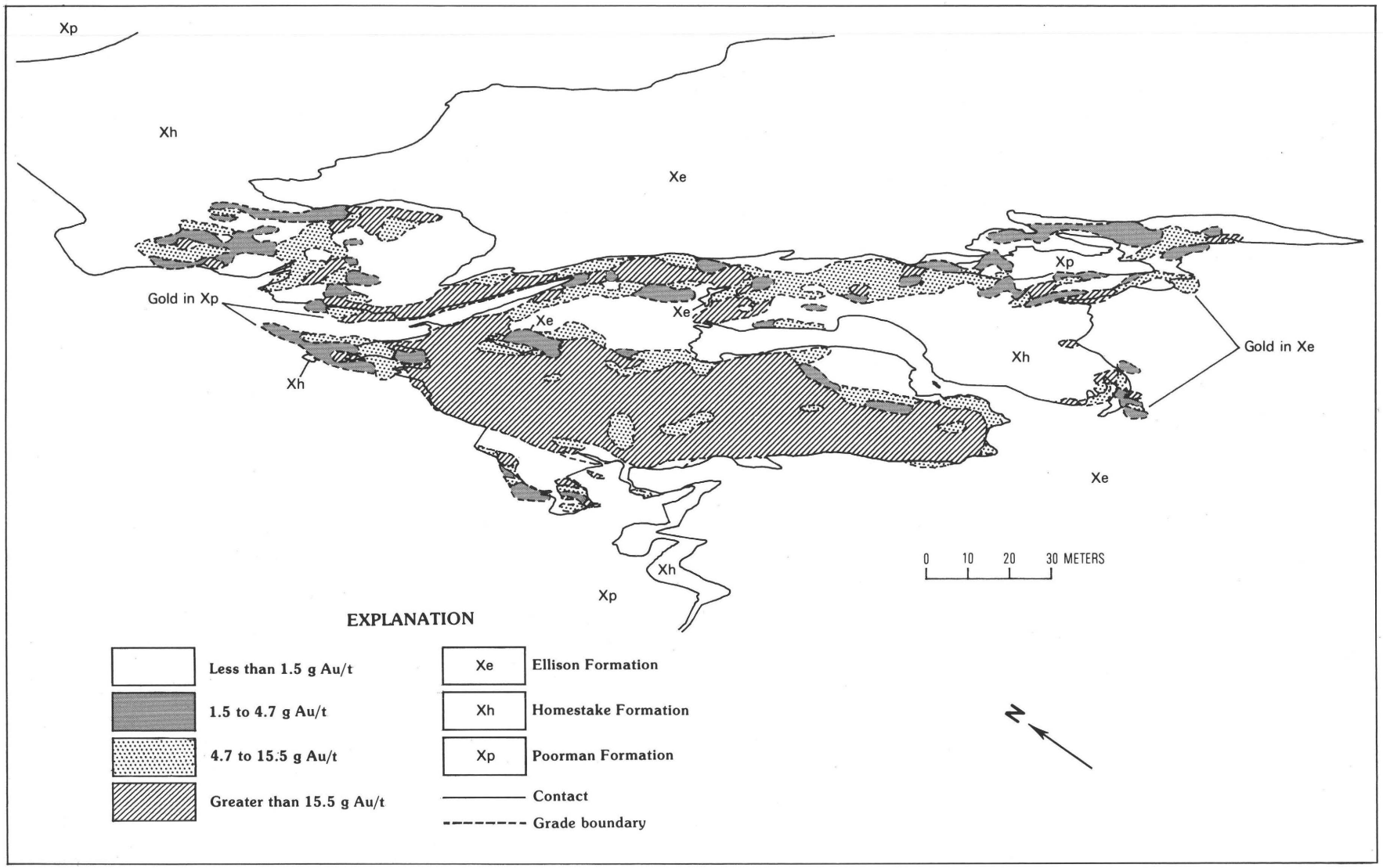

Figure J31. Geologic map showing gold grades for 2450 level, Main Ledge. This map depicts a core area position in the ore ledge. (See figs. J6 and J27 for relative location.)

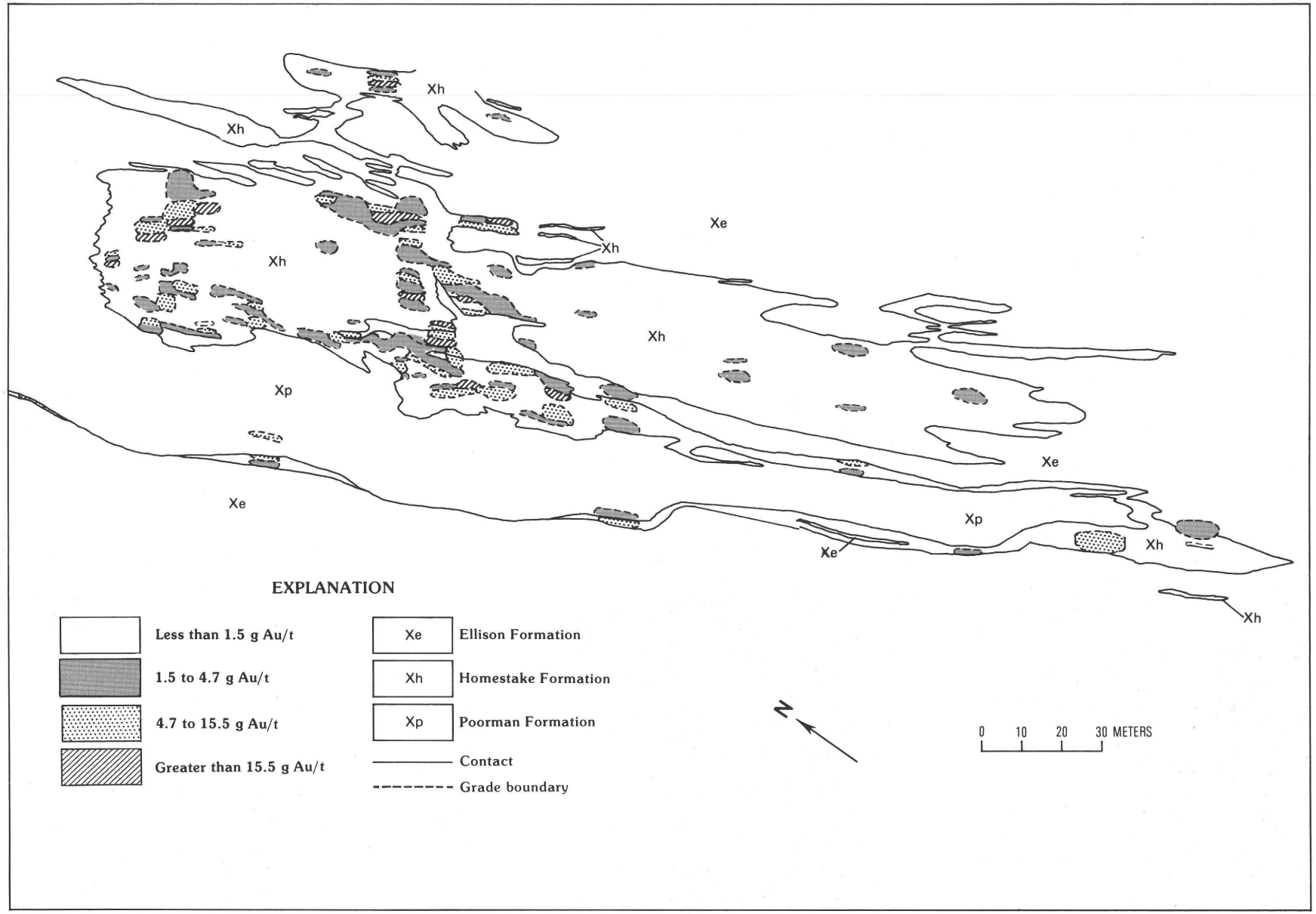

Figure J32. Geologic map showing gold grades for "D" limb of 9 Ledge, 5750 level. This map depicts a lower tail position in the ore ledge. (See figs. J6 and J28 for relative location.)

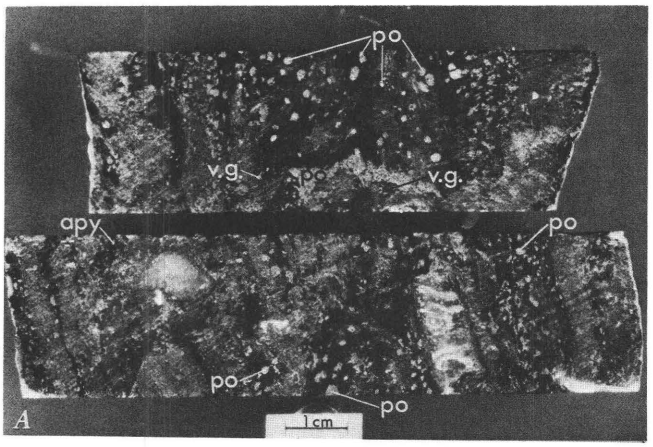

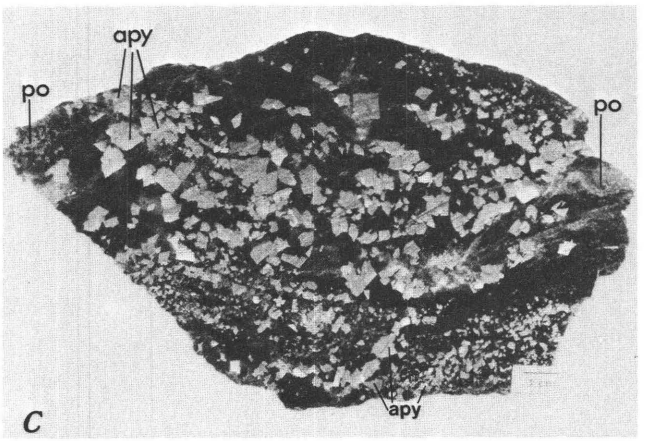

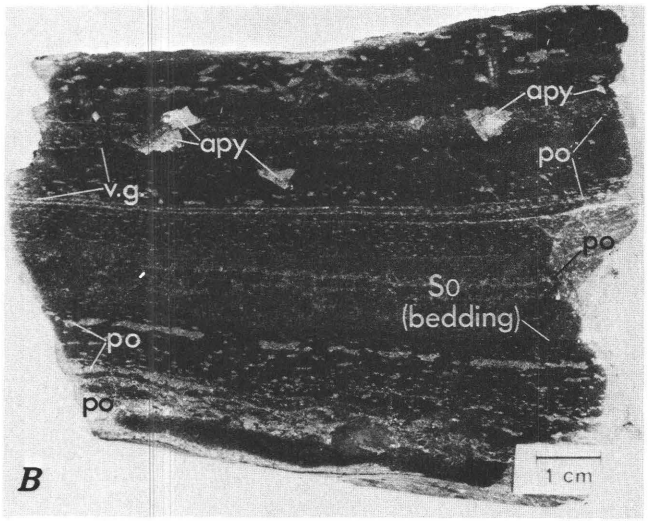

Figure J33. Photographs of typical ore specimens, Homestake mine; po, pyrrhotite; apy, arsenopyrite; v.g., coarse visible gold. *A*, Pyrrhotite blebs in grunerite- and siderite-rich layers interbedded with thin chert beds from drill core in a 15 Ledge ore body, 8000 level. Minor chlorite is present in the grunerite- and siderite-rich strata. Two small grains of coarse visible gold border irregular pyrrhotite blebs. A 2 m interval assayed 37.3 g Au/t. Modal sulfide contents are 8 percent pyrrhotite, <<1 percent coarse gold, and <<1 percent arsenopyrite. *B*, Typical layered pyrrhotite (some disseminations and blebs) interlayered with biotite-rich chert and siderite in an ore body in 21 Ledge, 7400 level. Thin layers that enclose thinner pyrrhotite layers contain minor chlorite, and are locally replaced by isolated arsenopyrite porphyroblasts. This layered texture is restricted to ore bodies. Two single grains of coarse visible gold occur within two pyrrhotite layers. Modal sulfide contents are 12–14 percent pyrrhotite, <1 percent arsenopyrite, and <<1 percent coarse visible gold. *C*, Coarse-grained arsenopyrite within a chlorite-rich siderite matrix from an ore body in 7 Ledge, 1550 level. Specimen came from a 2.0-m-wide Stage II quartz-vein selvage within which coarse visible gold is present locally. The gold borders and is within arsenopyrite porphyroblasts, and is enclosed as isolated platy grains in chlorite. This ore is typically of exceptional grade and averages >16.0 g Au/t. Modal sulfide contents are 15–20 percent arsenopyrite and <1 percent pyrrhotite.

(irregular blebs) quartz veins. Locally, irregular blebs in Stage II quartz veins are intergrown with arsenopyrite, and everywhere associated with low-grade (>1.0 g/t) to ore-grade (>4.7 g/t) gold. Elliptical blebs are not associated with gold. Pyrrhotite blebs in Stage III quartz veins are also of the irregular variety and are locally associated with anomalous gold (as much as 300 ppb).

Pyrrhotite layers occur as 1- to 2-mm-thick seams, or 1- to 4-cm-thick disseminations in layers alternating with parallel transposed beds of chert±biotite±chlorite in Homestake Formation. Pyrrhotite layers are found on foliation-bedding surfaces as microdilational infilling between stratigraphic beds and as replacement disseminations in certain strata (siderite beds) near or adjacent to Stage II quartz veins. Pyrrhotite layers are confined to ore bodies, contain sparse isolated grains of arsenopyrite porphyroblasts, locally contain coarse grains of gold, and assay greater than 1.0 g Au/t; indeed, they generally assay greater than 4.7 g Au/t. Pyrrhotite layers and blebs are commonly intergrown, and both locally replace pyrrhotite streaks. Zones of pyrrhotite layers invariably become discontinuous within a few meters from margins of Stage II quartz veins. This texture is exclusively associated with Stage II quartz veins within some ore bodies. Pyrrhotite layers are most common in western ore ledges at lower metamorphic grades and where middle D1b shear foliation is best developed. In ore bodies, combined pyrrhotite content (by volume) varies from 5 percent to more than 40 percent.

Arsenopyrite

Arsenopyrite is an important indicator of gold and is at least a minor constituent in parts of all ore bodies. Arsenopyrite content (by volume) varies in ore bodies from a trace to more than 15 percent. Typical occurrence of arsenopyrite is as tin-white, euhedral, pseudo-orthorhombic, prismatic crystals with diamond-shaped cross sections; only rarely is it deformed into stretched crystals. Crystals are

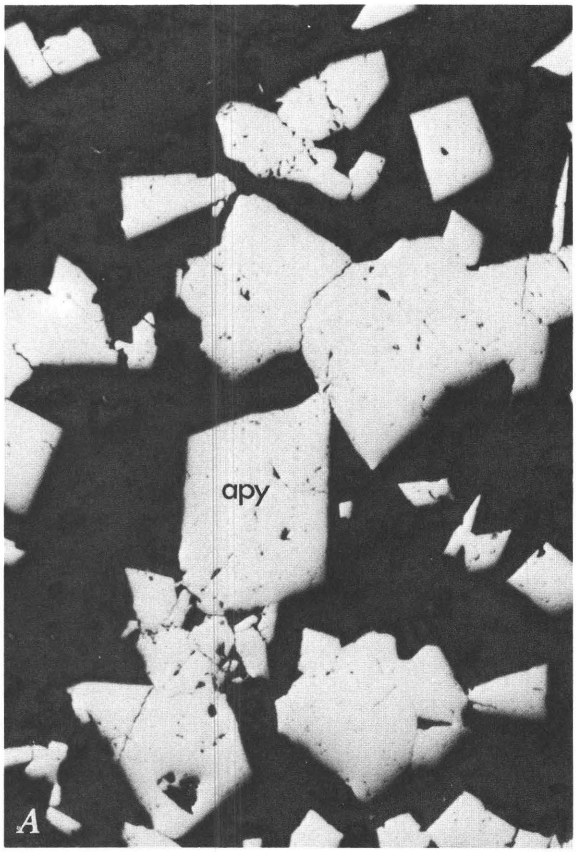

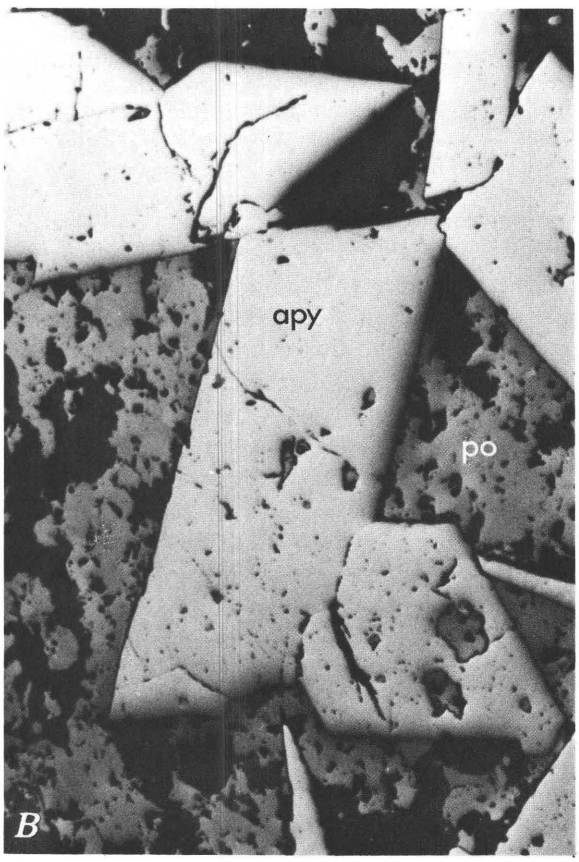

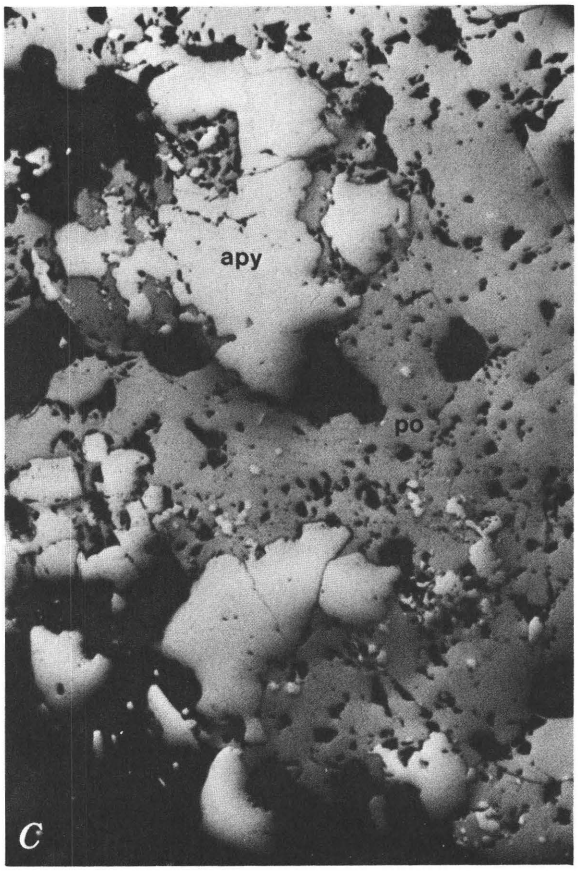

Figure J34. Photomicrographs showing typical arsenopyrite occurrence; po, pyrrhotite; apy, arsenopyrite. *A*, Coarse arsenopyrite from the selvage of a Stage II quartz vein. Coarse, disseminated, subhedral to euhedral arsenopyrite is shown in a chlorite matrix. Field of view is 4 mm vertically. *B*, Typical layered arsenopyrite, which at high magnification is resolved as euhedral arsenopyrite crystals whose interstices are filled with pyrrhotite. Field of view is 2 mm vertically. *C*, Replacement of arsenopyrite by pyrrhotite with "islands" of arsenopyrite in pyrrhotite. Field of view is 2 mm vertically.

generally from 2 mm to 2.5 cm long and are commonly striated parallel to [001] (Noble, 1950). Arsenopyrite is disseminated in the Homestake Formation (and locally in the Poorman and Ellison) adjacent to Stage II veins and may exist as densely crowded groups of crystals. Chlorite-rich and locally pyrrhotite rich rock adjacent to Stage II quartz veins, generally near or within ore bodies, contains the most abundant arsenopyrite (Noble, 1950; present authors). Arsenopyrite is generally, but not everywhere, associated with ore-grade (>4.7 g/t) gold. Stage II quartz veins occur without exception in the vicinity of abundant arsenopyrite concentrations.

Both coarse- and fine-grained varieties of arsenopyrite are commonly (though not everywhere) associated with ore-grade gold (>4.7 g Au/t). The coarse-grained

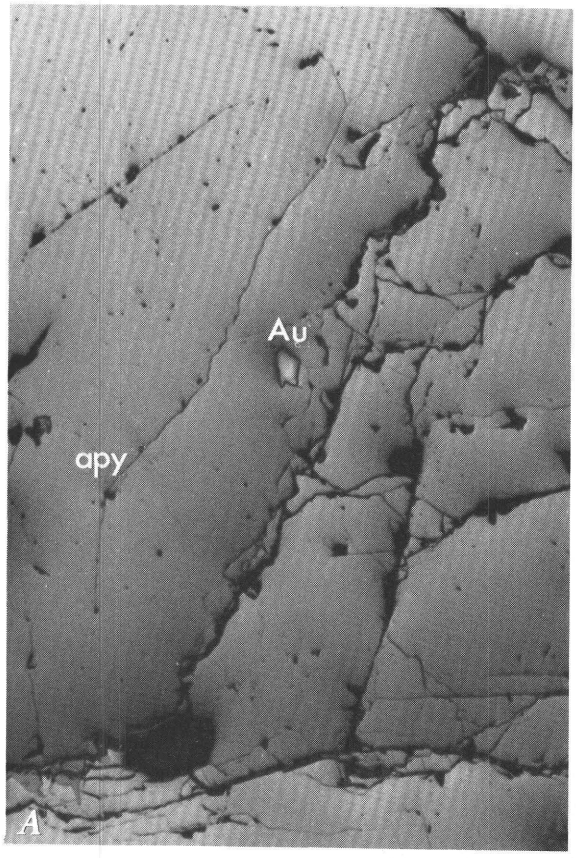

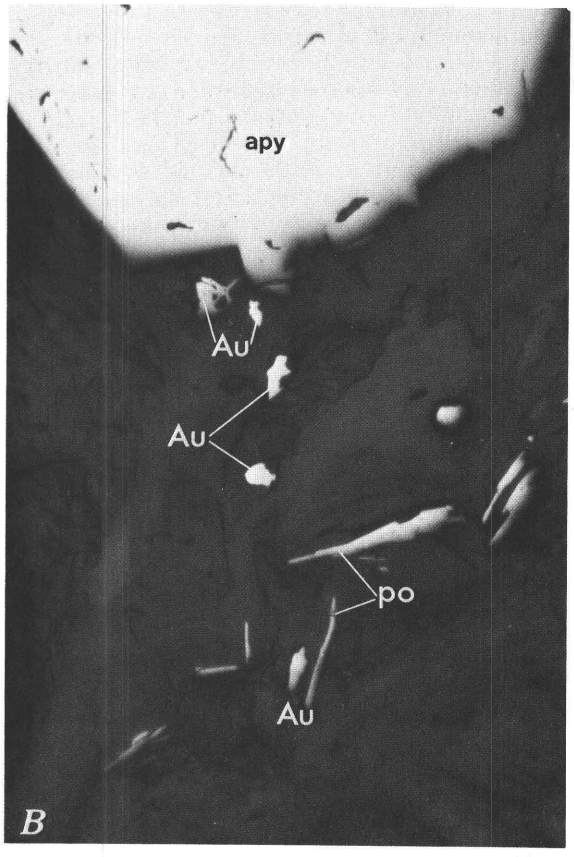

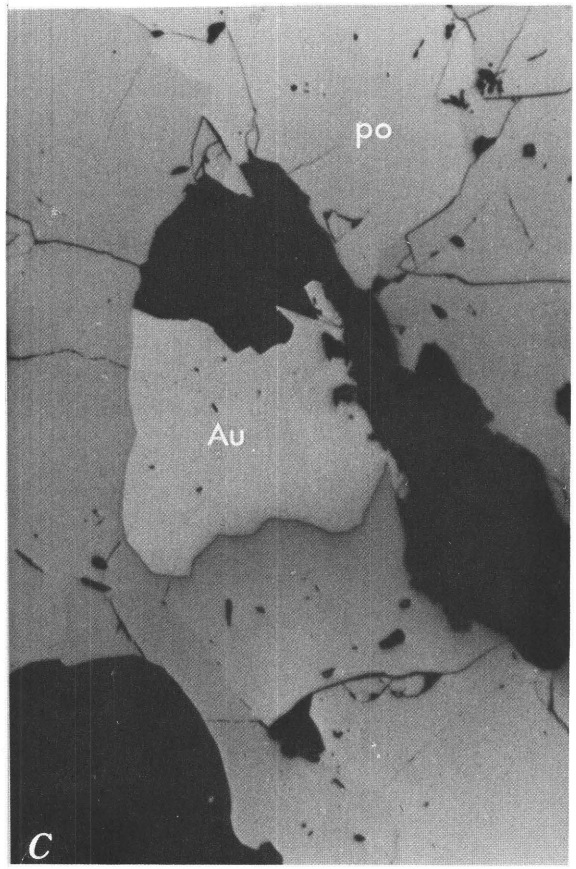

Figure J35. Photomicrographs showing occurrence of gold; apy, arsenopyrite; po, pyrrhotite; Au, gold. *A*, Gold grain in arsenopyrite. Gold grain is 0.1 mm in maximum dimension. *B*, Gold, pyrrhotite, and arsenopyrite in a matrix of siderite, chlorite, and biotite. Field of view is 2 mm wide. *C*, Gold intergrown with pyrrhotite. Field of view is 1 mm vertically.

variety is the more common and is found as (1) single porphyroblasts or aggregates within Stage II quartz veins, (2) single porphyroblasts or aggregates in selvages adjacent to Stage II quartz veins, and (3) random grain aggregates within or near ore bodies. Coarse-grained arsenopyrite is found intergrown with pyrrhotite blebs and layers. The fine-grained variety is found as selective replacements of biotite-rich layers or introduced along microdilatancies along middle D1b shear foliations. Arsenopyrite layers, like pyrrhotite, are discontinuous, commonly intergrown with pyrrhotite layers, and exclusively associated with margins of Stage II quartz veins. Arsenopyrite in these layers comprises randomly oriented aggregates of intergrown euhedral grains extending in two dimensions in the plane of middle D1b shear foliations or subparallel to compositional layering.

Pyrite

Early Proterozoic-age pyrite is found within most ore bodies. It is more abundant (by volume) in upper eastern ore

ledges (trace to 10 percent), and sparse in lower eastern and western ore ledges (<1 percent). Pyrite is found as medium-grained (1–5 mm) cubes in the upper mine levels, whereas in the lower mine levels it is very fine grained (<1 mm) and cubic, and generally requires detection by microscopic methods. It occurs as a fine-grained replacement of pyrrhotite streaks, blebs, and layers. Tertiary-age pyrite is coarse grained (3 mm to 1 cm), is spatially related to Tertiary igneous dikes and late vuggy quartz veins, and is clearly secondary, locally as a replacement of Precambrian pyrrhotite.

Gold

Gold is invariably associated with irregular pyrrhotite blebs and layers, and commonly with arsenopyrite. Most gold is anhedral, very fine grained (<<1 mm), and disseminated throughout the ore bodies; highest concentrations are near margins of some Stage II quartz veins. As documented by Noble (1950), gold in general is spatially associated with the assemblage composed of quartz-chlorite-pyrrhotite-arsenopyrite. The gold-bearing assemblage largely constitutes alteration selvages found along walls of Stage II quartz veins. Gold grains occur as microscopic to submicroscopic blebs or flakes found within and along grain boundaries of silicate, sulfide, and carbonate gangue minerals, as coarse intergrown networks with quartz, and as micrometer-thin smears on chlorite parting surfaces. Visible gold is also observed along grain boundaries of arsenopyrite and pyrrhotite, and along fractures in arsenopyrite, pyrrhotite, and garnet. Main and 9 Ledges contained the most abundant coarse gold on the upper levels; however, visible gold is common throughout the mine.

Gold is reported as 899 fine (based on mill recoveries), and the remaining 101 as silver. Based on microprobe analyses from 56 gold samples across the deposit (R.M. Honea, oral commun., Sept. 9, 1988), average gold and silver compositions of gold grains are 86.09 wt. percent and 13.91 wt. percent, respectively. High and low silver concentrations are 21.20 wt. percent and 6.21 wt. percent, respectively. Four samples contained silver exceeding 20.00 wt. percent. The gold:silver ratio averages 6.2. J.C. Groen (oral commun., July 15, 1988) analyzed 36 selected gold samples from all ore ledges across the mine. His gold:silver ratios ranged from 3.0 to 10.0, averaging 4.0. The combined data suggest an average gold:silver ratio of 5:1 for the Homestake deposit. Gold overall at Homestake does not contain enough silver to be classified as electrum. Gold fineness is calculated at 861 fine based on Honea's work, and 838 fine based on Groen's work. Percent of silver recovered at Homestake is much lower than that of gold, and has varied over time.

Other Minerals

Chalcopyrite is common in trace amounts in most ore bodies. It occurs as microscopic to <2 mm anhedral grains, commonly as streaks or blebs in pyrrhotite. Galena and particularly sphalerite are rare, and present only in certain quartz veins. The presence of minor löllingite has been verified by X-ray diffraction techniques in some ore bodies by us and by R.M. Honea (oral commun., Sept. 9, 1988). Magnetite, hematite, and ilmenite are minor accessory minerals; they are generally observed petrographically in polished thin sections.

Tertiary-Age Mineralization

Tertiary-age mineralization was temporally and spatially related to Tertiary igneous dikes and sills, and represents the latest stage of mineralization recognized in the mine. It was a minor event, noneconomic, characterized by minor calcite, quartz, pyrite, dolomite, siderite, sphalerite, galena, molybdenite, chalcopyrite, anhydrite, fluorite, gypsum, chlorite, barite, rhodochrosite, realgar, native arsenic, and rarely gold-silver tellurides (Noble, 1950; present authors). These minerals are found in late Tertiary quartz veins, disseminations, and open-space fillings in and around fractures cutting all Tertiary intrusive and nearby Precambrian rocks.

Major and Trace Element Geochemistry

A large geochemical database existing in Homestake files is currently being evaluated. A limited amount of new geochemical data for selected ore ledges is presented in table J8, and analogous data on barren (to weakly anomalous) iron-formation were given previously in table J4. The reader is referred to Bidgood (1977) and Fantone (1983) for other published geochemical data.

Data from table J8 combined with additional data from Homestake files (not shown) allow some generalizations that compare and contrast the geochemistry of barren and ore-bearing Homestake Formation. The formation, in general, can be characterized as having rather consistent values for CaO, MgO, Na_2O, MnO, TiO_2, and P_2O_5. Oxides that exhibit a depletion in ore-bearing Homestake relative to barren Homestake include SiO_2, FeO, and K_2O. Ore bodies tend to show a general enrichment in sulfur, CO_2, gold, arsenic, and silver with slightly elevated values for Fe_2O_3 and some metals of the first transition series (vanadium, chromium, cobalt, nickel, copper) along with lead and zinc. Tungsten is barely detectable in barren and mineralized rock at an average value of about 2.6 ppm. A distinct trend observed for these elements in both barren and mineralized iron-formation is as follows:

$$Cu \simeq Zn > V > Cr > Co > Pb > Ni > W$$

Table J8. Major, minor, and trace element geochemistry of mineralized Homestake Formation samples, Homestake mine

[Unpublished Homestake data. Trace element values in parts per million, major and minor element values in weight percent. 13 Ledge sample contains visible gold. Leaders (--), not determined. Samples analyzed by atomic absorption and ICP methods, Skyline Labs, Wheatridge, Colo. CO_2 determined by carbon analyzer. GDS, grunerite-dominant schist; SDP, siderite-dominant phyllite]

Rock type	Major and minor elements												
	SiO_2	Al_2O_3	Fe_2O_3	FeO	MgO	CaO	Na_2O	K_2O	MnO	TiO_2	P_2O_5	elemental S (tot)	CO_2
1) GDS (ore)	59.40	4.50	4.90	18.40	5.20	0.35	0.04	0.93	0.381	0.26	0.08	0.86	0.17
2) GDS (ore)	47.40	9.00	13.30	15.00	4.80	.63	.24	1.40	.465	.21	.04	.42	.14
3) GDS (ore)	29.20	11.30	11.60	24.80	7.80	1.10	.11	.35	.923	.40	.18	1.10	4.03
4) GDS (ore)	32.20	10.00	12.60	16.80	6.40	.94	.03	.40	.484	.37	.07	4.00	2.94
5) SDP (ore)	26.20	6.40	17.10	18.20	5.50	1.50	.03	.62	.960	.17	.04	4.20	6.53
6) SDP	47.70	3.60	4.00	22.60	5.10	2.90	.08	.68	.633	.12	.26	<0.02	6.48
7) SDP (ore)	25.50	11.30	15.19	7.30	4.00	5.40	.12	3.50	.910	.40	.04	5.90	8.23
8) SDP (ore)	54.30	4.00	9.80	14.30	4.20	1.80	<0.01	.37	.470	.12	<0.02	4.20	3.57

Sample	Trace elements														
	Au	Ag	Cu	Pb	Zn	Co	Ni	Cr	W	As	V	Zr	Ba	Sr	Rb
1) Main Ledge	6.80	0.6	40	<5	10	10	10	15	3	440	60	30	210	<10	30
2) Caledonia	8.10	6.9	150	85	190	20	10	25	5	47,000	80	55	190	30	30
3) 11 Ledge	12.68	.6	55	<5	95	20	20	30	4	2,400	100	--	50	20	--
4) 13 Ledge	67.54	4.1	35	<5	85	15	20	35	<2	60,500	885	80	<10	20	30
5) 15 Ledge	5.14	.7	135	<5	75	25	15	30	4	42,500	90	70	150	30	30
6) 15 Ledge	.16	<0.2	<5	<5	25	<5	<5	15	<2	<5	35	20	150	60	30
7) 17 Ledge	8.45	.2	10	125	65	15	--	--	<2	53,500	--	115	--	30	10
8) 21 Ledge	7.54	1.4	90	<5	50	15	10	30	2	1,300	45	30	100	40	20

In barren iron-formation, however, values for many of these elements are at or below detection limits for atomic absorption analytic methods, with the exception of copper, zinc, vanadium, and chromium. Other notable trace constituents in all Homestake Formation include the alkaline-earth components BaO, SrO, and Rb_2O. BaO is more abundant than the other two by an order of magnitude, although all three oxides combined rarely exceed 0.05 wt. percent.

In terms of constituents that are enriched in the ore bodies (sulfur, CO_2, gold, arsenic, and silver), sulfur correlates best with gold and is present in amounts ranging from <0.2 wt. percent total S to as much as 13.5 wt. percent. This correlation corresponds to the direct spatial association of ore-grade gold and abundant pyrrhotite in the vast majority of ore bodies. A typical example is shown for 21 Ledge in figure J36. Arsenic (as arsenopyrite) exhibits a weak to moderate correlation with gold (+ 0.5), although within an ore ledge arsenic is a general indicator of ore-grade gold (fig. J36). The presence of abundant arsenopyrite does not always indicate associated ore-grade gold, especially in extreme upper tail areas of a ledge. Arsenic values in ore samples range from below 5 ppm (detection limit by atomic absorption with hydride-generation analysis) to about 5 wt. percent. Anomalous silver is associated with gold. Silver values are generally below 0.2 ppm in barren Homestake Formation and range from 0.2 ppm to nearly 7.0 ppm in ore bodies.

Silver exists in solid solution in gold grains. As previously indicated, the silver content rarely exceeds 20 wt. percent as determined by electron microprobe. Based on available data, no systematic trends are recognizable in the gold:silver ratio within or between ore ledges.

Elevated CO_2 values in ore bodies can be directly attributed to introduced carbonate. The introduction of carbonate accompanied hydrothermal alteration and gold mineralization.

Other trace metals found in ore-bearing iron-formation that have not been detected in barren Homestake (AA/ICP methods) include tellurium and selenium in single-digit parts per million levels. A few platinum and

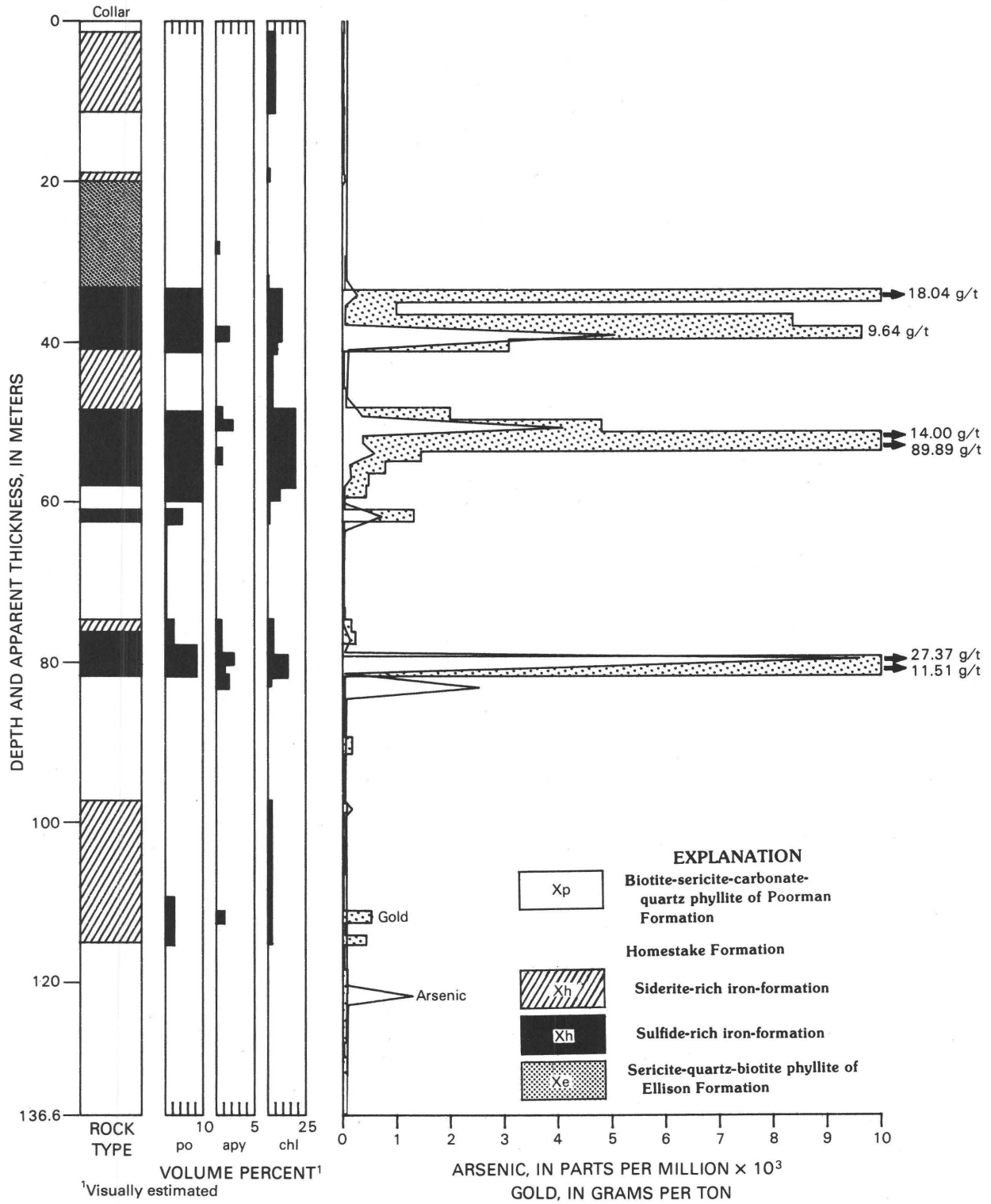

Figure J36. Distribution of gold, arsenic, total sulfide, and chlorite in drill hole 16802A, 21 Ledge, 7400 level. Pyrrhotite is present in Ellison and Poorman Formations in trace amounts (<1 volume percent); po, pyrrhotite; apy, arsenopyrite; chl, chlorite.

palladium analyses have been performed, but the elements have not been detected.

At the present time, no indicator element, element suite, or element ratio, with the possible exception of sulfur, shows any practical consistent or systematic trend that can be utilized to diagnostically discriminate gold concentrations. As with many gold deposits, the most effective geochemical indicator is gold itself.

Retrogressive Hydrothermal Alteration

Retrogressive hydrothermal alteration of Early Proterozoic rocks within the Homestake mine and Lead area took place in response to fluid movement through dilated segments of reactivated latest D1a and middle D1b shear zones synchronous with renewed thermal activity related to emplacement of early phases of the Crook Mountain Granite (this report; Bachman and others, 1990). Zones of high fluid transport and corresponding intense alteration were confined to dilatant parts of shear zones that opened preferentially within and adjacent to Homestake Formation and Yates unit of the Poorman Formation, owing to significant rheologic contrast with bounding phyllites. Alteration intensity was related to fluid-rock interaction, in turn dependent on fluid volume, transport, and access. In general, hydrothermal alteration effects are manifested principally by partial to complete mineral replacement that commonly entailed mass transfer. Specific alteration products are a function of bulk chemistry, pressure-temperature conditions, and fluid composition. Multiple fluid and alteration events are recognized and differentiated by spatial and temporal relations derived from detailed stratigraphic and structural analysis. The composite of the mineral alteration events can be related to prograde metamorphic processes, retrograde metamorphism, and a distinct retrogressive hydrothermal event that coincided with gold introduction. A detailed account of retrogressive hydrothermal alteration related to the latest fluid event (gold mineralization) is given in Campbell and others (1990).

Retrograde metamorphic conditions appear to have been short-lived, and to have terminated in latest D1a. Retrogressive hydrothermal activity may have been initiated in early D1b, but it was most active during gold mineralization in middle D1b. Extensive fluid movements controlled by shearing, and by mineral alteration, were associated with both early and middle D1b but were most intense during middle D1b. A composite mineral alteration history is shown in table J9.

Chlorite Alteration

Several generations of chlorite are found throughout the mine, the first two of which (Types I and II) were described previously in the section, "Prograde metamorphism." A third variety (Type III) is late and related largely to retrogressive hydrothermal alteration. Some of this third-generation chlorite is undoubtedly related to retrograde metamorphism but cannot be diagnostically distinguished at the present time.

Type III chlorite exists as matted aggregates with individual chlorite grains developed in random to nearly parallel orientation. Similar to Type I, Type III chlorite has anomalously low birefringence. Where it shows nearly parallel orientation with respect to bedding-foliation, it is difficult to distinguish from Type I chlorite, or Type II chlorite related to retrograde metamorphism, particularly in barren iron-formation or chloritic Ellison and Poorman rocks. Type III is the distinctive chlorite found in all ore bodies and is associated throughout the mine with middle D1b shears containing anomalous gold. Its distribution is largely within narrow, planar shear zones. This chlorite variety locally is more abundant than Type I or Type II. Middle D1b shears containing Type III chlorite crosscut earlier metamorphic mineral assemblages and overprint previously deformed strata. Type III chlorite is believed to have been directly related to flow of gold-bearing fluids through the ductile-brittle shear system, and thus to Stage II quartz veins and to gold mineralization.

Carbonate Alteration

Carbonate alteration occurred throughout the Homestake mine area and was especially extensive within the iron-formation. Different stages or periods of carbonate alteration occurred, but their temporal and spatial relations are poorly understood. Carbonate alteration was complicated because (1) carbonate recrystallization varied during prograde metamorphism and associated devolatilization reactions, (2) carbonate alteration took place during the retrograde metamorphism, and (3) carbonate introduction occurred during a later hydrothermal event related to gold mineralization. Fortunately for distinguishing different phases, early metamorphic carbonate indigenous to the iron-formation and to most of the carbonate-bearing semipelitic rocks is easily characterized; it is intergrown with quartz to display a fine-grained heterogranular polygonal texture. Any recrystallization or carbonate introduction, at least in iron-formation, is largely manifested in the form of subhedral to euhedral carbonate porphyroblasts. Most carbonate in the semipelitic rocks and iron-formation was an early and possibly original component. An introduced portion of uncertain volume is marked by abundant coarse siderite, and to a lesser extent ankerite, in the ore bodies. An elevated carbonate content characterizes a majority of the rocks in the Lead window in the Black Hills. Carbonate abundance and distribution at Homestake are similar to those of the large carbonate haloes associated with the major Canadian lode gold deposits, such as in the Abitibi region of Quebec and Ontario (Colvine and others, 1988).

Carbonate alteration associated with most ore bodies and subeconomic gold in the Homestake formed

Table J9. Mineral alteration history related to significant deformation events, Homestake mine

TIME	Deformational event	Thermal event	Description of alteration type
EARLY PROTEROZOIC ↑	Middle D1b (shearing)	Retrogressive hydrothermal alteration (≈1.72 Ga ?)	Replacement 1. Extensive chlorite, siderite, sericite, and minor garnet replacement of wall rock in and adjacent to middle D1b shears. 2. Sulfidation — arsenopyrite, pyrrhotite, and gold replacement of wall rock in and adjacent to middle D1b shears.
	Fluid generation related to emplacement of subjacent granitic pluton (?)		
	Latest D1a (shearing)	Retrograde metamorphism (?)	Metasomatism 1. Magnesium ± iron and (or) potassium + aluminum: biotite replacement of sericite in phyllites bounding sheared iron-formation; production of biotite in iron-formation. 2. Carbonatization, hydration ± potassium metasomatism: calcite and (or) dolomite and chlorite and (or) biotite alteration of sheared Yates unit.
		Prograde metamorphism	Remobilization Mobilization and concentration of graphite in structural traps.
	Fluid generation related to devolatilization during prograde metamorphism		
	Late D1a (folding)	Prograde metamorphism (≈1.84 Ga)	Metamorphism Formation of grunerite, garnet, and hornblende. $siderite+quartz+H_2O=grunerite+CO_2$] Xh $siderite+quartz+chlorite=grunerite+garnet+CO_2$ $chlorite+muscovite+quartz=almandine+biotite+H_2O$ (pelites)] Xp/Xe $chlorite+biotite+quartz=almandine+biotite+H_2O$ $actinolite+albite+ankerite=hornblende+andesine+CO_2+H_2O$ Xpy

coarse-grained, undeformed siderite (less commonly ankerite) porphyroblasts from 2 mm to 1 cm in maximum dimension that are scattered, generally throughout ore bodies, especially in zones of middle D1b shears. Coarse siderite is generally associated with abundant Type III chlorite within these shears. The presence of coarse siderite (and ankerite) with or without chlorite, however, does not necessarily indicate close proximity to ore bodies or sub-economic gold; it occurs also in barren iron-formation transected by middle D1b shears.

Bleached Zones and Sericite Alteration

Bleached zones at Homestake are sericite-rich zones that transect stratigraphic units, previously formed metamorphic mineral assemblages, and potassium-rich metasomatic haloes (for example, the biotite halo associated with iron-formation). These zones are most common (or more obvious) in graphite-bearing phyllites of the Poorman than in other formations. They generally exceed 5 m wide and extend more than 100 m along strike and dip. In most instances, contact relations with enclosing phyllite are transitional, generally within a width of 1 m. Relict host rock features such as faint banding with regular stratigraphic spacing are preserved in the bleached rock. Fabric in the rock, however, has been transposed by shearing into alignment with the associated shear plane, in places producing a phyllonite. Mineralogically these bleached zones consist dominantly of sericite, carbonate, quartz, and plagioclase with minor biotite. Mineralogy is related to the original bulk composition of the rock and to hydrothermal fluid composition. Chemical details are uncertain; however, initial data indicate that carbon, iron, and magnesium have been depleted, whereas CO_2 and possibly calcium have been introduced, at least in graphite-bearing phyllites. Commonly, these zones are close to ore bodies or subeconomic gold-mineralized rock. Bleached zones locally contain quartz veins. Most of the quartz veins are interpreted as Stage II (see section, "Quartz veins") and in some areas are associated with arsenopyrite and pyrrhotite and low but anomalous gold values (<1.0 g Au/t). Some zones of bleaching contain abundant Type III chlorite, are located below ore bodies, and have been interpreted by us to represent feeder conduits. The bleached zones signify paths of fluid flow along middle D1b shears and may represent small individual shears or splays related to or composing a larger shear or shear system generally developed near iron-formation.

Distribution of Hydrothermal Alteration Effects

Effects of hydrothermal alteration within ore ledges and around ore bodies throughout the mine have not been fully appreciated owing to (1) limited exposures across the ore system, and (2) lack of detailed mineralogic plan maps encompassing broad segments of the ore system. Quartz veins and associated haloes are local features and do not encase ore bodies (Noble, 1950; Wolfgram, 1977). More importantly, chlorite that occurs everywhere in and around ore ledges and ore bodies is too abundant and widespread to be a result of quartz-vein formation alone, but is probably related to a broader process that included formation of the quartz veins. Specifically, the fluid event that was responsible for Stage II quartz veins (see section, "Quartz veins") and associated gold mineralization is believed to have been responsible for the pervasive latest significant stage of chlorite (Type III) alteration.

Recently, we have begun to examine possible widespread hydrothermal alteration effects within and peripheral to ore bodies by preparing detailed mineralogic plan maps from mine workings and drill-hole data. We have completed maps of the 4100 and 5900 mine levels (not illustrated) showing ore-body positions and structural domains. Partial maps like those shown in figures J37 and J38 have been produced for key parts of selected ore ledges on other levels.

Chlorite, Type III specifically, is a common constituent in all ore bodies as recognized by Gustafson (1930, 1933), Noble (1950), Slaughter (1968), Chinn (1969), Bidgood (1977), and by the present workers. It is abundant (from 5 to >30 volume percent) in ore bodies and adjacent rocks throughout the ore-producing areas, and markedly decreases in abundance outside the ore environments where large concentrations are restricted to linear shear zones. The chlorite distribution in the mine is also confined to ductile-brittle shear zones (figs. J37, J38) and in large part represents a replacement of biotite, grunerite, and garnet. Restricted but mappable haloes encase ore bodies. Within and adjacent to shear zones, chlorite replacement affected most Early Proterozoic rock types in the mine. Based on recent diamond drilling, shear zones encompassing Main and 21 Ledges have been drilled in the Poorman Formation to several hundred meters below and along strike of the Homestake Formation. Abundant chlorite persists to that depth along with local, but uncommon, concentrations of pyrrhotite, arsenopyrite, and anomalous gold (as much as a few hundred parts per billion), indicating preferential shear development near the Homestake and leakage from nearby ore bodies.

Distribution of biotite-, sericite-, and graphite-bearing units has been compared to the distribution of chlorite and the rock types constituting iron-formation, especially in ore zones. In general, biotite- and sericite-bearing units represent stratigraphic units and rock types both, chemically modified during prograde and retrograde metamorphism, and hydrothermal alteration. Intense chloritization (along with possible further redistribution of graphite) in bleached and graphite-rich phyllites was the result of intense hydrothermal alteration related to gold mineralization and controlled by middle D1b shears. Distribution of these rock (alteration) types is shown in figures J37 and J38 along with the distribution of middle D1b ductile-brittle shears.

On the 2450 level of Main Ledge, grunerite dominates iron-formation outside the ore bodies. (Fig. J37 shows distribution of grunerite, and fig. J31 shows location of ore bodies and named formations at this level.) Individual ore bodies are chlorite rich relative to adjacent iron-formation. Chlorite-rich zones are evidence of intense fluid flow through grunerite-rich iron-formation along ductile-brittle shear zones, as they show systematic symmetry to the shear distribution. A small component of the chlorite is present as a result of replacement of biotite. A sericite-rich

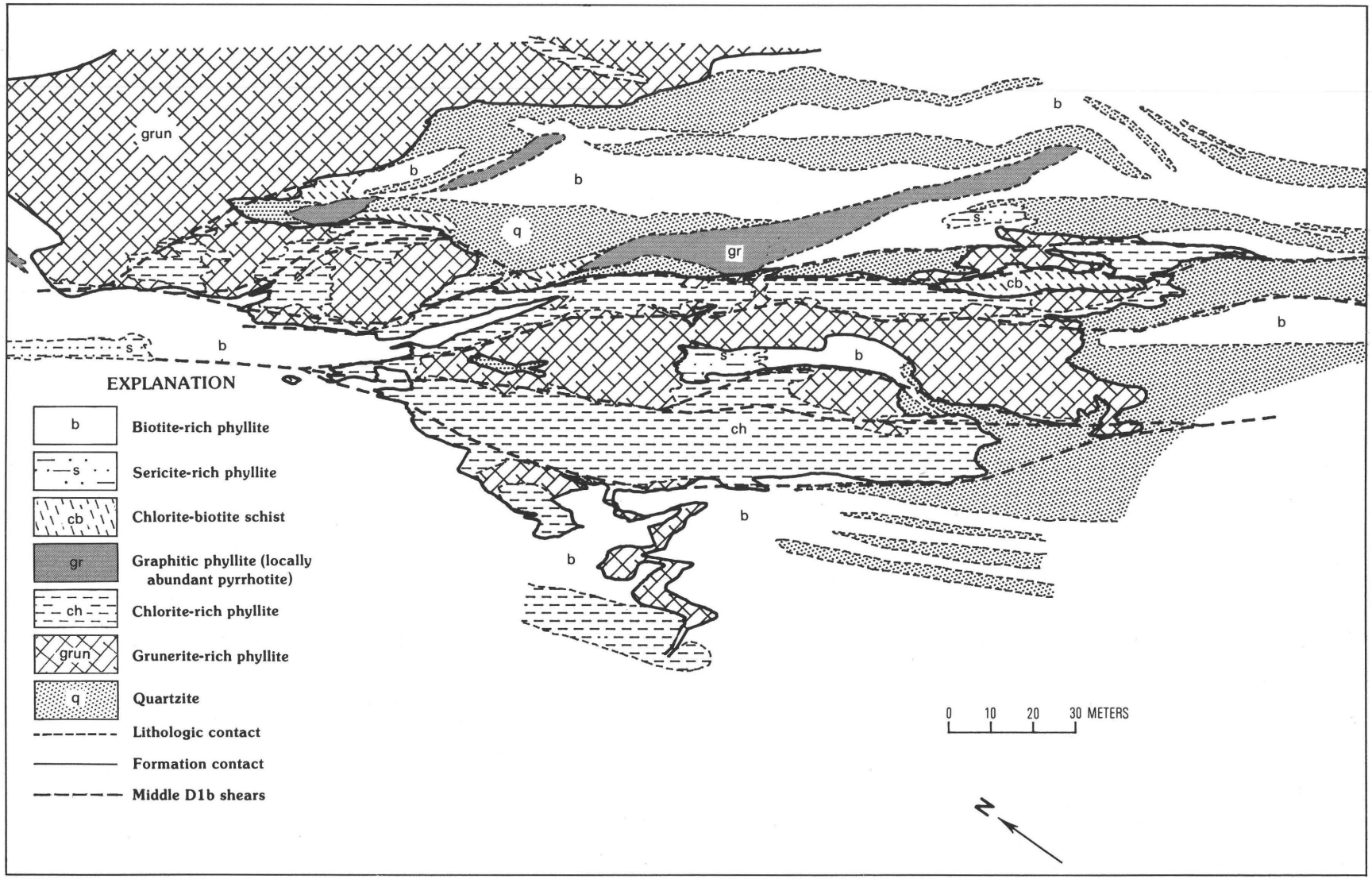

Figure J37. Geologic map showing distribution of rock types in Main Ledge, 2450 level. (See figs. J6 and J27 for relative location.)

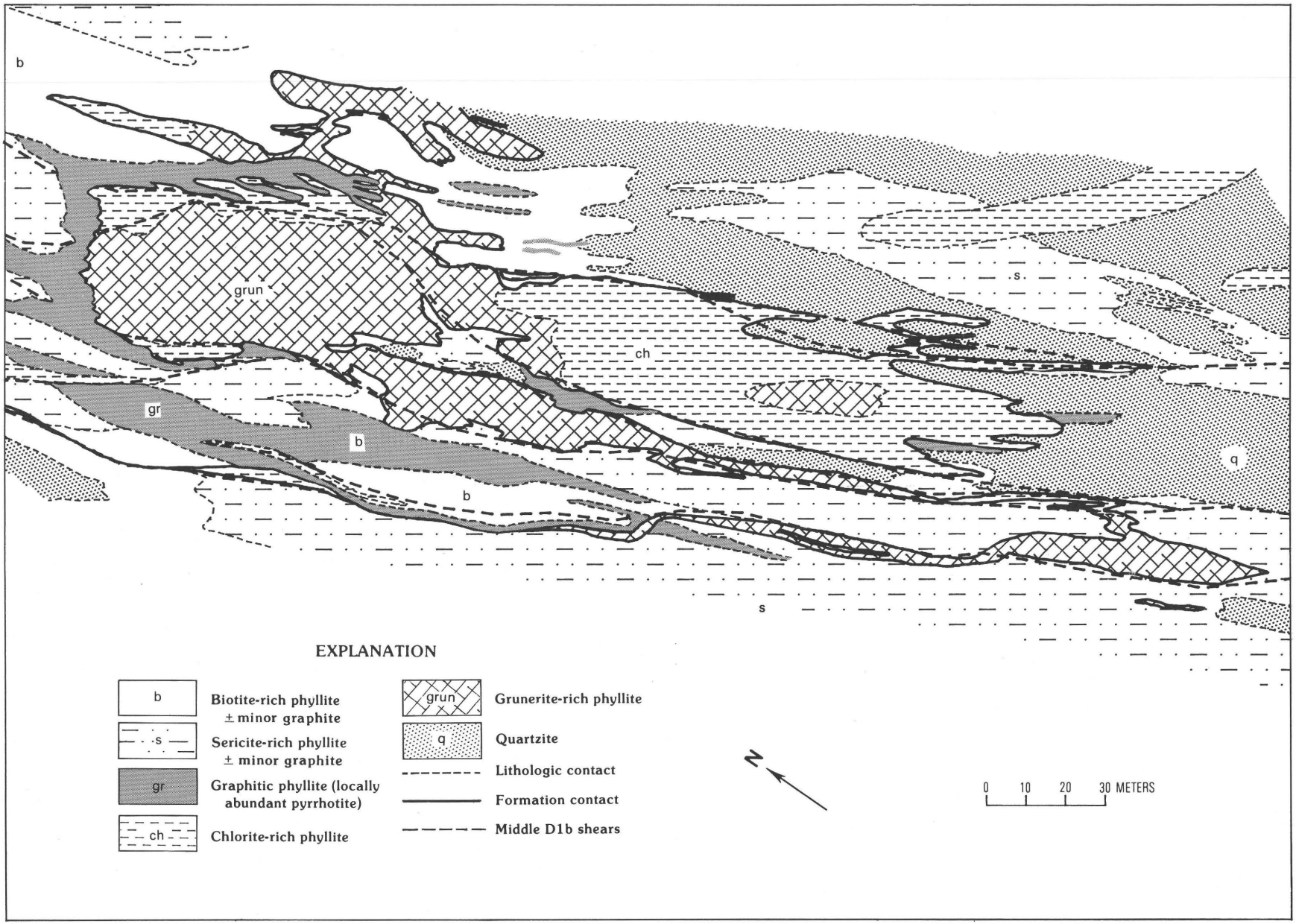

Figure J38. Geologic map showing distribution of rock types in "D" limb of 9 Ledge, 5750 level. (See figs. J6 and J28 for relative location.)

phyllite occurs as small irregular patches stratigraphically below and above the ore bodies in both the Poorman and Ellison Formations. Lenticular bodies of graphitic phyllite (without pyrrhotite) crosscut bedding in the Ellison adjacent to ore bodies. These sericite- and graphite-rich units are interpreted to represent remnants of hydrothermally altered rocks. In the transformation to chlorite-rich rocks, minor potassium may have been driven out of the Homestake and into adjacent formations (Wolfgram, 1977).

Analogous data are presented in figure J38 for "D" limb of 9 Ledge on the 5750 level. Ore bodies here are associated largely with grunerite-rich iron-formation and partly with chlorite-rich zones. (See fig. J32 for location of ore bodies.) Ore bodies are concentrated above graphitic phyllite in the Poorman that contains as much as 60 percent pyrrhotite (and consistently as much as 0.5 g Au/t). Parts of the Poorman and Ellison Formations contain zones rich in sericite. Several of these zones appear to crosscut quartzite units and are interpreted to represent hydrothermal alteration zones controlled by discordant, middle D1b shears. In both figures J37 and J38, a direct spatial and temporal relation is shown between mineral alteration patterns (distributions), ore bodies, and middle D1b shears, indicating strong structural control. Future research should improve the understanding of these relations on a mine-wide basis.

Quartz Veins

Quartz veins occur in all formations in the Homestake area, but they are most common in iron-formation of the Homestake, and less common in quartzite of the Ellison and phyllite of the Poorman or in Ellison semipelitic rocks. Quartz veins in amphibolite, specifically the Yates unit of the Poorman, are rare. In general, all quartz veins are milky white, discontinuous (particularly vertically), and generally unzoned. Quartz in veins is consistently coarse grained, crystalloblastic, and readily distinguishable from sedimentary chert, especially in the eastern ledges. Discordant and concordant quartz veins and irregular quartz masses (fig. J39) are found together commonly in all ore ledges and parts of all ore bodies (figs. J29, J30). Three distinct stages of Early Proterozoic quartz vein development can be described based on temporal relations, morphology, relation to bedding-foliation, mineralogy, and nature of selvage development. The three stages of quartz veins described here are listed in order of decreasing age (table J7).

Stage I

Stage I quartz veins are largely concordant to foliation and transposed bedding. They are folded and sheared locally throughout the mine, less than 1 m thick, and extend along strike for a few tens of meters. Stage I quartz veins are generally boudinaged, drag folded, and sheared in high-strain zones, creating irregularly shaped detached elongate pods of translucent grayish-white quartz exhibiting poorly developed selvages. The long axis of the vein pod is parallel to axial fabric produced in latest D1a. Associated pyrrhotite generally occurs as elliptical blebs localized near or on the margins of the veins. Alteration selvage mineralogy was largely dependent on host rock composition. For example, a vein transecting sericite schist may have a fine- to medium-grained sericite selvage. Where it traverses a pyrrhotite-bearing graphitic phyllite, the vein margin(s) may display a thin (<3 mm) mantle of pyrrhotite. In ore bodies, these early veins occur as detached boudins, isolated floating fold hinges, discontinuous lenses, and rounded fragments (figs. J29, J30). Stage I quartz veins may represent coarsened and (or) remobilized chert, but probably resulted from large-scale transport and deposition of silica during peak prograde metamorphism (table J7). We believe that they were produced synchronous with or just after peak prograde metamorphic conditions during latest D1a, when overall strain conditions were dominated by ductile shear deformation.

Stage II

Stage II quartz veins range from less than 1 cm to more than several meters thick, and they extend along strike from a few meters to greater than 350 m. These veins are roughly tabular, are concordant to discordant, and contain internal streaks, pods, and aggregates of chlorite and (or) biotite, pyrrhotite, arsenopyrite, and commonly coarse visible gold. Asymmetric vein selvages comprising chlorite, biotite, and minor ankerite are commonly 1 m or more thick, and are developed best in Homestake Formation (fig. J29), but they also are present in Ellison and Poorman Formations. Random, isolated, coarse-grained aggregates of irregular pyrrhotite blebs (fig. J33*A*) or pyrrhotite layers (fig. J33*B*) are commonly found concentrated on one quartz vein margin, whereas coarse arsenopyrite porphyroblasts or aggregates (fig. J33*C*; with or without pyrrhotite) characterize the other margin (as described by Wolfgram, 1977). Ore-grade gold (not in sufficient volume to constitute ore) is generally present in both quartz-vein selvages (pyrrhotite and arsenopyrite), but it is most common adjacent to quartz veins near ore bodies. The highest individual gold grades in an ore body combined with the most abundantly observed coarse visible gold, as noted by Noble (1950), are associated with abundant arsenopyrite (figs. J33*C*, J34*A*, and J34*B*) in thick (several meters) selvages, developed adjacent to the widest Stage II quartz veins. The largest ore bodies with the highest gold grades, such as the Main Ledge centroid (figs. J31 and J39), contain numerous Stage II quartz veins with well-developed vein selvages. This is a common observation in all ore

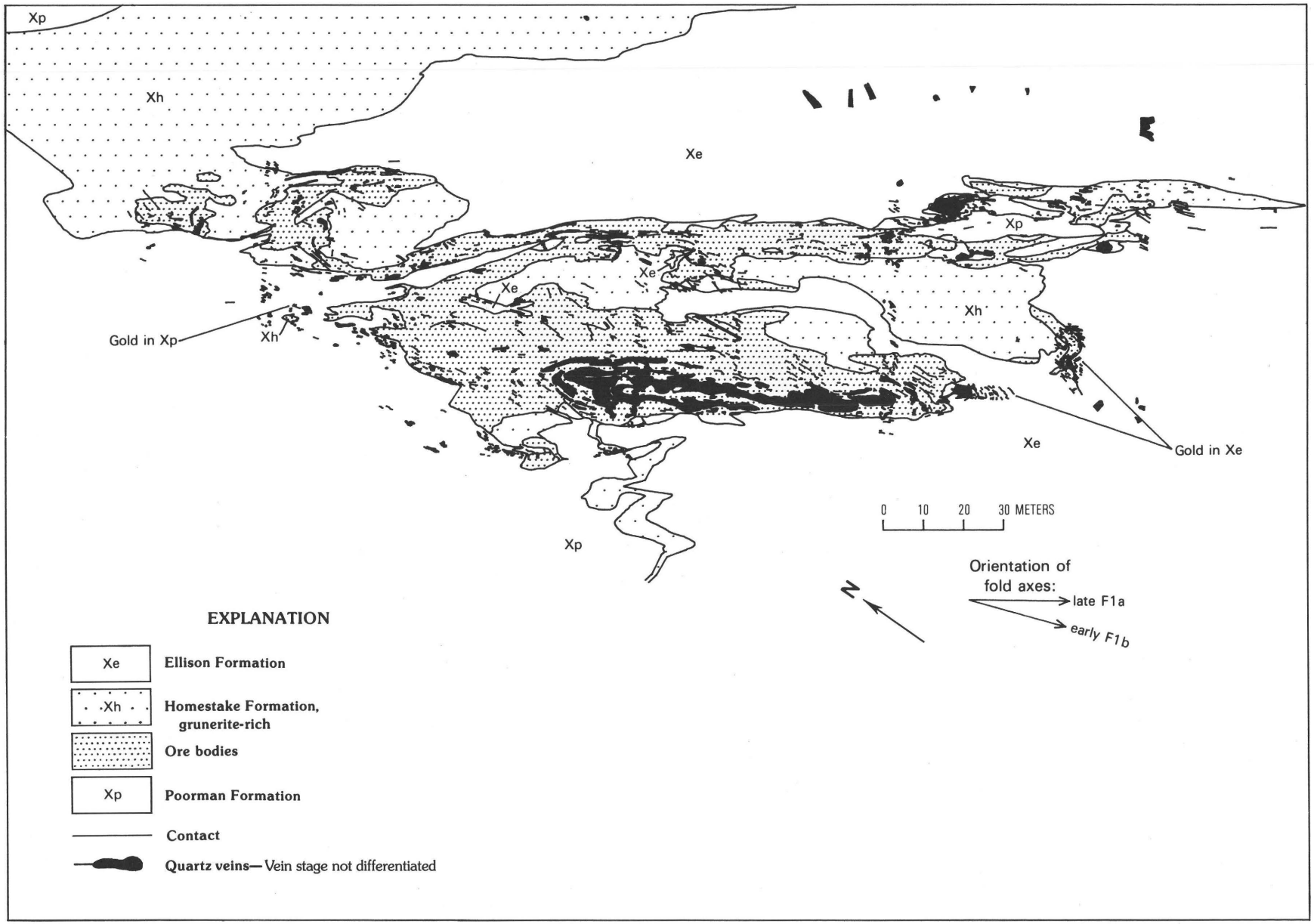

Figure J39. Geologic map showing quartz vein distribution, Main Ledge ore body, 2450 level. (See figs. J6 and J27 for relative location.)

ledges throughout the mine. Stage II quartz veins are rarely deformed, but post-ore shearing resulted in local drag folding and boudinage (fig. J29); the Stage II quartz veins consistently truncate Stage I quartz veins.

Stage II quartz veins in many ore bodies also commonly developed into large irregular masses or "blowouts." Quartz vein "blowouts" generally crosscut earlier developed tabular veins and commonly contain angular fragments or blocks of country rock. Arsenopyrite, pyrrhotite, and fine to coarse gold are associated and intergrown with chlorite locally along the margin of irregular quartz bodies (a small-scale example of quartz vein "blowouts" is illustrated in fig. J29). Tabular Stage II quartz veins and "blowouts" are of much larger volume than Stage I quartz veins, and we believe (1) that they developed in episodic pulses by injection into active shear zones during middle D1b, and (2) that they were locally deformed (fig. J29) during late D1b shearing (table J7). We also suggest that Stage II quartz veins were introduced in the ductile to ductile-brittle transition and were directly related to gold mineralization. Irregular Stage II quartz masses are interpreted as a product of extensional hydraulic fracturing in dilated parts of shear zones.

Stage III

Late barren quartz veins of Stage III truncate both Stage I and II quartz veins. They are markedly discordant and have poorly developed alteration selvages, if any; and they are undeformed. These veins average 5 cm thick, may attain thicknesses as much as 1 m, and extend several tens of meters laterally. They are planar, transect foliation, and truncate ore bodies at large angles (>30°) in throughgoing fashion. They were emplaced in late D1b (table J7). Stage III quartz veins consist primarily of milky quartz and commonly contain coarse ankerite and pyrrhotite, along with subordinate albite. Some veins locally contain narrow alteration selvages of biotite and (or) chlorite with sparse pyrrhotite, depending on host rock composition. Selvage development was dependent on proximity to extensive biotite and (or) chlorite alteration in or near ore bodies. Commonly, sparse pyrrhotite occurs as irregular blebs as much as several centimeters across scattered randomly throughout the veins.

Stage III quartz veins are more common in greenschist-facies rocks than elsewhere. They are interpreted to have been produced in late D1b following ore-stage mineralization. Open-space-filling textures characterize Stage III veins, suggesting development in a more brittle tectonic regime.

Interpretation

Metamorphic rocks in the Homestake mine span a wide range of pressure-temperature conditions and are unevenly traversed by quartz veins. Quartz veins undoubtedly represent extensional fractures along which fluid flow and mineral deposition were focused. Fluids move through rock pervasively along micro-cracks, pores, grain boundaries, foliation, bedding, or widely spaced fractures. These potential conduits would be held open under metamorphic conditions if fluid pressure was greater than lithostatic pressure. This condition existed at times in or near the Homestake Formation as evidenced by the abundance of ductile and ductile-brittle shears and associated quartz veins. Devolatilization reactions in iron-formation, along with pore fluid liberation, sustained high fluid flow and fluid pressure. Devolatilization also was responsible for generation of metamorphic mineral assemblages that represent specific pressure-temperature-composition conditions. Fluid flow was most likely channeled by deep-seated ductile shear zones, the conduits for the plumbing system, into the Homestake Formation, which served as a metamorphic aquifer during devolatilization. Stratigraphically and structurally controlled permeability variations strongly influenced fluid channeling. Characteristics of pelitic to semipelitic rocks (carbonate and fine-grained white mica) that inhibited metamorphic reactivity also restricted fluid channeling. Carbonates were deformed plastically, reducing porosity. Micas served to seal these rocks and restrict fluid flow along foliation in the absence of shears. Pelitic to semipelitic rocks characteristically surround the iron-formation and may have reduced fluid escape, resulting in increased fluid pressure that initiated fracturing and led to eventual quartz vein formation. If fluid pressure in the Homestake were increased to the point of shear failure (ductile mechanics) or extensional hydraulic fracturing (ductile-brittle transition), permeability would have increased fluid flow into shears or fractures. Temperature and pressure gradients would have subsequently led to quartz vein development. Deposition of quartz veins and ore components depended on continued fluid movement and channeling into shear zones or fractures where the fluids reacted with favorable host rocks.

The pressure gradients and chemical instabilities between fluids in the veins and fluids and bulk chemistry of the wallrock controlled vein selvage development and formation of mineral alteration assemblages adjacent to the veins. Stage I quartz veins and their associated fractures formed during prograde metamorphism and probably had lower fluid pressure than corresponding pore fluid pressure of the country rock. If so, the pressure would have driven fluid from wallrock into the fracture system, preventing significant wallrock alteration adjacent to Stage I quartz veins.

Conversely, to explain locally extensive chloritic alteration around Stage II and certain Stage III veins, fluid pressure in the veins would have been higher than pore fluid pressure in the wallrock. Such a condition may have obtained during retrogressive hydrothermal activity (cooling) in which younger veins were formed. The fluid

pressure in host rocks may have been reduced below that prevailing at hydrostatic conditions as a result of absorption of pore water during retrograde metamorphic reactions. Fluid pressure in quartz veins would have been higher than lithostatic pressure, driving chemically active fluid into vein walls to induce chemical reactions along vein margins. These conclusions are taken from Homestake internal reports; the mechanisms of vein selvage development are analogous to those discussed by Yardley (1986) for the Connemara Schists of Ireland.

DISCUSSION

The Homestake gold deposit, the largest deposit of its type known, is believed to have formed as the result of four principal factors: (1) favorable stratigraphy, (2) development of a progressive tectonic system with dilational shears, (3) an intensive thermal and fluid system, and (4) a gold source. In recent years progress has been made in understanding how stratigraphic, tectonic, and thermal processes interacted in time and space to produce the deposit. Our understanding of the source for gold is speculative at best and outside the scope of this study. The actual gold-mineralizing event, the focus of much of our interest, is only the end result of a complex sequence of prior events. Understanding these events and related processes is the key to definition of ore controls.

The importance of original stratigraphy as an ore control relates to the primary rheologic characteristics of individual rock units. Deposition of the voluminous Yates unit tholeiite (>1.97 Ga) is viewed as most significant because during later tectonism the competent Yates unit acted as a regional "hard knot," buffering strain and controlling folding and shearing in the bounding schist and phyllite. During the early stages of major "plate-scale" transcurrent movement (early D1a) the originally flat lying strata were differentially compressed about the Yates unit mass as the strata were transposed to nearly vertical. Deformational strain was selectively partitioned into narrower zones of ductile shearing along the margins of the elongated Yates unit mass. The Homestake Formation, relatively competent although at district scale volumetrically insignificant, was folded and sheared producing a near-perfect structural host. The spatially continuous nature of the iron-formation in the Homestake and increased permeability produced by shearing provided an efficient fluid path along the plunging iron-formation and at the steeply dipping interface between the metatholeiite and schist.

Contemporaneous with the early transcurrent shearing was the development of a regional "hot spot" northeast of and below the current mine. This "hot spot" is believed to have been the focus of thermal activity in the district and also of subsequent fluid generation. Through progressive ductile shearing (latest D1a), preexisting foliation and bedding were transposed into parallelism with the developing shear zones, producing increased permeability. These permeable shear zones became fluid release conduits for devolatilization products that buffered preexisting metamorphic assemblages. Within the mine area, ductile shear zones controlled fluid movement, thereby controlling the distribution of thermal energy and metamorphic processes. This series of changes effectively produced a structurally controlled isothermal zone surface, the upper greenschist–lower amphibolite facies transition zone. In this context, we characterize regional prograde and retrograde metamorphism as dynamothermal, developing synchronously with and controlled by early ductile deformation (late and latest D1a) at 1.84 Ga.

Fluids generated during prograde and retrograde metamorphism, although thought to contain no precious metals, produced significant district-scale metasomatic alteration and local graphite remobilization. This alteration and remobilization defined zones of high fluid transport that correlate to dilated segments of individual ductile shears. The general form and orientation of iron-formation in the Homestake after D1a deformation and regional metamorphism appear to have strongly resembled those currently observed, but without the gold ore bodies and related retrogressive hydrothermal alteration effects. The folded and sheared iron-formation map pattern and fold plunge were apparently established during D1a, and not substantially modified by later events.

The start of deformation D1b reflected a significant change in the regional stress field that was characterized by early, relatively simple northeast-southwest compression and which produced upright folds and later semiductile high-angle reverse shears. Deformation during D1b indicates mechanics at or near the ductile-brittle transition, semibrittle deformation dominating the later stages of D1b. High fluid pressures, possibly exceeding lithostatic pressures, are indicated and may have been important to D1b shear development. Semibrittle deformation mechanics suggest lower relative rock temperatures as compared to peak metamorphism (540 °C). Synchronous with development of D1b structures was a diapiric emplacement of the Crook Mountain Granite. The granite formed as an anatectic response to a "hot spot" which developed northeast of the mine; the hot spot coincided spatially with earlier thermal activity that occurred during regional metamorphism. The granite is considered coeval with the 1.72 Ga Harney Peak Granite in the southern Black Hills. Fluid generation associated with "hot-spot" activity and development of the Crook Mountain Granite is considered by us to have been substantial. Redden and others (1990) suggested significant fluid generation associated with Harney Peak-type granites in general. We postulate that during the early stages of "hot-spot" activity, gold-bearing fluids (derived deep from within the tectono-stratigraphic section) were mobilized and entered a reactivated shear system; gold

deposition occurred in the Homestake Formation. Gold mineralization in the Homestake took place in late-stage ductile-brittle shears (middle D1b) that appear to have dilated largely during reverse movement (northeast sides up). These late shears and associated mineralization effects crosscut earlier deformational fabrics and metamorphic mineral assemblages. The late D1b kink folds formed as a consequence of the final stages of granite emplacement and are postore. These facts are perhaps the most significant and compelling line of evidence that may date gold mineralization substantially later than peak prograde metamorphism estimated at 1.84 Ga (Zartman and Stern, 1967); this line of evidence provides a possible genetic link between mineralization and the early development of granite before 1.72 Ga.

S.F. Emmons (in Irving and others, 1904) was the first to suggest a Precambrian genesis for the Homestake gold deposit. Precambrian hydrothermal or syngenetic variations on genesis were shared by Paige (1924), Connolly (1927), Gustafson (1930, 1933), McLaughlin (1933), Slaughter (1968), Chinn (1969), Rye (1972), Rye and Rye (1974), and Rye and others (1974). The latter three publications suggested on the basis of initial isotopic studies that early gold mineralization was related to a paleo-hot spring or sedimentary exhalative origin. Bidgood (1977), on the basis of petrographic and trace element studies, suggested that introduction of gold and other constituents into the Homestake Formation by hot spring activity was unlikely. However, he did interpret disseminated gold as possibly concentrated by sedimentary or biological processes. Wolfgram (1977) suggested that ore components at Homestake were derived from weathering of volcanic rocks and became incorporated in the iron-formation by biological processes during sedimentation. Hosted and Wright (1923), and Noble (1950) were the two major proponents of a Tertiary age for the Homestake gold deposit, related to Tertiary igneous and hydrothermal activity.

We favor a postpeak metamorphic age (<1.84 Ga) and an epigenetic origin for gold-ore mineralization at Homestake, an origin which best fits the geologic form of the deposit as presently observed. We speculate that sulfidation that accompanied the introduction of sulfur, silica, arsenic, gold, and other elements into a structurally prepared and chemically reactive, iron-rich, siliceous, carbonate-facies host rock during the late-stage middle D1b ductile-brittle shear event was the most likely process to account for deposit genesis. Tabular to pipelike ore bodies were preferentially localized within dilation zones along a network of reactivated ductile-brittle shears. The geologic environment of ore deposition presented herein is similar to ore environments in Precambrian terrains reported elsewhere by Groves and others (1987), Cameron (1989), and DeRoo (1989).

Manuscript received by scientific editors December 1988

REFERENCES CITED

Allsman, P.T., 1940, Reconnaissance of gold-mining districts in the Black Hills, South Dakota: U.S. Bureau of Mines Bulletin 427, 146 p.

Bachman, R.L., and Campbell, T.J., 1990, Early Proterozoic tectonism, metamorphism, and metalization in the Black Hills, South Dakota—A plate-tectonic model: Geological Association of Canada/Mineralogical Association of Canada Program with Abstracts, 1990 Annual Meeting, v. 15, p. A5.

Bachman, R.L., Sneyd, D.S., and Campbell, T.J., 1990, The Crook Mountain Granite and its possible relation to Early Proterozoic gold mineralization, Homestake Mine, Black Hills, South Dakota: Geological Society of America, Rocky Mountain Section, Abstracts with Programs, v. 22, no. 6, p. A2.

Beach, A., 1980, Retrogressive metamorphic processes in shear zones with special reference to the Lewisian complex: Journal of Structural Geology, v. 2, p. 257–263.

Bickford, M.E., Van Schmus, W.R., and Zietz, Isidore, 1986, Proterozoic history of the midcontinent region of North America: Geology, v. 14, p. 492–496.

Bidgood, T.W., 1977, Petrography and trace element distribution across a gold orebody in the Homestake mine, Lead, South Dakota: Rapid City, S. Dak., South Dakota School of Mines and Technology Ph. D dissertation, 97 p.

Bondesen, E., 1970, The stratigraphy and deformation of the Precambrian rocks of the Graenseland area, SW Greenland: Meddelelser om Grönland 185, 125 p.

Broussard, M.L., ed., 1975, Deltas—Models for exploration: Houston, Texas, Houston Geological Society, 555 p.

Button, A., 1976, Iron-formation as an end member in carbonate sedimentary cycles in the Transvaal Supergroup, South Africa: Economic Geology, v. 71, p. 193–201.

Caddey, S.W., Bachman, R.L., and Otto, R.P., 1990, 15 Ledge ore discovery, Homestake Mine, Lead, South Dakota: Fourth Western Regional Conference on Precious Metals and the Environment, Black Hills Section, Society for Mining Metallurgy and Exploration, 1990 Meeting Proceedings Volume, p. 405–423.

Cameron, E.M., 1989, Derivation of gold by oxidative metamorphism of a deep ductile shear zone—Part 1, Conceptual model: Journal of Geochemical Exploration, v. 31, no. 2, p. 135–147.

Campbell, T.J., Sneyd, D.S., and Marlowe, K.E., 1990, Early Proterozoic mineral alteration, Homestake gold mine, Lead, South Dakota: Geological Association of Canada/Mineralogical Association of Canada Program with Abstracts, 1990 Annual Meeting, v. 15, p. A20.

Chinn, W., 1969, Structural and mineralogical studies of the Homestake mine, Lead, South Dakota: Berkeley, Calif., University of California Ph. D. thesis, 190 p.

Colvine, A.C., Fyon, J.A., Heather, K.B., Marmont, S., Smith, P.M., and Troop, D.G., 1988, Archean lode gold deposits in Ontario: Ontario Geological Survey Miscellaneous Paper 139, 136 p.

Connolly, J.P., 1927, The Tertiary mineralization of the northern Black Hills: South Dakota School of Mines and Technology Bulletin 15, 130 p.

Darton, N.H., and Paige, S., 1925, Central Black Hills, South Dakota: U.S. Geological Survey Geologic Atlas of the United States, Folio 219, 34 p.

DeRoo, J.A., 1989, The Elura Ag-Pb-Zn mine in Australia—Ore genesis in a shale belt by syndeformational metasomatism along hydrothermal fluid conduits: Economic Geology, v. 84, p. 256–278.

DeWitt, Ed, Redden, J.A., Wilson, A.B., and Buscher, D., 1986, Mineral resource potential and geology of the Black Hills National Forest, South Dakota and Wyoming: U.S. Geological Survey Bulletin 1580, 135 p.

Dodge, T.A., 1942, Amphibolites of the Lead area, northern Black Hills, South Dakota: Geological Society of America Bulletin, v. 53, p. 561–584.

Fantone, K., 1983, Geochemistry and petrology of the carbonate iron-formations and ferruginous cherts of the northeastern Black Hills, South Dakota: Rapid City, S. Dak., South Dakota School of Mines and Technology M.S. thesis, 107 p.

Fielder, M., 1970, The treasure of Homestake gold: Aberdeen, S. Dak., North Plains Press, 478 p.

Fisher, W.L., Brown, L.F., Jr., Scott, A.J., and McGowen, J.H., 1969, Delta systems in the exploration for oil and gas: Austin, Texas, Texas Bureau of Economic Geology, 78 p.

Floran, R.J., 1975, Mineralogy and petrology of the sedimentary and contact metamorphosed Gunflint Iron-Formation, Ontario-Minnesota: State University of New York at Stony Brook Ph. D. dissertation, 336 p.

Floran, R.J., and Papike, J.J., 1978, Mineralogy and petrology of the Gunflint Iron-Formation, Minnesota-Ontario—Correlation of compositional and assemblage variations at low to moderate grade: Journal of Petrology, v. 19, p. 214–288.

Folk, R.L., 1968, Petrology of sedimentary rocks: Austin, Texas, Hemphill's Book Store, 170 p.

Ghent, E.D., and Stout, M.Z., 1981, Geobarometry and geothermometry of plagioclase-biotite-garnet-muscovite assemblages: Contributions to Mineralogy and Petrology, v. 76, p. 92–97.

Goodwin, A.M., 1956, Facies relations in the Gunflint Iron-Formation: Economic Geology, v. 51, p. 565–595.

Gosselin, D.C., Papike, J.J., Zartman, R.E., and Peterman, Z.E., 1988, Archean rocks of the Black Hills, South Dakota—Reworked basement from the southern extension of the trans-Hudson orogen: Geological Society of America Bulletin, v. 100, p. 1244–1259.

Groves, D.I., Phillips, N., Ho, S.E., Houstoun, S.M., and Standing, C.A., 1987, Craton-scale distribution of Archean greenstone gold deposits—Predictive capacity of the metamorphic model: Economic Geology, v. 82, p. 2045–2058.

Gustafson, J.K., 1930, The Homestake gold-bearing formation: Cambridge, Mass., Harvard University Ph. D. thesis, 173 p.

_____ 1933, Metamorphism and hydrothermal alteration of the Homestake gold-bearing formation: Economic Geology, v. 28, p. 123–262.

Homestake Mining Company, 1988, Annual Shareholders Report: p. 6–7, 18.

Hosted, J.O., and Wright, L.B., 1923, Geology of the Homestake orebodies and the Lead area of South Dakota: Engineering and Mining Journal Press, v. 115, no. 18, p. 793–799; no. 19, p. 836–843.

Irvine, T.N., and Baragar, W.R.A., 1971, A guide to the chemical classification of igneous rocks: Canadian Journal of Earth Science, v. 8, p. 523–548.

Irving, J.D., Emmons, S.F., and Jaggar, T.A., Jr., 1904, Economic resources of the northern Black Hills: U.S. Geological Survey Professional Paper 26, 222 p.

James, H.L., 1954, Sedimentary facies of iron-formation: Economic Geology, v. 49, p. 235–293.

Jensen, L.S., 1976, A new cation plot for classifying subalkalic rocks: Ontario Department of Mines Miscellaneous Paper 66, 22 p.

Kath, R., 1989, Metamorphic mineral assemblages associated with the grunerite and garnet-grunerite isograds in the Homestake Iron-Formation, Lead, South Dakota—Phase relations for potassic and aluminous iron-formations: Geological Society of America Abstracts with Programs, v. 21, no. 6, p. A275.

_____ 1990, Mineralogy and petrology of the Homestake Iron-Formation, Lead, South Dakota—Conditions and assemblages of metamorphism related to P–T path and fluid evolution: Rapid City, S. Dak., South Dakota School of Mines and Technology Ph. D. dissertation.

Kerrich, R., 1986, Fluid transport in lineaments: Royal Society of London Philosophical Transactions, v. 317A, p. 219–251.

Krauskopf, K.B., 1967, Introduction to geochemistry: New York, McGraw-Hill, p. 63–85.

Labotka, T.C., 1985, Petrogenesis of metamorphic rocks beneath the Stillwater Complex—Assemblages and conditions of metamorphism, *in* Czamanske, G.K., and Zientek, M.L., eds., The Stillwater Complex, Montana—Geology and guide: Montana Bureau of Mines and Geology Special Publication 92, p. 70–76.

Labotka, T.C., Vaniman, D.T., and Papike, J.J., 1982, Contact metamorphic effects of the Stillwater Complex, Montana—The concordant iron-formation; A reply to the role of buffering in metamorphism of iron-formation: American Mineralogist, v. 67, p. 149–152.

Leake, B.E., 1978, Nomenclature of amphiboles: American Mineralogist, v. 63, p. 1023–1052.

McBride, E.F., 1963, A classification of modern sandstones: Journal of Sedimentary Petrology, v. 33, p. 664–669.

McCarthy, T.R., 1976, The metamorphic petrology of the sideroplesite and cummingtonite schist facies of the Homestake Formation, Homestake mine, Lead, South Dakota: Madison, Wis., University of Wisconsin M.S. thesis, 73 p.

McLaughlin, D.H., 1933, The Homestake orebodies, Lead, South Dakota, *in* Lindgren, Waldemar, Ore deposits of the Western States (Lindgren Volume): American Institute of Mining and Metallurgical Engineers, p. 563–565 and 722–729.

Noble, J.A., 1939, Geology of the Homestake gold mine: Cambridge, Mass., Harvard University Ph. D. dissertation, 278 p.

_____ 1950, Ore mineralization in the Homestake gold mine, Lead, South Dakota: Geological Society of America Bulletin, v. 61, no. 3, p. 221–252.

Noble, J.A., and Harder, J.O., 1948, Stratigraphy and metamorphism in a part of the northern Black Hills and the Homestake mine, Lead, South Dakota: Geological Society of America Bulletin, v. 59, p. 941–975.

Noble, J.A., Harder, J.O., and Slaughter, A.L., 1949, Structure of a part of the northern Black Hills and the Homestake mine, Lead, South Dakota: Geological Society of America Bulletin, v. 60, p. 321–352.

Norby, J.W., 1984, Geology and geochemistry of Precambrian amphibolites and associated gold mineralization, Tinton district, Lawrence County, South Dakota, and Crook County, Wyoming: Rapid City, S. Dak., South Dakota School of Mines and Technology M.S. thesis, 144 p.

Norton, J.J., 1989, Bald Mountain gold mining region, northern Black Hills, South Dakota, *in* Shawe, D.R., Ashley, R.P., and Carter, L.M.H., eds., Geology and resources of gold in the United States: U.S. Geological Survey Bulletin 1857–C, p. C1–C13.

Paige, S., 1924, Geology of the region around Lead, South Dakota: U.S. Geological Survey Bulletin 765, 56 p.

Park, A.F., 1988, Geometry of sheath folds and related fabrics at the Luikonlahti mine, Svecokarelides, eastern Finland: Journal of Structural Geology, v. 10, no. 5, p. 487–498.

Pearce, T.H., Gorman, B.E., and Birkett, T.C., 1975, The TiO_2-K_2O-P_2O_5 diagram—A method of discriminating between oceanic and non-oceanic basalts: Earth and Planetary Science Letters, v. 19, p. 290–300.

Ramsay, J.G., and Huber, M.I., 1983, The techniques of modern structural geology, Volume 1, Strain analysis: New York, Academic Press, 307 p.

Ratté , J.C., and Zartman, R.E., 1970, Bear Mountain gneiss dome, Black Hills, South Dakota—Age and structure: Geological Society of America Abstracts with Programs, v. 2, no. 5, p. 345.

Redden, J.A., and French, G.McN., 1989, Geologic setting and potential exploration guides for gold deposits, Black Hills, South Dakota, *in* Shawe, D.R., Ashley, R.P., and Carter, L.M.H., eds., Geology and resources of gold in the United States: U.S. Geological Survey Bulletin 1857–B, p. B45–B74.

Redden, J.A., and Norton, J.J., 1975, Precambrian geology of the Black Hills, *in* U.S. Congress, Senate Committee on Interior and Insular Affairs: U.S. 94th Congress, 1st session, p. 18–21.

Redden, J.A., Peterman, Z.E., Zartman, R.E., and DeWitt, Ed, 1990, Early Proterozoic Trans-Hudson orogen of North America, *in* Geological Survey of Canada Special Paper 37: p. 229–251.

Roberts, W.L., Campbell, T.J., and Rapp, G.R., Jr., 1990, Encyclopedia of minerals, second edition: New York, Van Nostrand-Reinhold, Inc., 1008 p.

Roscoe, S.M., 1969, Huronian rocks and uraniferous conglomerates in the Canadian Shield: Geological Survey of Canada Paper 68–40, 205 p.

Rye, D.M., 1972, The stable and lead isotopes of part of the northern Black Hills—Age and origin of the Homestake and surrounding orebodies: Minneapolis, Minn., University of Minnesota Ph. D. dissertation, 119 p.

Rye, D.M., Doe, B.R., and Delevaux, M.H., 1974, Homestake gold mine, South Dakota—II, Lead isotopes, mineralization ages, and source of lead in ores of the northern Black Hills: Economic Geology, v. 69, p. 814–822.

Rye, D.M., and Rye, R.O., 1974, Homestake gold mine, South Dakota—I, Stable isotope studies: Economic Geology, v. 69, p. 293–317.

Shapiro, L.H., and Gries, J.P., 1970, Ore deposits in rocks of Paleozoic and Tertiary age of the northern Black Hills, South Dakota: U.S. Geological Survey Open-File Report 70–300, 235 p.

Sims, P.K., Kisvarsanyi, E.B., and Morey, G.B., 1987, Geology and metallogeny of Archean and Proterozoic basement terranes in the northern midcontinent, U.S.A.—An overview: U.S. Geological Survey Bulletin 1815, 51 p.

Slaughter, A.L., 1968, The Homestake mine, *in* Ridge, J.D., ed., Ore deposits of the United States, 1933–1967 (Graton-Sales Volume II): New York, American Institute of Mining and Metallurgy, Petroleum Engineers, p. 1436–1459.

Tapper, C.J., 1984, Geochemistry of greenstone and amphibolite in the eastern Black Hills, South Dakota: Rapid City, S. Dak., South Dakota School of Mines and Technology M.S. thesis, 90 p.

Thompson, J.B., 1957, The graphical analysis of mineral assemblages in pelitic schists: American Mineralogist, v. 42, p. 842–858.

Thompson, J.B., and Norton, S.A., 1968, Paleozoic regional metamorphism in New England and adjacent areas, *in* Studies of Appalachian geology: New York, John Wiley, p. 319–327.

Tilley, C.E., 1925, Metamorphic zones in the southern highlands of Scotland: Geological Society of London Quarterly Journal, v. 81, p. 100–112.

Vaniman, D.T., Papike, J.J., and Labotka, T.C., 1980, Contact metamorphic effects of the Stillwater Complex, Montana—The concordant iron-formation: American Mineralogist, v. 65, p. 1087–1102.

Wayland, R.G., 1936, Cummingtonite from the Black Hills, South Dakota: American Mineralogist, v. 21, no. 9, p. 607–610.

Winkler, H.G.F., 1979, Petrogenesis of the metamorphic rocks, 5th edition: New York, Springer-Verlag, 348 p.

Wolfgram, Diane, 1977, Wallrock alteration and the localization of gold in the Homestake mine, Lead, South Dakota: Berkeley, Calif., University of California Ph. D. dissertation, 139 p.

Woolnough, W.G., 1941, Origin of banded iron deposits—A suggestion: Economic Geology, v. 36, p. 465–489.

Yardley, B.W.D., 1986, Fluid migration and veining in the Connemara schists, Ireland, *in* Walther, J.V., and Wood, B.J., eds., Fluid-rock interactions during metamorphism: Advances in Physical Geochemistry, v. 5, p. 109–131.

Zartman, R.E., and Stern, T.W., 1967, Isotopic age and geologic relationships of the Little Elk Granite, northern Black Hills, South Dakota, *in* Geological Survey research 1967: U.S. Geological Survey Professional Paper 575–D, p. D157–D163.

☆U.S. GOVERNMENT PRINTING OFFICE: 1992-673-049/46028

SELECTED SERIES OF U.S. GEOLOGICAL SURVEY PUBLICATIONS

Periodicals

Earthquakes & Volcanoes (issued bimonthly).
Preliminary Determination of Epicenters (issued monthly).

Technical Books and Reports

Professional Papers are mainly comprehensive scientific reports of wide and lasting interest and importance to professional scientists and engineers. Included are reports on the results of resource studies and of topographic, hydrologic, and geologic investigations. They also include collections of related papers addressing different aspects of a single scientific topic.

Bulletins contain significant data and interpretations that are of lasting scientific interest but are generally more limited in scope or geographic coverage than Professional Papers. They include the results of resource studies and of geologic and topographic investigations; as well as collections of short papers related to a specific topic.

Water-Supply Papers are comprehensive reports that present significant interpretive results of hydrologic investigations of wide interest to professional geologists, hydrologists, and engineers. The series covers investigations in all phases of hydrology, including hydrology, availability of water, quality of water, and use of water.

Circulars present administrative information or important scientific information of wide popular interest in a format designed for distribution at no cost to the public. Information is usually of short-term interest.

Water-Resources Investigations Reports are papers of an interpretive nature made available to the public outside the formal USGS publications series. Copies are reproduced on request unlike formal USGS publications, and they are also available for public inspection at depositories indicated in USGS catalogs.

Open-File Reports include unpublished manuscript reports, maps, and other material that are made available for public consultation at depositories. They are a nonpermanent form of publication that maybe cited in other publications as sources of information.

Maps

Geologic Quadrangle Maps are multicolor geologic maps on topographic bases in 7 1/2- or 15-minute quadrangle formats (scales mainly 1:24,000 or 1:62,500) showing bedrock, surficial, or engineering geology. Maps generally include brief texts; some maps include structure and columnar sections only.

Geophysical Investigations Maps are on topographic or planimetric bases at various scales, they show results of surveys using geophysical techniques, such as gravity, magnetic, seismic, or radioactivity, which reflect subsurface structures that are of economic or geologic significance. Many maps include correlations with the geology.

Miscellaneous Investigations Series Maps are on planimetric or topographic bases of regular and irregular areas at various scales; they present a wide variety of format and subject matter. The series also includes 7 1/2-minute quadrangle photogeologic maps on planimetric bases which show geology as interpreted from aerial photographs. The series also includes maps of Mars and the Moon.

Coal Investigations Maps are geologic maps on topographic or planimetric bases at various scales showing bedrock or surficial geology, stratigraphy, and structural relations in certain coal-resource areas.

Oil and Gas Investigations Charts show stratigraphic information for certain oil and gas fields and other areas having petroleum potential.

Miscellaneous Field Studies Maps are multicolor or black-and-white maps on topographic or planimetric bases on quadrangle or irregular areas at various scales. Pre-1971 maps show bedrock geology in relation to specific mining or mineral-deposit problems; post-1971 maps are primarily black-and-white maps on various subjects such as environmental studies or wilderness mineral investigations.

Hydrologic Investigations Atlases are multicolored or black-and-white maps on topographic or planimetric bases presenting a wide range of geohydrologic data of both regular and irregular areas; the principal scale is 1:24,000, and regional studies are at 1:250,000 scale or smaller.

Catalogs

Permanent catalogs, as well as some others, giving comprehensive listings of U.S. Geological Survey publications are available under the conditions indicated below from the U.S. Geological Survey, Books and Open-File Reports Sales, Box 25425, Denver, CO 80225. (See latest Price and Availability List.)

"Publications of the Geological Survey, 1879-1961" may be purchased by mail and over the counter in paperback book form and as a set microfiche.

"Publications of the Geological Survey, 1962-1970" may be purchased by mail and over the counter in paperback book form and as a set of microfiche.

"Publications of the U.S. Geological Survey, 1971-1981" may be purchased by mail and over the counter in paperback book form (two volumes, publications listing and index) and as a set of microfiche.

Supplements for 1982, 1983, 1984, 1985, 1986, and for subsequent years since the last permanent catalog may be purchased by mail and over the counter in paperback book form.

State catalogs, "List of U.S. Geological Survey Geologic and Water-Supply Reports and Maps For (State)," may be purchased by mail and over the counter in paperback booklet form only.

"Price and Availability List of U.S. Geological Survey Publications," issued annually, is available free of charge in paperback booklet form only.

Selected copies of a monthly catalog "New Publications of the U.S. Geological Survey" is available free of charge by mail or may be obtained over the counter in paperback booklet form only. Those wishing a free subscription to the monthly catalog "New Publications of the U.S. Geological Survey" should write to the U.S. Geological Survey, 582 National Center, Reston, VA 22092.

Note.–Prices of Government publications listed in older catalogs, announcements, and publications may be incorrect. Therefore, the prices charged may differ from the prices in catalogs, announcements, and publications.